# JOINT CHANNEL - PHYSICAL LAYER NETWORK CODING IN MULTI-WAY WIRELESS RELAY SYSTEMS

by

Dananjaya Nuwan Balasuriya

A Thesis Submitted for the Partial Fulfillment of the Requirements for the Degree of

Doctor of Philosophy

Department of Electronic and Telecommunication Engineering

University of Moratuwa

January 2021

## Declaration

I certify that this thesis does not incorporate without acknowledgement any material previously submitted for a degree or diploma in any university; and to the best of my knowledge it does not contain any material which had been previously published by another person except where due reference is made in the text.

.....

Dananjaya Nuwan Balasuriya

Certified by:

.....  .....

Dr. K.C.B. Wavegedara  Prof. S.A.D. Dias

# Abstract

During the last two decades or so, physical layer network coding (PNC) has received a considerable attention as it provides superior spectral efficiency over conventional relaying, in wireless relay systems. However, error performance of the network coded relay systems is inferior to that of conventional relaying under poor quality channel conditions. On the other hand, channel coding provides improved error performance over noisy and fading channels. In channel and PNC coded wireless relay systems, a better performance can be achieved by performing channel decoding and network coding at the relay jointly compared to separately. However, the existing joint channel decoding and network coding algorithms cannot achieve a good trade-off between error performance and spectral efficiency when applied in a multi-way wireless relay system. This is mainly due to the fact that the existing algorithms operate the constituent sub-decoders independently. With the advancement of new trends such as Internet of Things (IoT), multi-way wireless relay system has been a popular network topology, hence joint channel decoding and network coding algorithms having very good spectral efficiency-error performance trade-offs are highly desired.

This thesis presents, as the key technical contribution to the existing body of knowledge, a joint channel-physical layer network coding (JCPNC) algorithm for multi-way wireless relay systems, which achieves an improved trade-off between error performance and spectral efficiency. This improved performance is a result of harnessing additional time diversity by exchanging information between constituent sub-decoders. Several

diversity combining schemes are proposed and they are compared with each other. The thesis also presents an improved symbol value selection algorithm for the conventional non-binary symbol-flipping low density parity check decoder which is adopted to produce a low-complexity JCPNC algorithm. Moreover, a novel JCPNC algorithm which can be employed in asymmetric multi-way wireless relay systems, is developed. Finally, the convergence behaviour of the proposed JCPNC algorithm is analyzed using extrinsic information transfer (EXIT) characteristics of the constituent sub-decoders.

The error performance of the proposed algorithms is extensively investigated using computer simulations. The simulation results demonstrate that the proposed JCPNC algorithm and its variants achieve superior spectral efficiency-error performance trade-offs than the existing counterpart JCPNC algorithms.

# Acknowledgments

Playing multiple roles as a father, a husband, a son, a brother, a teacher, a good friend and many more consumes a lot of one's energy. While playing all these multiple roles in day to day life, carrying out PhD level research is a mammoth task. However, thanks to many individuals it was possible for me to paddle through rough waters and reach the sea. Thus, helpful hands of many individuals are blended into this thesis.

First, I would like to express my sincere gratitude to my supervisors Dr. K.C.B. Wavegedara and Prof. S.A.D. Dias, whose guidance had been immensely valuable throughout this period. Their patience at my rough times and encouragements and invaluable advices at all times became the driving forces for this thesis. I am also very grateful to my workplace colleagues at The Open University of Sri Lanka, specially Dr. K.A.C. Udayakumar for the constant support granted to me in numerous ways. My family has been a wall of support during this whole period. I am forever indebted to my mother for the emotional care she had provided and my loving wife for all the support she has extended over the years, being a part of my life in good and bad times. Though my two young sons did not like their father being too much attached to research, their affection kept my mindset balanced to carryout quality research amidst a busy schedule. Finally, there is one person outstandingly stood behind my success. One who had only been grade ten educated but possessed life knowledge beyond a PhD, who dreamt his son conquering the highest peak in education one day. It is his vision that drove me to the peak. I dedicate this thesis to him, to my dear father.

# Contents

**Abstract** **i**

**Acknowledgments** **iii**

**List of Tables** **ix**

**List of Figures** **xii**

**List of Abbreviations** **xv**

**1 Introduction** **1**

1.1 An Overview of the Wireless Relay Channel . . . . . 2

1.2 Introduction to Network Coding . . . . . 3

1.3 Physical Layer Network Coding . . . . . 7

1.4 Channel Coding . . . . . 9

1.5 Joint Channel-Network Coding . . . . . 10

1.6 JCPNC Algorithms for Different Network Topologies . . . . . 11

1.7 JCPNC Algorithms for Different Channel Coding Types . . . . . 14
1.8 Theme and Objectives of the Thesis . . . . . 15
1.9 Outline of the Thesis . . . . . 16
1.10 Scope and Limitations of the Study . . . . . 18

**2 Proposed Joint Channel-Network Coding Algorithm for Multi-way Relay Systems 19**

2.1 Introduction . . . . . 19
2.2 System Model . . . . . 21
2.3 Joint Decoding at the Relay . . . . . 25
2.3.1 Separating $c_b$ information at the relay . . . . . 25
2.3.2 Exchanging $c_b$ information between $c_a \oplus c_b$ and $c_b \oplus c_c$ decoders . 27
2.3.3 Re-calculation of Joint Probabilities . . . . . 30
2.4 Extending the Joint Decoding Algorithm to MPSK Modulated Muti-way Relay Systems . . . . . 31
2.4.1 New System Model . . . . . 31
2.4.2 Pair-wise Iterative Joint Decoding at the Relay . . . . . 33
2.4.3 Improved Iterative Joint Decoding at the Relay . . . . . 38
2.4.4 Analysis of Computational Complexity . . . . . 45
2.5 Numerical Results and Discussion . . . . . 48
2.6 Conclusion . . . . . 54

**3 Low-Complexity Joint Channel-Network Coding Algorithm for Multi-Way Relay Systems** **59**

3.1 Introduction . . . . . 59

3.2 System Model . . . . . 61

3.3 Low-complexity Joint Decoding at the Relay . . . . . 62

3.3.1 Initialization . . . . . 63

3.3.2 Modified Bit-flipping Algorithm . . . . . 64

3.3.3 Information Exchange Between Decoders . . . . . 66

3.3.4 Finalization . . . . . 68

3.4 Computational Complexity Analysis . . . . . 68

3.5 Improved Low-complexity Joint Channel Network Coding Algorithms for Multi-Way Relay Systems . . . . . 70

3.5.1 Introduction . . . . . 71

3.5.2 System Model . . . . . 72

3.5.3 Non-binary LDPC Decoding . . . . . 73

3.5.4 Proposed Symbol-value Selection . . . . . 77

3.5.5 Computational Complexity . . . . . 79

3.6 Simulation Results and Discussion . . . . . 83

3.7 Conclusion . . . . . 88

**4 Joint Channel-Network Coding in Unequally Error Protected Multi-way Wireless Relay Systems** **91**

4.1 Introduction . . . . . 91
4.2 System Model . . . . . 93
4.3 Throughput Enhancement . . . . . 96
4.4 Iterative Joint Decoding at the Relay . . . . . 97
4.4.1 Initialization . . . . . 97
4.4.2 Iterative Decoding . . . . . 98
4.4.3 Finalization . . . . . 101
4.5 Extending the Unequal Error Protection Scheme to $\mathcal{M} > 3$ . . . . . 101
4.5.1 Throughput . . . . . 102
4.5.2 Scaled Joint Decoder Algorithm . . . . . 103
4.6 Numerical Results and Discussion . . . . . 103
4.7 Conclusion . . . . . 105

**5 EXIT Analysis of the JCPNC Algorithm 110**

5.1 Introduction . . . . . 110
5.2 System Model . . . . . 111
5.3 Log Domain Joint Decoder . . . . . 112
5.3.1 Initialization . . . . . 113
5.3.2 Variable Node Decoder . . . . . 115
5.3.3 Check Node Decoder . . . . . 115
5.3.4 Finalization . . . . . 117
5.4 EXIT Analyzis for the JCPNC . . . . . 117

5.4.1 $J_V$ Function . . . . . 118
5.4.2 VND EXIT Curve . . . . . 119
5.4.3 CND EXIT Curve . . . . . 120
5.5 Example EXIT Analysis for the JCPNC Algorithm . . . . . 121
5.6 EXIT Analyzis for the JCPNC in Multi-way Relay Systems . . . . . 127
5.7 Conclusion . . . . . 131

**6 Conclusion and Suggestions for Further Work 133**

6.1 Conclusion . . . . . 133
6.2 Further Work . . . . . 136

**Bibliography 138**

# List of Tables


1.1 Physical layer network coding symbol mapping . . . . . 8

1.2 JCPNC algorithms for different channel codes . . . . . 13

1.3 JCPNC algorithms for different network topologies . . . . . 14

1.4 JCPNC algorithms for different channel coding types . . . . . 15

2.1 PNC symbol mapping for BPSK modulation . . . . . 27

2.2 Per iteration, number of mathematical operations involved under different information exchange schemes . . . . . 47

2.3 Percentage number of times the algorithm converges at different number of iterations for $255 \times 175$ LDPC code with QPSK modulation . . . . . 57

2.4 Per iteration, number of mathematical operations involved under different information exchange schemes in $255 \times 175$ binary LDPC code with QPSK modulation . . . . . 58

3.1 Combined transmitted signal constellation . . . . . 63

3.2 Comparison of computational complexity . . . . . 69

3.3 Number of real operations for the symbol flipping algorithm . . . . . 80

3.4 Number of real operations for the symbol flipping algorithm for $204 \times 102$, GF(4) LDPC code. . . . . 82

3.5 Number of real operations for the symbol flipping algorithm for $63 \times 37$, GF(16) LDPC code. . . . . 82

3.6 Number of real operations for the symbol flipping algorithm for $1023 \times 781$, GF(16) LDPC code. . . . . 83

4.1 Spectral efficiency for different code rates . . . . . 104

5.1 Mean and variance values for LLR . . . . . 115

5.2 $\lambda(.)$ and $\nu(.)$ functions . . . . . 119

5.3 EXIT trajectory for $E_b/N_0 = 2dB$ when $h_A = 0.3$ and $h_B = 0.5$ . . . . . 123

5.4 EXIT trajectory for $E_b/N_0 = 7dB$ when $h_A = 0.3$ and $h_B = 0.5$ . . . . . 124

5.5 EXIT trajectory for $E_b/N_0 = 3dB$ when $h_A = 0.9$ and $h_B = 1.1$ . . . . . 125

5.6 EXIT trajectory for $E_b/N_0 = 5dB$ when $h_A = 0.9$ and $h_B = 1.1$ . . . . . 126

5.7 EXIT trajectory of the BC decoder for $E_b/N_0 = 5dB$ with information exchange . . . . . 129

5.8 EXIT trajectory of the AB decoder for $E_b/N_0 = 7dB$ with information exchange . . . . . 129

5.9 EXIT trajectory of the BC decoder for $E_b/N_0 = 4dB$ with information exchange . . . . . 130

5.10 EXIT trajectory of the AB decoder for $E_b/N_0 = 4dB$ with information exchange . . . . . 130

# List of Figures


1.1 A wireless relay system . . . . . 2

1.2 Bidirectional relaying between nodes A and B with a single relay . . . . . 4

1.3 Network coding in a bidirectional relay system . . . . . 5

1.4 Conventional relaying in the butterfly relay network . . . . . 6

1.5 Network coding in the butterfly relay network . . . . . 7

2.1 Three-way relay system (a) MAC phase of A & B transfer (b) MAC phase of B & C transfer (c) Broadcast phase of A & B transfer (d) Broadcast phase of B & C transfer . . . . . 22

2.2 Proposed joint channel decoder-network encoder . . . . . 26

2.3 Comparison of decoder BER performance for $255 \times 175$ LDPC code. . . . 49

2.4 Comparison of decoder BER performance for $1057 \times 813$ LDPC code. . . 50

2.5 BER performance of the proposed algorithm for $255 \times 175$ binary LDPC code with QPSK modulation. . . . . 51

2.6 BER performance of the proposed algorithm for $1057 \times 813$ binary LDPC code with 8-PSK modulation. . . . . 52
2.7 BER performance of the proposed algorithm for $255 \times 175$ binary LDPC code with 16-PSK modulation. . . . . 53
2.8 BER performance of the proposed algorithm for $204 \times 102$ GF(4) LDPC code with QPSK modulation. . . . . 54
2.9 BER performance of the proposed algorithm for $255 \times 175$ binary LDPC code under different modulation orders. . . . . 55
2.10 FER performance of the proposed algorithm for $255 \times 175$ binary LDPC code with QPSK modulation. . . . . 56
2.11 Comparison of decoder BER performance for $255 \times 175$ LDPC code for 5, 10 and 20 decoding iterations. . . . . 57
2.12 BER performance of the proposed algorithm for $255 \times 175$ binary LDPC code with QPSK modulation after 1, 3 and 10 decoder iterations. . . . . 58

3.1 Information exchange . . . . . 67
3.2 Histogram for the average number of iterations per decoded codeword for $255 \times 175$ LDPC code. . . . . 70
3.3 System model . . . . . 73
3.4 Comparison of decoder BER performance for $204 \times 102$, GF(4) LDPC code. 84
3.5 Comparison of decoder BER performance for $63 \times 37$, GF(16) LDPC code. 85

3.6 Comparison of decoder BER performance for $1023 \times 781$, GF(16) LDPC code. . . . . 86

3.7 Comparison of decoder BER performance for $255 \times 175$ LDPC code. . . . 88

3.8 Comparison of decoder BER performance for $1023 \times 781$ LDPC code. . . 89

4.1 Asymmetric information exchange . . . . . 95

4.2 Proposed decoder arrangement . . . . . 99

4.3 Spectral efficiency for different code rates . . . . . 104

4.4 BER performance for $63 \times 37$ LDPC code . . . . . 106

4.5 BER performance for $255 \times 175$ LDPC code . . . . . 107

4.6 Convergence of the proposed decoder algorithm . . . . . 108

4.7 BER performance for a four-way relay system . . . . . 109

5.1 Two-way relay system (I) MAC phase of A & B transfer (II) Broadcast phase of A & B transfer . . . . . 111

5.2 Iterative decoder . . . . . 114

5.3 BER performance of the individual AB and BC decoders for $255 \times 175$ binary LDPC code . . . . . 127

5.4 BER performance of the joint decoder for $255 \times 175$ binary LDPC code . 131

# List of Abbreviations

| | |
|---|---|
| **ALLR** | average log-likelihood ratio |
| **AP** | average probability |
| **AWGN** | additive white Gaussian noise |
| **BAP** | bit-wise average probability |
| **BBP** | bit-wise best probability |
| **BER** | bit error rate |
| **BF** | bit flipping |
| **BP** | belief propagation |
| **BPS** | best probability selection |
| **BPSK** | binary phase shift keying |
| **BWSP** | bit-wise weighted sum probability |
| **CND** | check node decoder |
| **EXIT** | extrinsic information transfer |
| **FER** | frame error rate |
| **FG-LDPC** | finite geometry-low density parity check |
| **GF** | Galois field |
| **IoT** | internet of things |
| **JCPNC** | joint channel-physical layer network coding |
| **JCNC** | joint channel-network coding |
| **LDPC** | low density parity check codes |
| **LLR** | log-likelihood ratio |
| **MAC** | medium access control |
| **MIMO** | multiple input-multiple output |

| | |
|---|---|
| **MPSK** | M-ary phase shift keying |
| **MVA** | multiple-vote symbol flipping algorithm |
| **MVPSF** | multiple-vote parallel symbol flipping |
| **NOMA** | non-orthogonal multiple access |
| **PNC** | physical layer network coding |
| **PSF** | parallel symbol flipping |
| **QAM** | quadrature amplitude modulation |
| **QPSK** | quadrature phase shift keying |
| **RA** | repeat accumulate |
| **RBA** | reliability-based symbol value selection algorithm |
| **SNR** | signal power to noise power ratio |
| **UAV** | unmanned aerial vehicle |
| **VND** | variable node decoder |
| **WSN** | wireless sensor network |
| **WSP** | weighted sum probability |

# Chapter 1

# Introduction

Today's high demand for high speed data communication over the wireless channels has generated new spectral efficient communication requirements. Communicating high volumes of data through limited capacity channels with minimum amount of errors, introduces the need for efficient source coding for signal compression and channel coding for error correction [1, 2]. At the same time, Network coding has attracted a high recent research interest as another way of achieving spectral efficiency in wireless relay channels [3–7].

In this introductory chapter, first the basic communication process over a wireless relay channel is introduced. Second, a description of the different network coding approaches will be followed by an introduction to channel coding and the joint channel-network coding (JCNC). Moreover, the chapter presents the existing algorithms for joint channel-network coding in different relay network typologies and with different channel coding

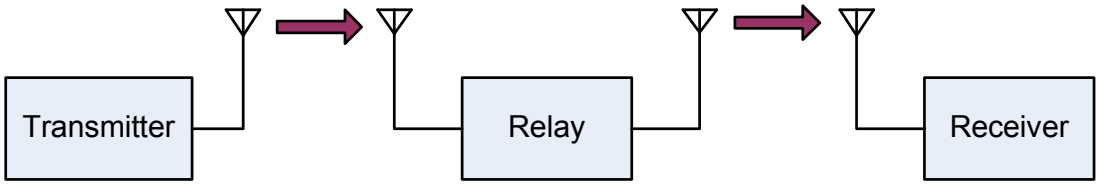


Figure 1.1: A wireless relay system

types.

## 1.1 An Overview of the Wireless Relay Channel

Radio waves are a kind of electromagnetic radiation which looses power while traveling over distances. In addition to that, at the receiver's antenna, noise is added to the received signal. It is of the highest importance to have an acceptable signal to noise power ratio (SNR) at the receiver to achieve a successful detection of the original message. However, at a certain distance from the transmitter the received signal power to noise ratio reaches a threshold beyond which successful detection is not possible. Hence, whenever the transmitter and the receiver are separated by a distance larger than this maximum distance, additional measures must be taken to improve the receiver SNR. Although the received signal power can be increased by increasing the transmit power, the power constraints at the transmitter limits the possibility of this solution. Therefore, in order to have an acceptable SNR at the receiver, an alternative technology is preferred.

One of the widely deployed such alternatives is the use of relays (Fig.1.1). Relays are placed in-between the transmitter and the receiver and the relays capture the signal, filter noise, amplify the message signal and then re-transmit. This amplified and re-transmitted signal is received by the receiver. Although the simple relays follow an amplify and forward (repeat) approach, an advanced version called *re-generators* performs detection, additional processing followed by re-modulation before the re-transmitting. Apart from the range improvement introduced above, relays can also form duplicate channels, which can combat fading.

Meanwhile, in most of the communication systems such as wireless sensor networks and cellular mobile systems, bidirectional communication is required and duplex channels are preferred. However, having full duplex bidirectional channels requires time, space, code or frequency division duplexing to eliminate the interferences between bidirectional communications. In relay systems too bidirectional relaying is very common and a duplexing method is required to isolate the two channels (Fig. 1.2).

## 1.2 Introduction to Network Coding

In relay-based communication systems, network coding was introduced as a method of combining two digital bit streams at a relay in order to achieve a compression [3]. Thereby, a considerable spectral efficiency can be obtained compared to the conventional relay channels. The application of network coding can be in many network topologies

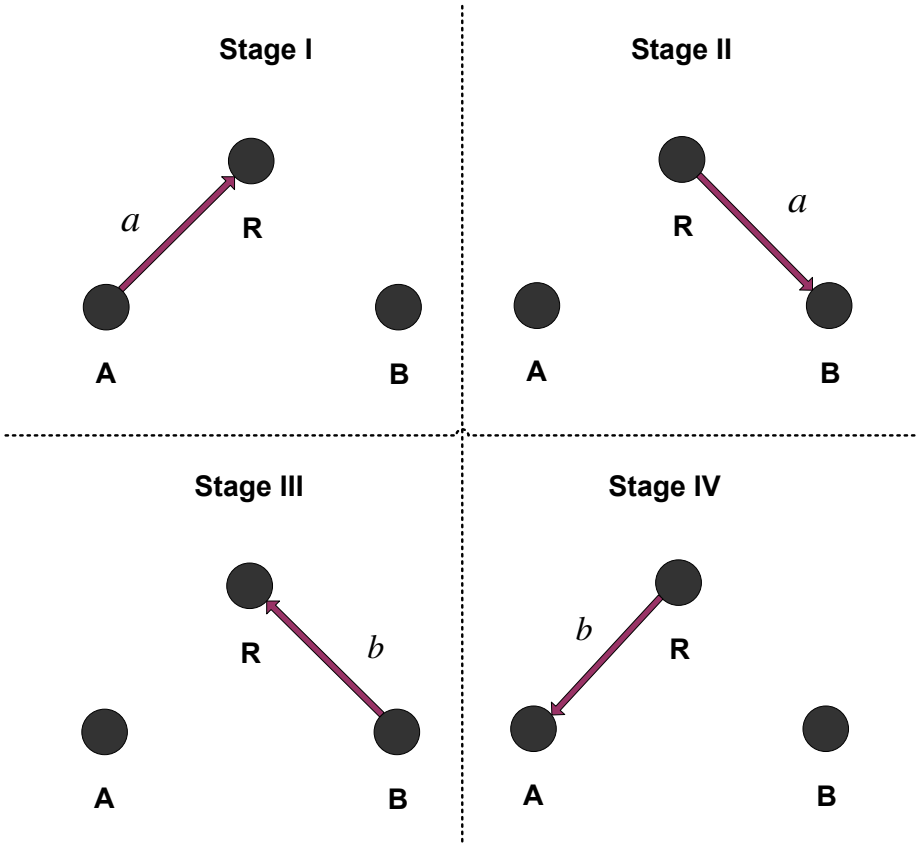


Figure 1.2: Bidirectional relaying between nodes A and B with a single relay

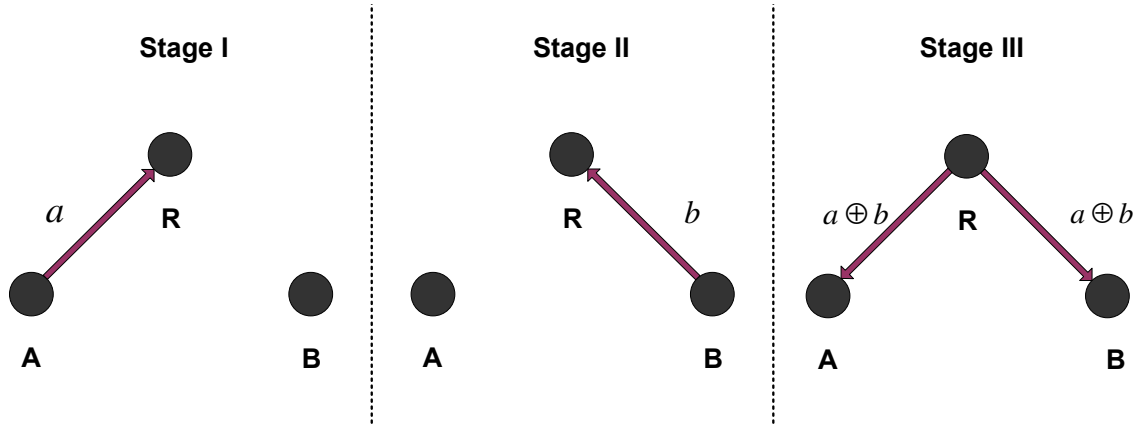


Figure 1.3: Network coding in a bidirectional relay system

whereas one of its main application areas is the bidirectional relay channel.

Let A and B be two nodes, which have to share their information via a relay R as shown in (Fig. 1.3). Note that the relay has been deployed to overcome the communication limitation created by the distance between A and B.

For simplicity let's assume Binary Phase Shift Keying (BPSK) modulation. First, node A modulates and transmits its data bit ($a$) within the first time-slot which is received by the relay. Then, node B transmits its modulated data bit ($b$) within the second time-slot, again received by the relay. After receiving both these signals, the relay detects the individual bits and combines them with $XOR$ operation. During the third time-slot, the combined bit ($a \oplus b$) is being modulated and broadcasted, and is received by both nodes A and B. At A, since $a$ is its own information, $a$ is known. Hence, $a \oplus (a \oplus b)$ will result in $b$. Similarly at node B, $a$ can be calculated by performing $b \oplus (a \oplus b)$. It is noteworthy that the time-slot requirement for this bit exchange is three

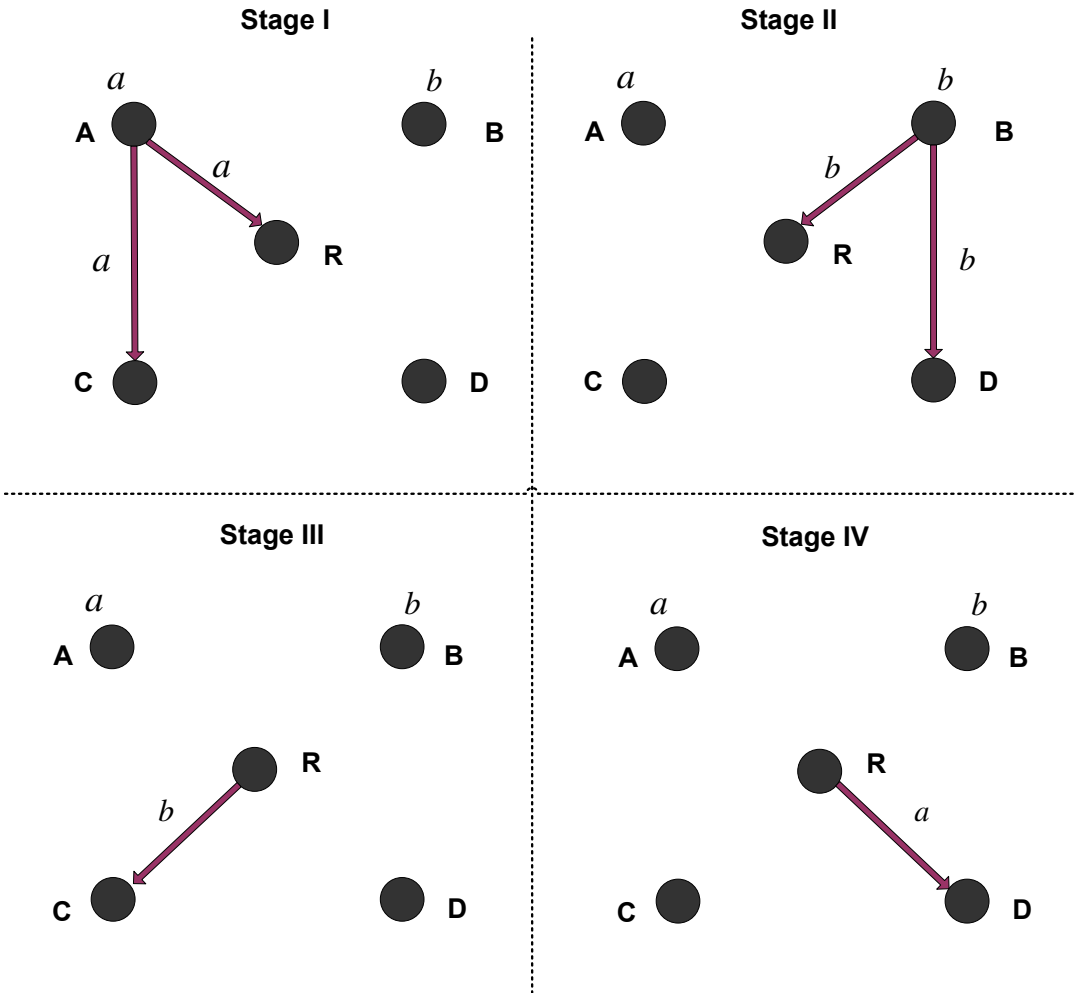


Figure 1.4: Conventional relaying in the butterfly relay network

compared to four time-slots in conventional bidirectional relaying as in Fig. 1.2. The reduced time-slot requirement enhances the spectral efficiency of the communication by 33%.

Another common relay network configuration is the *butterfly* network, where two transmitters communicate their information to two receivers via a single relay as shown in Fig. 1.4. Note that nodes C and D are out of the ranges of nodes B and A, respectively.

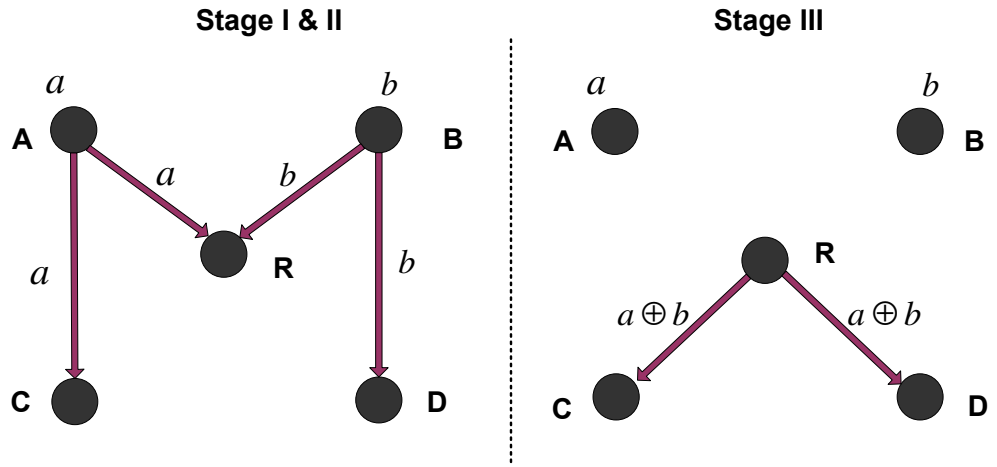


Figure 1.5: Network coding in the butterfly relay network

During the first two time-slots, nodes A and B transmit their information bits ($a$ and $b$), which is received by R and C, and R and D, respectively. In a conventional non-network coded situation, the relay may use two more time-slots to transfer $a$ and $b$ bits to nodes C and D. However, with network coding, the received bits at the relay are recombined to form $a \oplus b$ and the combined bit is broadcasted during the third time-slot as shown in Fig.1.5. Upon receiving the XORed values, the nodes C and D can resolve both $a$ and $b$ individually, which will result in an enhanced spectral efficiency compared to conventional relaying.

## 1.3 Physical Layer Network Coding

In the aforementioned network coding schemes, two time-slots are required to convey the two bits of the two communicating nodes to the relay (we name this phase as the

*"relay phase"*). One more time-slot is required for the *"broadcast phase"* where the relay broadcasts the combined bit.

If the modulated symbols $s_a$ and $s_b$ corresponding to bits $a$ and $b$ are transmitted simultaneously using the same frequency channel, an overlapped signal appears at the relay. It is shown that this received overlapped signal can be uniquely mapped to the binary $XOR$ combined bit $a \oplus b$ [8].

For example, consider a BPSK modulated scheme where the modulation mapping is such that $\{0, 1\} \rightarrow \{-1, +1\}$.

Table 1.1: Physical layer network coding symbol mapping

| a | b | $s_a$ | $s_b$ | $s_{ab} = s_a + s_b$ | $a \oplus b$ |
|---|---|---|---|---|---|
| 0 | 0 | -1 | -1 | -2 | 0 |
| 0 | 1 | -1 | +1 | 0 | 1 |
| 1 | 0 | +1 | -1 | 0 | 1 |
| 1 | 1 | +1 | +1 | +2 | 0 |

At the relay, the unique mapping scheme between the received signals constellation points $s_{ab}$ and $a \oplus b$ is shown in Table:1.1 [8]. This version of network coding is known as physical layer network coding (PNC) [9–15] and has become very popular as it requires only two time-slots for a complete bi-directional information exchange compared to four time-slots in conventional relaying. Note that PNC obtains a 100% capacity improvement compared to conventional relaying. PNC has been widely considered for many research scenarios and has been applied in many network topologies. Furthermore, in additive white Gaussian noise (AWGN) channels, a suitable detection scheme

such as maximum likelihood detection can be used to estimate,

$$\hat{s}_{ab} = arg \min_{s_{ab}} |r_{ab} - s_{ab}|, \tag{1.1}$$

where $r_{ab}$ is the received combined signal value at the relay. Thus, $a \oplus b$ can in turn be estimated from the received signal at the relay.

## 1.4 Channel Coding

In a typical wireless communication channel, there are many channel impairments such as noise, fading, shadowing, etc.. These effects introduce errors to a communicated digital bit stream. On the other hand, it is of highest importance to convey the information from transmitter to the receiver with very high reliability. In order to provide a reliable communication over the hostile wireless channel, channel coding schemes are deployed [16]. The key idea behind channel coding is to add redundant bits to the original information bit stream, which are correlated to the information bits. Hence in the presence of errors, these correlations can be used to detect and correct errors.

Channel coding can broadly be classified in to,

- Linear block codes,
- Convolutional codes.

The performance of a channel code depends on a few factors such as the code rate (ratio between the number of information bits to the number of total bits), code type and the decoding algorithms. Moreover, turbo codes [17] and low density parity check codes (LDPC) [18, 19] which can reach performances close to the well known Shannon's theoretical upper bound [20] have been popular choices in recent standard wireless communication systems. Further, Repeat accumulate (RA) codes too give an acceptable performance with reduced complexity in implementation [21].

## 1.5 Joint Channel-Network Coding

In wireless relay channels where network coding is deployed to obtain spectral efficiency, noise and other adverse effects stated above may introduce bit errors. In order to overcome the bit errors, channel coding is being deployed in such systems [22, 23]. In relay networks where PNC and linear block channel coding is employed together, joint channel decoding and network coding can be performed which utilizes the linearity property of the channel codes as follows.

Consider the same bidirectional relay scenario as in Section 1.3. Let the two individual bit streams ($\mathbf{a}$ and $\mathbf{b}$) are channel coded with the same linear block channel code to produce $\mathbf{c}_a$ and $\mathbf{c}_b$.

The linearity property states that the addition (bit wise $XOR$) of two valid codewords is also a valid codeword [2]. This implies that $\mathbf{c_a} \oplus \mathbf{c}_b$ is also a valid codeword and is

the result of encoding $\mathbf{a} \oplus \mathbf{b}$ with the same channel code. $\mathbf{c}_a \oplus \mathbf{c}_b$ can then be channel decoded using a suitable algorithm to produce $\mathbf{a} \oplus \mathbf{b}$ at the relay. Note that joint channel decoding and network coding provides higher bit error rate (BER) performances than in separately channel decoded and network coded systems [23–27].

Joint channel decoding and network coding which is commonly referred to as joint channel network coding (JCNC) is a fairly explored area in wireless sensor network (WSN) and relay based cellular systems applications. Further, most of these explorations have been extended to the algorithms using PNC which is known as joint channel physical layer network coding (JCPNC) [28–37]. Both JCNC and JCPNC approaches harness both reliability advantage of channel codes as well as the spectral efficiency advantage of network coding schemes.

## 1.6 JCPNC Algorithms for Different Network Topologies

Single hop relay topologies in practical wireless sensor and cellular networks are fourfold. They can be,

- Two-way relay channels where two nodes are exchanging their information via a single relay,
- butterfly channels where two nodes communicate their information to two receiver nodes via a single relay (Fig. 1.4),

- multi-way relay channel where multiple nodes exchange their information via a single relay

  and

- multi-relayed networks where multiple nodes transfer their information to multiple receivers via multiple relays.

In the literature, JCPNC algorithms have been considered for all of the aforementioned channels (Table 1.2). Moreover, it has been extensively employed in two-way relay channels. Application of the JCPNC algorithms to butterfly networks is also considered and is very much similar to their application in two-way relay channels. Meanwhile, for the multi-way relay channel, a JCPNC algorithm is defined as an extension of the algorithm for the two-way relay channel where only two nodes are scheduled to communicate at a time. In here, scheduling algorithms based on different schemes such as round robin scheduling, channel condition based opportunistic scheduling are used for scheduling.

Though different channel codes are deployed in different relay network topologies presented above, multi-way relay channel is paid relatively less attention (Non-existance of prior work is indicated by $\times$).

However, the multi-way relay channel is very common in WSN applications and also in latest wireless cellular systems. Meanwhile, internet of things (IoT) has attracted a huge attention recently, as a technology which can bring any information to ones' fingertips [38,39]. With this recent high interest in IoT, wireless sensor networks have come to the

forefront of today's communication [40]. Wireless sensor networks are generally relay based and the multi-way relay systems are very common in IoT applications. Wireless sensor nodes which exchange their information through a relay node deployed on a satellite, a balloon or on an unmanned aerial vehicle (UAV) is very common. Hence the JCPNC in such channels is worth a consideration.

Table 1.2: JCPNC algorithms for different channel codes

| | LDPC | Turbo Codes | RA Codes |
|---|---|---|---|
| Two-way Relay Channel | [22, 42–44] | [23, 45, 46] | [31] |
| Multi-way Relay Channel | × | × | × |
| Multi-relayed Channel | [47, 48] | × | × |

On the other hand, although the JCPNC algorithm for a multi-way relay channel of [41] provides a trade-off between the reliability and the spectral efficiency, it is worth to analyze ways of further improving the trade-off.

At the same time, though the JCPNC for the two-way relay channel has been defined for all BPSK, quadrature phase shift keying (QPSK) and quadrature amplitude modulation (QAM) modulated systems, the JCPNC for multi-way relay channel is investigated only with BPSK modulation (Table 1.3). With many of today's communication systems employing higher order modulations than BPSK in order to achieve a high spectral efficiency, JCPNC with a higher order modulation scheme is worth to be analyzed.

Table 1.3: JCPNC algorithms for different network topologies

| | BPSK | QPSK |
|---|---|---|
| Two-way Relay Channel | [42, 43] | [49] |
| Multi-way Relay Channel | [41] | × |
| Multi-relayed Channel | [47, 48] | × |

## 1.7 JCPNC Algorithms for Different Channel Coding Types

Meanwhile, different schemes of channel coding can be considered in JCNC and JCPNC deployed networks. Most of the networks use LDPC codes, turbo codes or RA codes as the channel code due to their capacity approaching performance. At the same time, the channel codes can be deployed in multiple ways in relay based systems (Table 1.4). The simplest scheme is the one considered in the Section 1.5 in which the nodes which communicate via the relay are encoding their individual bit streams with the same channel code. With the use of the linearity property of the considered channel codes, the $XOR$ combined bit stream also becomes a valid codeword which is then decoded to produce the combined bit stream. This approach had been considered with both types of codes listed above.

Another approach is to use distributed channel encoding where the separate bit streams of the nodes are separately encoded using distributed, component generator matrices and collectively decoded at the relay to produce the XORed bit stream. JCPNC with such an approach has been investigated with the use of turbo codes. However, there are

open research gaps of such distributed channel coding approaches using JCPNC with LDPC and RA codes.

Most importantly in two-way, multi-way or in multi-relayed networks, there are more than one communication channel involved. In these different channels, fading may be different whereas one channel may undergo less fading while one channel may undergo deep fading. In such scenarios, using the same channel code is really unfair and will not yield the best trade-off between the decoder complexity and reliability. Deploying a high performing (hence complex) channel code for the deep fading channel and using a simpler (hence less performing) channel code for the less fading channel can be expected to achieve a better trade-off between complexity and reliability.

Accommodating the above idea with JCNC or JCPNC has not being considered so far. Investigating the JCPNC in above unexplored scenarios is worthwhile.

Table 1.4: JCPNC algorithms for different channel coding types

| | LDPC | Turbo Codes | RA Codes |
|---|---|---|---|
| Distributed Channel Coding | [50] | [46, 51] | × |
| Same Channel Coding | [42, 43, 47, 48] | [45] | [29, 31] |
| Different Channel Coding | × | × | × |

## 1.8 Theme and Objectives of the Thesis

As already discussed in Sections 1.6 and 1.7, it is apparent that some of the practical areas in JCPNC have not been investigated so far. This study focuses on these unexplored

areas. The main objective of this research is to develop improved JCPNC algorithms for multi-node wireless relay systems communicating via a single relay.

The specific objectives of this research can be summarized as follows.

1. To develop an improved, scalable joint channel-network coding algorithm to be employed at the relay of multi-way wireless relay systems.

2. To improve the above algorithm in 1. and develop a JCPNC-based receiver algorithm for multi-way relay systems using higher order modulation schemes such as QPSK.

3. To develop a reduced complexity joint decoding algorithm to be used in multi-way wireless relay systems.

4. To develop a receiver algorithm for JCPNC-based multi-way relay systems using distributed channel codes.

5. To develop a receiver algorithm for JCPNC-based multi-way relay systems with unequal channel codes deployed in different channels.

6. To analyze the algorithm developed in 1. using extrinsic information transfer (EXIT) characteristics.

## 1.9 Outline of the Thesis

The rest of the thesis is organized as follows.

- Chapter 2 presents a joint channel decoding and network coding algorithm to be employed at relay node of the multi-way wireless relay systems which harnesses the diversity introduced due to the transmission of some nodes' information bits twice. Multiple techniques of diversity combining are also derived. The algorithm is first presented for BPSK modulated systems and then generalized for $M$-ary phase shift keying (MPSK) modulated relay systems. Superior BER performance of the proposed algorithms over the JCPNC algorithms in which the diversity is not harnessed are verified via simulations. Moreover, the complexities of the proposed algorithms are also investigated.

- Chapter 3 presents a novel low-complexity decoding algorithm for non-binary LDPC codes whose key element is a novel flipped symbol value selection step. This algorithm is then utilized to produce a low complexity JCPNC algorithm for the multi-way wireless relay channel in which diversity information is used to improve the error performance. Complexities of the proposed algorithms are compared with those of the existing algorithms.

- Chapter 4 presents a variant of the proposed joint channel decoding and network coding algorithm, which operates with asymmetric, distributed channel codes employed at different constituent channels of the multi-way relay system. However, in here too the diversity information exchange takes place. BER performance and the spectral efficiency of the proposed algorithm is investigated.

- EXIT chart based convergence analysis has been widely used in iterative decoder algorithm analysis. Chapter 5 analyses proposed iterative joint channel decoding and network coding algorithm using EXIT characteristics.

- Finally, Chapter 6 concludes the thesis highlighting several possible future research avenues.

## 1.10 Scope and Limitations of the Study

Scope of this study is centered around developing novel receiver algorithms for the relay of a multi-way wireless relay system. Due to the time and the complexity constraints, the study was limited in certain aspects which can be listed as follows.

- The channels between the nodes and the relay were assumed to be quasi-static block Rayleigh fading, where channel is static for the duration of a block of bits. However, the practical channels can be varying even within the duration of a block of bits.

- Channel state information was assumed to be fully available at all nodes participating in the communication, whereas full channel state information may not be available in a practical situation.

- Due to prohibitively high complexity, only the JCPNC algorithm for the BPSK modulated systems was analyzed using EXIT characteristics.

# Chapter 2

# Proposed Joint Channel-Network Coding Algorithm for Multi-way Relay Systems

## 2.1 Introduction

Among wireless relay systems, multi-way relay systems in which multiple nodes exchange their information via a single relay, whose applications range from wireless sensor networks to wireless teleconferencing networks have drawn considerable attention. In the literature, many attempts have been made to adopt PNC in multi-way relay systems [52–55]. Among them, use of joint network-superposition coding [52] and deploying multiple input-multiple output (MIMO) antenna arrays [53,54] have been two very pop-

ular techniques to exchange bit streams from multiple communicating nodes spending a small number of time-slots. In all these approaches, all the nodes who participate in the information exchange transmit at the same time during the MAC phase. Thereafter, the relay node detects the individual participating nodes' bits using this received combined signal. Thus, the errors introduced due to a poor quality channel between the relay node and any of the nodes may cause errors in the detection of information bit sequences of other nodes. As a remedy to this problem, a multi-node information exchange scheme based on opportunistic scheduling was proposed in [56]. Of [56], the main idea is pair-wise communication during MAC phase and channel-condition based communicating node pair selection. At a time, a pair of nodes communicates and exchanges information as in a simple two-way relay channel. Moreover, nodes associated with relatively fair quality channels are scheduled for communication in a manner so that pairs formed are overlapping. Apart from that, in order to make sure a fair chance is given to the nodes associated with deep fading channels, a fair scheduling scheme is also incorporated to the node pair scheduling algorithm. In this chapter, it is first shown that the minimum number of time-slots required to exchange the total information set from $\mathcal{M}$ nodes using a pairwise relaying approach is $2(\mathcal{M}-1)$.

Moreover, in a multi-way relay channel where a pair-wise information exchange is carried out as in [56], channel coding can be employed and a joint channel network coding process provides an improved decoding performance.

With the node pairs selected for communication are overlapping, the same informa-

tion from some nodes is transmitted twice under two different channel conditions. This multiple transmission of same information can be exploited to obtain a diversity gain. However, the existing joint channel-network coding algorithms as in [31] is incapable of exploiting this additional diversity. Hence, this chapter presents a joint channel network coding algorithm in which a joint decoding is performed on bit blocks belonging to different pairs of nodes with the decoders corresponding to different pairs of nodes exchanging soft information corresponding to nodes transmitting twice, between them. Furthermore, a number of schemes of soft information exchange between parallely operating decoders are proposed. For simplicity, the proposed joint channel-network coding algorithm is first developed and presented for a three-way relay channel. Then the same is extended to a $\mathcal{M}$-way relay system $\{\mathcal{M} > 3\}$.

The rest of the chapter is organized as follows. Section 2.2 presents the system model and Section 2.3 introduces the proposed joint decoding algorithm under BPSK modulation. Then in Section 2.4, we extend the proposed algorithm to MPSK modulated systems. In Section 2.5, a set of numerical results and a discussion is included and Section 2.6 concludes the chapter.

## 2.2 System Model

In this chapter a three-way relay system is considered in which A, B and C nodes exchange their information via a relay R as shown in Fig.2.1 [41]. To present the

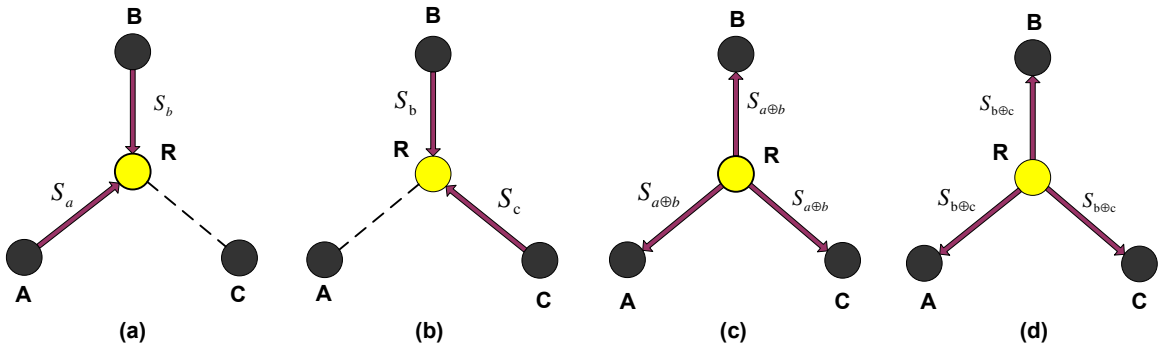


Figure 2.1: Three-way relay system (a) MAC phase of A & B transfer (b) MAC phase of B & C transfer (c) Broadcast phase of A & B transfer (d) Broadcast phase of B & C transfer

proposed algorithm, let us assume that the channel pair selection algorithm in [41] first selects A and B nodes to transmit their bit sequences and then B and C nodes to transmit their bit sequences. All three communicating nodes encode their bit vectors $\mathbf{x}_a, \mathbf{x}_b$ and $\mathbf{x}_c$ using the same $(n-\kappa)\times n$ binary LDPC channel code and produce three symbol vectors $\mathbf{c}_a, \mathbf{c}_b$ and $\mathbf{c}_c$ of $n$ code bits in each. The channel coded bit streams are then modulated and transmitted in pairs as in [41]. In this chapter, let us initially consider BPSK modulation due to its simplicity. Considering the discrete-time base band equivalent of the wireless relay system, let the modulation signal constellation be $\{-1, 1\}$. Thus the modulator maps the $n$-bit channel encoder output sequences $\mathbf{c}_\alpha \in \{0,1\}^n$, $\alpha = a, b, c$ to the $n$ dimensional symbol vectors $\mathbf{s}_\alpha = [s_\alpha(1), \ldots, s_\alpha(n)]$, where $s_\alpha(j) \in \{-1, 1\}$ for $j \in [1, n]$.

During the first $n$ bit-intervals, A and B transmit their $n$ bit information vectors $\mathbf{s}_a$ and $\mathbf{s}_b$ simultaneously. Hence, the relay receives an overlapped version of the two signal vectors

which is denoted by the $\mathbf{y}_{ab}$. Note that the algorithm in [41] performs detection, joint channel decoding - network coding on this received signal vector and then broadcasts the XOR bit combination vector. Unlike the algorithm in [41], in here, during the next $n$ bit-intervals nodes B and C transmit their information bit vectors $\mathbf{s}_b$ and $\mathbf{s}_c$. These signals are also received as an overlapped signal and let us denote the same as $\mathbf{y}_{bc}$. Corresponding to the $j$-th bit of each codeword

$$y_{ab}(j) = h_{A1}(j)s_a(j) + h_{B1}(j)s_b(j) + n_{ab1}(j) \quad (2.1)$$

$$y_{bc}(j) = h_{B2}(j)s_b(j) + h_{C2}(j)s_c(j) + n_{bc2}(j). \quad (2.2)$$

Here, $h_{A1}, \{h_{B1}, h_{B2}\}$ and $h_{C2}$ are complex channel coefficients of quasi-static block fading A-R, B-R and C-R channels respectively. Furthermore, $n_{ab1}(j)$, $n_{bc2}(j)$ represents the complex additive white Gaussian noise (AWGN) samples having zero mean and variance $\sigma^2$ per real dimension added during AB and BC nodes' communications. Let us omit the bit index $j$ for the sake of simplicity. Furthermore, let us assume that the full channel state information is available at the relay. If $y_{ab}$ and $y_{bc}$ are detected without errors, they can be uniquely mapped to $c_a \oplus c_b$ and $c_b \oplus c_c$ at the relay. The detected XOR bit vectors are then separately channel coded using the same channel code, modulated and then transmitted as a broadcast to all three nodes. Upon receiving the broadcast, the nodes detect and channel decode for $c_a \oplus c_b$ and $c_b \oplus c_c$. This broadcasting scheme consumes two bit-intervals per each bit. At node B, using the knowledge of its own

information $c_b$, $c_b \oplus (c_a \oplus c_b)$ and $c_b \oplus (c_b \oplus c_c)$ can calculate $c_a$ and $c_c$ respectively. At node A, using the knowledge of its own information $c_a$, $c_a \oplus (c_a \oplus c_b)$ and $[c_a \oplus (c_a \oplus c_b)] \oplus (c_b \oplus c_c)$ can calculate $c_b$ and $c_c$ respectively. Similarly at node C, $c_c \oplus (c_b \oplus c_c)$ and $[c_c \oplus (c_b \oplus c_c)] \oplus (c_a \oplus c_b)$ can calculate $c_b$ and $c_a$ respectively.

***Lemma 1.*** The minimum number of time-slots required for a complete information exchange in a $\mathcal{M}$-way relay system, $2(\mathcal{M} - 1)$.

*Proof:*

- Let the vertices and edges in a graph represent the multi-way relay system's nodes and the simultaneously communicating node pairs, respectively.
- A fully connected, cycle free graph (i.e. a tree) is required to have a complete information exchange.
- By definition, a tree with $\mathcal{M}$ vertices consists of $(\mathcal{M} - 1)$ edges. Thus, a full information exchange requires at least $(\mathcal{M} - 1)$ communications.
- In physical layer network coding, each bidirectional communication consumes 2 time-slots.
- Thus, for an $\mathcal{M}$-way system we need $2(\mathcal{M} - 1)$ time-slots for the complete information exchange.

## 2.3 Joint Decoding at the Relay

In this thesis, the main interest is in channel decoding and network coding at the end of the medium access control phase. Joint channel decoding-network coding can be performed using $y_{ab}$ and $y_{bc}$ received values as in [41] exploiting the linearity of the channel code.

As stated in Section 2.1, node B's information is transmitted twice under two different channel conditions. Moreover, in the two decoders, $c_b$ information is decoded separately associated with two different pieces of information $c_a$ and $c_c$. This time diversity can be exploited to improve the detection of $c_b$ bit information at the relay. However, in a conventional detection scheme where $c_a \oplus c_b$ and $c_b \oplus c_c$ are detected independently, this diversity is totally neglected. This section proposes a joint decoding scheme in which the aforementioned time-diversity of $c_b$ is considered and utilized to improve the performance at the relay. The diversity exploitation is performed by exchanging information between different decoders as shown in Fig. 2.2. However, the key challenge in this approach is the absence of $c_b$ information explicitly for the exchange as the decoding is done for $c_a \oplus c_b$ and $c_b \oplus c_c$.

### 2.3.1 Separating $c_b$ information at the relay

In a conventional PNC communication, $y_{ab}$ is mapped to $c_a \oplus c_b$ using $Pr\left(s_{ab}|y_{ab}\right)$ during the medium access control phase of A and B nodes' information exchange. Alternatively, [42] proposes a novel belief propagation based joint LDPC decoding and

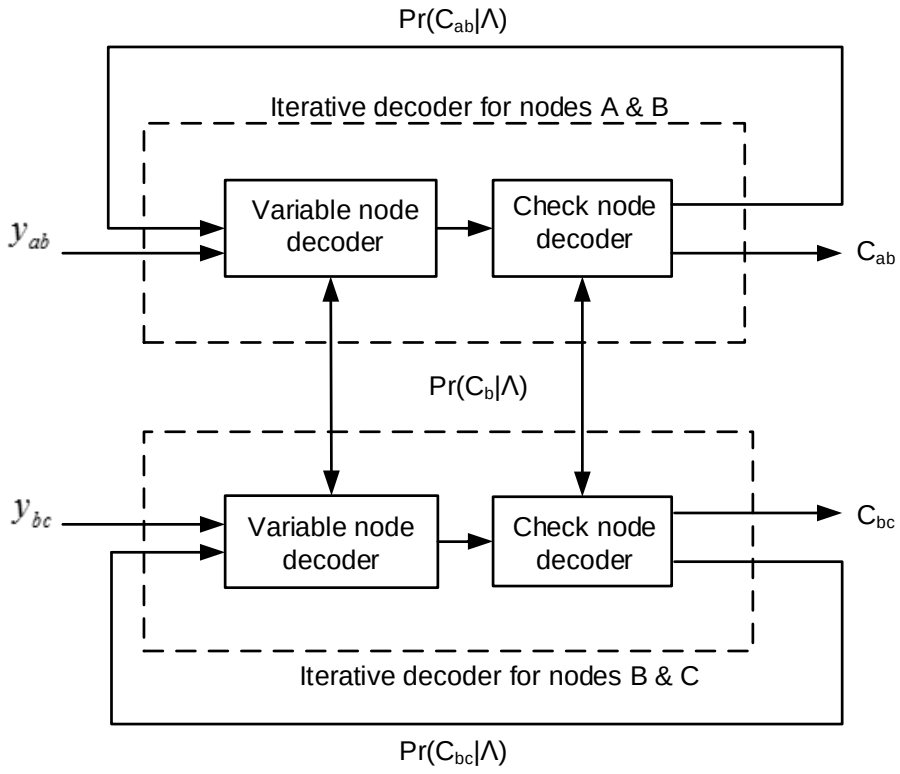


Figure 2.2: Proposed joint channel decoder-network encoder

network coding algorithm which exploits the difference in the channel coefficients to calculate $Pr\left(c_{ab}=\mathcal{C}_0|y_{ab}\right), Pr\left(c_{ab}=\mathcal{C}_1|y_{ab}\right), Pr\left(c_{ab}=\mathcal{C}_2|y_{ab}\right)$ and $Pr\left(c_{ab}=\mathcal{C}_3|y_{ab}\right)$ where $\mathcal{C}_i$, $i=0,\ldots,3$ are as given in Table 2.1.

Moreover, at the end of each iteration, this algorithm calculates four separate probabilities $p_0 = Pr\left(c_{ab}=\mathcal{C}_0|\Lambda\right)$, $p_1 = Pr\left(c_{ab}=\mathcal{C}_1|\Lambda\right)$, $p_2 = Pr\left(c_{ab}=\mathcal{C}_2|\Lambda\right)$ and $p_3 = Pr\left(c_{ab}=\mathcal{C}_3|\Lambda\right)$, compared to two XOR bit's complementary probabilities in a conventional LDPC channel decoder. Here, $\Lambda$ refers to the priori information resulted from the previous iteration. The proposed joint decoder algorithm makes use of the same iterative algorithm in [42], Hence, $Pr(c_b|\Lambda)$ can be explicitly calculated at the end of

Table 2.1: PNC symbol mapping for BPSK modulation

| $c_{ab}$ | $s_a$ | $s_b$ | $s_{ab}$ |
|---|---|---|---|
| $\mathcal{C}_0$ | $-1$ | $-1$ | $-h_A - h_B$ |
| $\mathcal{C}_1$ | $-1$ | $+1$ | $-h_A + h_B$ |
| $\mathcal{C}_2$ | $+1$ | $-1$ | $h_A - h_B$ |
| $\mathcal{C}_3$ | $+1$ | $+1$ | $h_A + h_B$ |

each iteration as,

$$\begin{aligned} Pr(c_a = 1|\Lambda) &= p_2 + p_3 \\ Pr(c_a = 0|\Lambda) &= p_0 + p_1 \\ Pr(c_b = 1|\Lambda) &= p_1 + p_3 \\ Pr(c_b = 0|\Lambda) &= p_0 + p_2. \end{aligned} \tag{2.3}$$

Similarly, by performing joint LDPC decoding and PNC coding on $y_{bc}$, $Pr(c_b = 1|\Lambda), Pr(c_b = 0|\Lambda), Pr(c_c = 1|\Lambda)$ and $Pr(c_c = 0|\Lambda)$ can also be calculated.

### 2.3.2 Exchanging $c_b$ information between $c_a \oplus c_b$ and $c_b \oplus c_c$ decoders

The key contribution of this research is the exchange of information between separate decoders. For calculating a new $c_b$ probability at the end of each iteration after exchanging the $c_b$ information between the two decoders, three schemes are proposed.

*Average Probability (AP):*

The new probability value of $c_b$ is calculated by averaging the two $c_b$ probability information from the two decoders.

$$Pr(c_b = 1|\Lambda) = \frac{(Pr_{ab}(c_b=1|\Lambda)+Pr_{bc}(c_b=1|\Lambda))}{2}$$
$$Pr(c_b = 0|\Lambda) = \frac{(Pr_{ab}(c_b=0|\Lambda)+Pr_{bc}(c_b=0|\Lambda))}{2}.$$

This new $c_b$ probability value is then used in the two $c_a \oplus c_b$ and $c_b \oplus c_c$ decoders.

*Best Probability Selection (BPS):*

$|LLR_\mu(c_b|\Lambda)| = \left|\log\left(\frac{Pr_\mu(c_b=1|\Lambda)}{Pr_\mu(c_b=0|\Lambda)}\right)\right|$, $\mu \in \{ab, bc\}$ is a very good measure of the reliability of the calculated probability.

Then the new probability value for $c_b$ is calculated as,

$$[Pr(c_b = 0|\Lambda), Pr(c_b = 1|\Lambda)] = \begin{cases} [Pr_{ab}(c_b = 0|\Lambda), Pr_{ab}(c_b = 1|\Lambda)] & \text{if } |LLR_{ab}(c_b|\Lambda)| \geq |LLR_{bc}(c_b|\Lambda)| \\ [Pr_{bc}(c_b = 0|\Lambda), Pr_{bc}(c_b = 1|\Lambda)] & \text{Otherwise.} \end{cases} \tag{2.4}$$

The $c_b$ bit's probability value with the lower reliability is replaced with the high reliable probability value available at the other decoder. It is noteworthy that this scheme is resembling the popular *selection combining* [57].

*Average Log-likelihood-ratio (ALLR):*

Main drawback of the above BPS scheme is that the information transfer is unidirectional. Thus, only one of the decoders' $c_b$ bit information is updated during an iteration

which results in a performance degradation. On the other hand, a bidirectional information transfer can yield a better overall performance. Note that *maximal ratio combining* [57,58] is a very popular diversity combining technique in which the different copies of the same signal received separately are weighted averaged to form a combined signal. This combining method can be utilized to combine the two probabilities in the joint decoder such that a bidirectional information transfer occurs. Under the channel condition having a fading coefficient of $h_B$, AWGN with zero mean and variance $\sigma^2$ and BPSK modulation

$$LLR(c_b|\Lambda) = \log \frac{P(c_b = 1|\Lambda)}{P(c_b = 0|\Lambda)} = \log \frac{e^{-\frac{(y-h_B)^2}{2\sigma^2}}}{e^{-\frac{(y+h_B)^2}{2\sigma^2}}} = \frac{2}{\sigma^2} y h_B, \tag{2.5}$$

where received value is represented by $y$. Consider the maximal ratio combined signal $y = h_{B1}y_{B1} + h_{B2}y_{B2}$, where $h_{B2}, h_{B2}, y_{B1}, y_{B2}$ correspond to two diversity paths participating in the combining. Since $y_{B1}$ and $y_{B2}$ are both Gaussian random variables $y$ too becomes a Gaussian random variable. Therefore $\sigma_y^2 = (h_{B1}^2 + h_{B2}^2)\,\sigma^2$. Furthermore,

$$\begin{aligned} LLR_y(c_b|\Lambda) &= \frac{2}{\sigma_y^2} y h_B \\ &= \frac{\kappa}{\sigma^2}(h_{B1}y_{B1} + h_{B2}y_{B2}) \\ &= \kappa \frac{[LLR_{ab}(c_b|\Lambda) + LLR_{bc}(c_b|\Lambda)]}{2}, \end{aligned} \tag{2.6}$$

where $\kappa = \frac{h_{B1}+h_{B2}}{h_{B1}^2+h_{B2}^2}$. Hence, weighted combining of the received values $y$ is equivalent to averaging of $LLR(c_b|\Lambda)$ of the two available copies of $c_b$ information. Thus the combined LLR is given by,

$$LLR(c_b|\Lambda) = \frac{1}{2}\left(\frac{h_{B1}+h_{B2}}{h_{B1}^2+h_{B2}^2}\right)\left[LLR_{ab}(c_b|\Lambda) + LLR_{bc}(c_b|\Lambda)\right]. \tag{2.7}$$

Further, $Pr(c_b = 0|\Lambda) = \frac{1}{1+e^{LLR(c_b|\Lambda)}}$ and $Pr(c_b = 1|\Lambda) = \frac{e^{LLR(c_b|\Lambda)}}{1+e^{LLR(c_b|\Lambda)}}$ can calculate b's probability information following the information exchange.

### 2.3.3 Re-calculation of Joint Probabilities

After the information exchange, probabilities $\{p_0, \ldots, p_3\}$ can be recalculated as

$$\begin{aligned} p_0 &= Pr(c_a = 0|\Lambda)Pr(c_b = 0|\Lambda) \\ p_1 &= Pr(c_a = 0|\Lambda)Pr(c_b = 1|\Lambda) \\ p_2 &= Pr(c_a = 1|\Lambda)Pr(c_b = 0|\Lambda) \\ p_3 &= Pr(c_a = 1|\Lambda)Pr(c_b = 1|\Lambda). \end{aligned} \tag{2.8}$$

Also the probabilities $\{p_0, p_1, p_2, p_3\}$ at the decoder for $c_{bc}$ can too be calculated. During the next iteration, the calculated joint probability information are utilized in the two LDPC decoders.

## 2.4 Extending the Joint Decoding Algorithm to MPSK Modulated Muti-way Relay Systems

The algorithm presented so far is limited to BPSK modulated multi-way relay systems. However, almost all of the today's communication systems deploy higher order modulation schemes in seek of a high spectral efficiency, in which multiple bits of information are encapsulated in to a single symbol. To cater for such systems, this section proposes an extension of the joint decoder algorithm for a multi-way wireless relay system employing MPSK modulation.

### 2.4.1 New System Model

Following two different communication models are considered in the development of the proposed joint decoder algorithm.

#### Model I

Let $m = \log_2(M)$ where $m \in \mathbb{Z}^+$. The information bit stream at a node is separated to $m$ sub-streams such that first bit is in sub-stream 1, second bit is in sub-stream 2,..., $(m+1)$-th bit is again in sub-stream 1. All nodes block their bit sub-streams to sets of sub-vectors which are then encoded using the same $(n-\kappa) \times n$ binary LDPC channel code. Thereafter, groups of $m$ code bits are formed by taking bit values at the same bit position in each resultant binary codeword. A MPSK modulation scheme is used to

modulate the vectors having such groups of $m$ bits. The modulation results in a $M$-ary symbol vector. Finally, the scheme in Fig. 2.1 is employed to transmit three such $n$ dimensional symbol vectors at nodes A, B and C.

**Model II**

In Model II, we consider the consecutive $m$ bits together to form $m$ bit groups. Each group of $m$ bits is mapped to a GF($M = 2^m$) symbol and the resultant Galois Field (GF) symbol stream GF($M$) at each node is encoded with a $(n - \kappa) \times n$ non-binary LDPC channel code in GF($M$). Thereafter, three $M$-ary symbol vectors are formed by modulating each GF($M$) non-binary code symbol using a MPSK modulation scheme. The modulator output symbols are transmitted as in Fig. 2.1.

Let the base band discrete-time modulation signal constellation be $e^{j\frac{2\pi}{M}\gamma}$, where $\gamma = \{0, \ldots, M-1\}$. Hence the modulators map the three $n$-symbol GF($M$) codewords $\mathbf{c}_a$, $\mathbf{c}_b$ and $\mathbf{c}_c$ to the $n-$dimensional MPSK symbol vectors $\mathbf{s}_a = \{s_a(1), s_a(2), \ldots, s_a(n)\}$, $\mathbf{s}_b = \{s_b(1), \ldots, s_b(n)\}$ and $\mathbf{s}_c = \{s_c(1), s_c(2), \ldots, s_c(n)\}$.

Similar to the BPSK modulated scenario, nodes A and B transmit their individual blocks of $n$ code symbols simultaneously during $n$ symbol intervals of the first time-slot. The relay node receives the overlapped signal vector $\mathbf{y}_{ab}$ resulted from the simultaneous transmissions from nodes A and B. Let us again assume the complete channel state information to be available at the relay node. Thus, a joint channel decoding and

network coding can be carried out at the relay node as described in Section 2.4.3. After obtaining the resultant XORed symbol vectors corresponding to nodes A-B and B-C communications over the first two time-slots, they are again channel coded using the same $(n - \kappa) \times n$ channel code, modulated with the same MPSK modulation scheme and broadcasted by the relay during next two time-slots of $n$ symbol intervals each. This communication scheme can provide the complete information set to all nodes in the relay system.

### 2.4.2 Pair-wise Iterative Joint Decoding at the Relay

Similar to Section 2.3, in this section a joint decoder algorithm is proposed to be employed at the relay node in order to exploit the time diversity available due to the transmission of MPSK modulated information symbol vector of node B twice under two different channel conditions. The basis for the proposed algorithm is the JCPNC algorithm of [44] developed for two-way relay systems using BPSK modulation, where joint probabilities for different bit combinations are calculated at each iteration. However, the algorithm in [44] is limited to BPSK modulation. Thus, the algorithm of [44] is first extend to a MPSK modulated system.

Let us consider the first time-slot of the MAC phase during which nodes A and B transmit simultaneously.

**Initialization**

There are $M^2$ equally likely error free possible constellation points for the joint estimate at the relay node as a result of $M$-ary modulation employed at each of the two nodes A and B. These composite constellation points are given by $e^{j\frac{2\pi}{M}\gamma} + e^{j\frac{2\pi}{M}\theta}$ where $\gamma, \theta \in \{0, \ldots, M-1\}$. Thus the transmitted symbol pair $s_{ab} = \{s_a s_b\} = \Upsilon(i)$, $i \in \{0, \ldots, M^2-1\}$ has a-priori probability,

$$Pr\left\{s_{ab} = \Upsilon(i)\right\} = \frac{1}{M^2} \tag{2.9}$$

where $\Upsilon(i)$ is a base band equivalent MPSK symbol pair combination. The conditional probability of received signal $y_{ab}$ given an $i$-th symbol pair being transmitted is,

$$Pr\{y_{ab}\,|s_{ab} = \Upsilon(i)\} = \frac{1}{2\pi\sigma^2} exp - \left(\frac{\|y_{ab} - \Upsilon(i)\|^2}{2\sigma^2}\right). \tag{2.10}$$

Thus, the conditional a-posteriori probability that signal $\Upsilon(i)$ was transmitted given the received signal $y_{ab}$ is,

$$\begin{aligned} p_i &= Pr\{s_{ab} = \Upsilon(i)\,|y_{ab}\} \\ &= Pr\{y_{ab}\,|s_{ab} = \Upsilon(i)\} \times \frac{Pr(s_{ab} = \Upsilon(i))}{Pr(y_{ab})} \\ &= Pr\{y_{ab}\,|s_{ab} = \Upsilon(i)\} \times C \end{aligned} \tag{2.11}$$

where $C = \frac{1}{M^2 Pr(y_{ab})}$ is a constant. Note that the property $\sum_{\forall i} p_i = 1$ can be used to calculate $C$.

**Variable node to check node message**

Let us consider an equivalent Tanner graph representation of the LDPC code [16]. Then the joint decoding process performs an iterative message passing between the check nodes and the variable nodes in the Tanner graph. The same message passing scheme of [44] is used here, in which the initial value vector of the passed messages are selected to be the set of probabilities $\mathbf{p} = \{p_0, p_1, \ldots, p_{M^2-1}\}$ in (2.11). Let VAR and CHK represents the messages passed from the variable nodes and check nodes, respectively. Consider a degree three variable node and $\mathbf{p} = \{p_0, p_1, \ldots, p_{M^2-1}\}$ and $\mathbf{q} = \{q_0, q_1, \ldots, q_{M^2-1}\}$ be the $M^2$ dimensional probability message vectors received from two of the connected check nodes. Then $\text{VAR}(\mathbf{p}, \mathbf{q}) = \{r_0, r_1, \ldots, r_{M^2-1}\}$ represents the message passed to the other check node. Here, $r_i = Pr\{c_{ab}(j) = \zeta(i) \,|\mathbf{p}, \mathbf{q}\}$ with $c_{ab}(j)$ and $\zeta(i)$ refers to the $j$-th channel encoder output symbol and the $i$-th channel encoder output realization value, respectively.

$$\begin{aligned} r_i &= \frac{Pr\{\mathbf{p}, \mathbf{q} \,|c_{ab}(j) = \zeta(i)\} Pr\{c_{ab}(j) = \zeta(i)\}}{Pr(\mathbf{p}, \mathbf{q})} \\ &= \frac{Pr\{c_{ab}(j) = \zeta(i) \,|\mathbf{p}\} Pr\{c_{ab}(j) = \zeta(i) \,|\mathbf{q}\} Pr(\mathbf{p}) Pr(\mathbf{q})}{Pr\{c_{ab}(j) = \zeta(i)\} Pr(\mathbf{p}, \mathbf{q})} \\ &= \beta p_i q_i. \end{aligned} \tag{2.12}$$

Here $\beta = \frac{Pr(\mathbf{p})Pr(\mathbf{q})}{Pr\{c_{ab}(j)=\zeta(i)\}Pr(\mathbf{p},\mathbf{q})} = \frac{1}{\mathbf{p}\mathbf{q}^T}$ is a normalizing factor. Moreover, $\text{VAR}(\mathbf{p}, \mathbf{q}, \ldots) = \text{VAR}(\mathbf{p}, \text{VAR}(\mathbf{q}, \text{VAR}(\ldots)))$ can be used to calculate the messages from variable nodes connected to more than three check nodes.

**Check node to variable node message**

Calculation of the check node to variable node message differs from one to other for the two communication models described in Sub-section 2.4.1 Thus, we present the two calculations separately as follows.

*Model I*

When the GF($M^2$) sum of the participating $M^2$-ary symbols is equal to zero, a parity check is satisfied. Let us first consider a check node having a degree three. When the probability message vectors $\mathbf{p}$ and $\mathbf{q}$ are received from two connected variable nodes $c_{ab}(\nu)$ and $c_{ab}(\mu)$, the message passed to the third variable node is $\mathrm{CHK}(\mathbf{p}, \mathbf{q}) = \{s_0, s_1, \ldots, s_{M^2-1}\}$ where,

$$\begin{aligned} s_\tau &= Pr\{c_{ab}(j) = \zeta(\tau) \,|\mathbf{p}, \mathbf{q}\} \\ &= \sum_{i=0}^{M^2-1} Pr\{c_{ab}(\nu) = \zeta(i), c_{ab}(\mu) = \zeta(\Psi_{\tau,i}) \,|\mathbf{p}, \mathbf{q}\} \\ &= \sum_{i=0}^{M^2-1} p_i q_{\Psi_{\tau,i}}. \end{aligned} \tag{2.13}$$

Here $\Psi_{\tau,i}$ is the integer converted version of $\zeta(\tau) \oplus \zeta(i)$, while $\oplus$ representing a GF($M^2$) sum.

*Model II*

Calculation of the output message is slightly different when non-binary LDPC channel coding is used. In such a case, when parity check matrix coefficient weighted addition

of participating GF($M^2$) composite symbols equals zero, a parity check equation is satisfied. Thus, the check node to variable node message passed, given the input message vectors $\mathbf{p}$ and $\mathbf{q}$ coming from the two other connected variable nodes $c_{ab}(\nu)$ and $c_{ab}(\mu)$ has the same format as (2.13). However in this case,

$$t \otimes \zeta(\Psi_{\tau,i}) = (t_\tau \otimes \zeta(\tau)) \oplus (t_i \otimes \zeta(i)) \,. \tag{2.14}$$

Here, $\otimes$ stands for a GF($M$) multiplication and $t, t_\tau, t_i$ are the corresponding non-binary parity check matrix coefficient values. With the property that $t^{M-1} = 1$ in GF($M$), we have $t^{-1} = t^{M-2}$. Hence, $\Psi_{\tau,i}$ gives the integer conversion of $t^{M-2} \otimes [(t_\tau \otimes \zeta(\tau)) \oplus (t_i \otimes \zeta(i))]$.

Moreover, the check nodes output messages when the degree is larger than three can be calculated using $\mathrm{CHK}(\mathbf{p}, \mathbf{q}, \ldots) = \mathrm{CHK}(\mathbf{p}, \mathrm{CHK}(\mathbf{q}, \mathrm{CHK}(\ldots)))$.

**Finalization**

Soft information to PNC coded symbol mapping at the end of each iteration is carried out as,

$$c_{ab}(j) \;=\; \zeta(\eta), \tag{2.15}$$

where $\eta = \arg\max_i \ p_i$ for the $j$-th symbol.

At the end of the PNC mapping, the resultant XORed codewords are checked for the satisfaction of the parity checks. The joint decoding algorithm is terminated when a given number of iterations is completed or if all the parity checkings are satisfied.

### 2.4.3 Improved Iterative Joint Decoding at the Relay

This sub-section presents the proposed iterative joint channel decoding and physical layer network coding algorithm which can harness the diversity gain present at the relay. In Sub-section 2.4.2 an extension of the algorithm of [44] was derived to determine the set of probabilities corresponding to all possible different symbol value combinations, during each iteration at each of the two decoders. Algorithm in Section 2.4.2 can be used to perform node pair-wise joint decoding in the proposed algorithm, in a way that during each iteration a $M^2$ dimensional probability vector corresponding to all the possible received value constellation points at each symbol position is calculated.

**Extracting node B information at the relay and exchanging information between parallel decoders**

Consider an arbitrary iteration. Let us denote the node pair A and B's probability value vector at symbol position $j$ to be $\mathbf{p}(j) = \{p_0(j), \ldots, p_{M^2-1}(j)\}$, $p_l(j) = Pr(c_{ab}(j) = \zeta(l)|\Lambda)$, $l \in \{0, 1, \ldots, M^2 - 1\}$ where $\Lambda$ stands for a-priori information resulting from the previous iteration.

Further, let $\zeta(l) = \{\mathcal{A}(l'), \mathcal{B}(l'')\}$, $l', l'' \in \{0, 1, \ldots, M-1\}$ where $\mathcal{A}(l')$ and $\mathcal{B}(l'')$ represent GF($M$) symbol values of nodes A and B respectively which construct $\zeta(l)$. Let $c_{b1}(j)$ represents the $j$-th symbol of node B during the first time-slot of the MAC phase. Then,

$$Pr\left(c_{b1}(j) = \mathcal{B}(l'')|\Lambda\right) = \sum_{\forall l} Pr(c_{ab}(j) = \zeta^{B(l'')}(l)|\Lambda). \tag{2.16}$$

Here, $\zeta^{B(l'')}(l)$ is a joint symbol which has $\mathcal{B}(l'')$ as a part.

Let $\mathbf{p}_{b1} = \{Pr\left(c_{b1}(j) = \mathcal{B}(0)|\Lambda\right), \ldots, Pr\left(c_{b1}(j) = \mathcal{B}(M-1)|\Lambda\right)\}$. $Pr(c_{b2}(j) = \mathcal{B}(l'')|\Lambda)$ can also be calculated at the joint decoder for node pair B and C.

Let, $\mathbf{p}_{b2} = \{Pr\left(c_{b2}(j) = \mathcal{B}(0)|\Lambda\right), \ldots, Pr\left(c_{b2}(j) = \mathcal{B}(M-1)|\Lambda\right)\}$.

Three schemes to exchange the soft information between the two parallely operating decoders are proposed.

*Average Probability (AP):*

Consider the two probability vectors $\mathbf{p}_{b1}$ and $\mathbf{p}_{b2}$ from the two decoders. New updated probability vector is calculate by element-wise averaging $\mathbf{p}_{b1}$ and $\mathbf{p}_{b2}$ and this updated information is used as the node B's symbol probability vector at the two decoders.

$$\mathbf{p}_b = \frac{1}{2}\left[\mathbf{p}_{b1} + \mathbf{p}_{b2}\right]. \tag{2.17}$$

*Best Probability (BP):*

Note that the ratio between the highest symbol value probability ($p^H$) and the next

highest symbol value probability ($p^L$) is a clear measure of the reliability of the current symbol value at that position. Thus,

$$\begin{aligned} rel(b_1) &= \left| log\left(\frac{p_{b1}^H}{p_{b1}^L}\right)\right| \\ rel(b_2) &= \left| log\left(\frac{p_{b2}^H}{p_{b2}^L}\right)\right|. \end{aligned} \tag{2.18}$$

Then the updated probability value vector for node B is selected by,

$$\mathbf{p}_b = \begin{cases} \mathbf{p}_{b1} & \text{if } rel(b_1) > rel(b_2) \\ \mathbf{p}_{b2} & \text{Otherwise} \end{cases} \tag{2.19}$$

*Weighted Sum Probability (WSP):*

Recall that in BPS approach, only one decoder's information is updated during an iteration. Thus, one of the main short-comings of the BPS approach is that its uni-directional information exchange. However, a bi-directional soft information exchange can be expected to yield an improved performance. It is worth to emphasize that during the soft information combining process, the soft information of a symbol with a high reliability has to be highlighted while the soft information of a symbol with a low reliability has to be suppressed. In order to cater for this requirement, a weighting scheme is proposed in which the soft information is weighted with its corresponding normalized reliability. This weighted averaging closely resembles *maximal ratio combining*. Let us denote the weights by $w_1 = \frac{rel(b_1)}{rel(b_1)+rel(b_2)}$ and $w_2 = \frac{rel(b_2)}{rel(b_1)+rel(b_2)}$. Thus, the updated combined soft

information is

$$\mathbf{p}_b = w_1\mathbf{p}_{b1} + w_2\mathbf{p}_{b2}. \tag{2.20}$$

This scheme is expected to provide a good bit error rate (BER) performance improvement as in optimal *ALLR* scheme in [61].

**Bit wise information exchange**

Another method to exchange the information between the parallely operating decoders is to perform the information exchange at the bit level. In here, the individual bit probabilities are calculated and the bit-level soft information is exchanged between the two decoders. We propose three schemes for this bit-level information exchange.

*Bit-wise Average Probability (BAP):*

In this approach, the bit level soft information vectors corresponding to Node B are calculated at each of the decoders by combining the corresponding symbol probabilities. Then, the two bit level soft information vectors are averaged. Let $b'_1$ and $b'_2$ represents the two decoders' probability values corresponding to a certain bit position. Then the averaged bit probability is given by,

$$Pr(b') = \frac{1}{2}\left(Pr(b'_1) + Pr(b'_2)\right). \tag{2.21}$$

*Bit-wise Best Probability (BBP):*

We know that the reliability values of a certain bit position are given by $rel(b'_1) =$

$\left|log\left[\frac{Pr(b'_1=1)}{Pr(b'_1=0)}\right]\right|$ and $rel(b'_2) = \left|log\left[\frac{Pr(b'_2=1)}{Pr(b'_2=0)}\right]\right|$. Thus, a combined probability value for the considered bit position can be calculated by selecting the probability value with the higher reliability.

$$Pr(b') = \begin{cases} Pr(b'_1) & \text{if } rel(b'_1) > rel(b'_2) \\ Pr(b'_2) & \text{Otherwise.} \end{cases} \tag{2.22}$$

*Bit-wise Weighted Sum Probability (BWSP):*

Let us consider weighing factors $w'_1 = \frac{rel(b'_1)}{rel(b'_1)+rel(b'_2)}$ and $w'_2 = \frac{rel(b'_2)}{rel(b'_1)+rel(b'_2)}$. A combined probability corresponding to node B's bit can be calculated as,

$$Pr(b') = w'_1 Pr(b'_1) + w'_2 Pr(b'_2). \tag{2.23}$$

It is straight forward to calculate $\mathbf{p}_b$ using the bit-probability vectors obtained as above.

We are also interested in studying how the errors which were introduced during initial symbol estimation propagate when the proposed combining process is carried out at either the symbol level or at the bit level.

***Lemma 2.*** The lowest error in average can be obtained when combining is carried out at the symbol level.

*Proof:*

Let $x_\iota$ s be variables with associated errors $\delta x_\iota$ respectively. Then, if $z = \sum_{\forall \iota} \alpha_\iota x_\iota$

with constant $\alpha_\iota$ s,

$$\delta z = \sum_{\forall \iota} \alpha_\iota \delta x_\iota. \tag{2.24}$$

Moreover, if $u = \prod_{\forall \iota} x_\iota$, $\frac{\delta u}{u} = \sum_{\forall \iota} \frac{\delta x_\iota}{x_\iota}$ [59, 60]. Thus,

$$\delta u = \sum_{\forall \iota} \delta x_\iota \prod_{\forall \iota', \iota' \neq \iota} x_{\iota'}. \tag{2.25}$$

Let us consider an $(M = 2^m)$-ary symbol set at each of the parallelly operating two decoders. Furthermore, let the $M$-ary symbol soft information corresponding to node B at the two decoders are denoted by $p_{b1}(\iota)$ and $p_{b2}(\iota)$, $\iota = 0, 1, \ldots, 2^m - 1$. To combine and calculate bit level soft information $2^{m-1}$ symbol probabilities are added together. This addition calculates $m$ soft information pairs at bit level.

Moreover, let's assume that each $M$-ary symbol soft information value is having an equal error $\Delta$.

Hence for a certain bit position $k$, a combined bit level soft information can be calculated as,

$p_k = w_1' \sum_{2^{m-1}} p_{b1}(\iota) + w_2' \sum_{2^{m-1}} p_{b2}(\iota)$, where $w_1' + w_2' = 1$. $k = 0, 1, \ldots, m$. According to (2.24), $p_k$ is associated with an error $\Delta p_k = w_1' \times 2^{m-1}\Delta + w_2' \times 2^{m-1}\Delta = 2^{m-1}\Delta$.

Probabilities of the recombined symbols are given by $p_t = \prod_m p_k$.

Thus with (2.25), the corresponding error $\Delta p_t = \sum_m \Delta p_k \left( \prod_{m-1, k' \neq k} p_{k'} \right)$. Then

the error in average is given by,

$$\begin{aligned}\Delta_{\text{avg}} &= \frac{\sum_{2^m}\Delta p_t}{2^m} \\ &= \frac{1}{2^m}\sum_{2^m}\Delta p_k \sum_{m}\left(\prod_{m-1,k'\neq k} p_{k'}\right) \\ &= \frac{2^{m-1}\Delta}{2^m}\sum_{2^m}\sum_{m}\left(\prod_{m-1,k'\neq k} p_{k'}\right).\end{aligned} \tag{2.26}$$

Let's assume,

$$\sum_{2^m}\sum_{m}\left(\prod_{m-1,k'\neq k} p_{k'}\right) = 2m. \tag{2.27}$$

Note that only 2 bit probabilities are introduced in addition to $2m$ existing probability values when moving from $M$-ary to $(M+1)$-ary. Hence, $p_t$ multiplication involves only two additional terms. New $2m$ number of terms are affected from and encompasses the new probability terms. Therefore number of probability values increase by 2 more, $\sum_{2^{m+1}}\sum_{m+1}\left(\prod_{m,k'\neq k} p_{k'}\right) = 2m+2 = 2(m+1)$.

Thus, if (2.27) is true for $m \;\rightarrow$ it is true for $m+1$.

For $m = 2$: Assume that the two bits in a symbol are given by $b^{(1)}$ and $b^{(2)}$ where the most significant bit is represented by $b^{(1)}$. Let $p_{b^{(2)}=0}$, $p_{b^{(2)}=1}$, $p_{b^{(1)}=0}$ and $p_{b^{(1)}=1}$ represent individual bit probabilities. Thus,

$$\begin{aligned}\sum_{2^2}\sum_{2} p_{k'} &= (p_{b^{(2)}=0} + p_{b^{(1)}=0}) + (p_{b^{(2)}=1} + p_{b^{(1)}=0}) \\ &+ (p_{b^{(1)}=1} + p_{b^{(2)}=0}) + (p_{b^{(1)}=1} + p_{b^{(2)}=1})\end{aligned} \tag{2.28}$$

$$= 2\left[(p_{b^{(2)}=0} + p_{b^{(2)}=1}) + (p_{b^{(1)}=0} + p_{b^{(1)}=1})\right]$$

$$= 2[1+1] = 2 \times 2.$$

Hence, (2.27) is true for $m = 2$.

Thus by the principle of mathematical induction, for any $m \geq 2$, (2.27) is true.

Thus with (2.26), $\Delta_{\text{avg}} = \frac{\Delta}{2} \times 2m = m\Delta$.

When a direct combining at symbol level occurs $p(\iota) = w_1 p_{b1}(\iota) + w_2 p_{b2}(\iota)$, $w_1 + w_2 = 1$, $j = 0, 1, \ldots, 2^m - 1$. By (2.24), $\Delta p(\iota) = w_1\Delta + w_2\Delta = \Delta$.

Hence, it is clear that a lower error value in average can be obtained when symbol level combining is carried out.

**Calculating the New Joint Probability Values**

The probability soft information vectors corresponding to node pair A and B, and node pair B and C decoders' inputs can be recalculated using the extracted soft information of nodes A and C, as above. Thereafter, during the next iteration, these recalculated new joint probabilities are inputted to the individual decoders.

### 2.4.4 Analysis of Computational Complexity

This sub-section analyses the computational complexity involved in the information exchange during a single iteration of the decoder. The computational complexity is shown in Table 2.2, in terms of the number of real mathematical operations performed.

It also lists the computational complexity for different information exchange schemes presented in Sub-section 2.4.3.

Table 2.2: Per iteration, number of mathematical operations involved under different information exchange schemes

| Scheme | Per iteration, number of mathematical operations |
|---|---|
| Separate | 0 |
| AP | $2nM(M-1)(\mathcal{M}-2)+2nM(\mathcal{M}-2)+2nM^2(\mathcal{M}-1)$ |
| BPS | $2nM(M-1)(\mathcal{M}-2)+7n(\mathcal{M}-2)+2nM^2(\mathcal{M}-1)$ |
| WSP | $2nM(M-1)(\mathcal{M}-2)+12n(\mathcal{M}-2)+3nM(\mathcal{M}-2)+2nM^2(\mathcal{M}-1)$ |
| BAP | $2n\lceil mM+M(M-1)\rceil(\mathcal{M}-2)+4nm(\mathcal{M}-2)+n(m-1)M(\mathcal{M}-2)+2nM^2(\mathcal{M}-1)$ |
| BBP | $2n\lceil mM+M(M-1)\rceil(\mathcal{M}-2)+7nm(\mathcal{M}-2)+n(m-1)M(\mathcal{M}-2)+2nM^2(\mathcal{M}-1)$ |
| BWSP | $2n\lceil mM+M(M-1)\rceil(\mathcal{M}-2)+12nm(\mathcal{M}-2)+3nmM(\mathcal{M}-2)+n(m-1)M(\mathcal{M}-2)+2nM^2(\mathcal{M}-1)$ |

Note that $w_r$ and $w_c$ represent the row weight and the column weight of the LDPC parity check matrix. At the same time, per iteration number of mathematical operation requirement of the belief propagation (BP) based decoders' probability soft information updating is given by $4nM^2w_c(w_c-2)(\mathcal{M}-1)+\kappa M^2(3M^2-1)w_r(w_r-2)(\mathcal{M}-1)$. It is worth to note that the number of mathematical operations required for information exchange increases exponentially in the order of 2 with the increased modulation order while the number of mathematical operations required for the BP decoder increases exponentially in the order of 4.

## 2.5 Numerical Results and Discussion

This section presents the BER performance of the proposed JCPNC algorithm for a BPSK modulated three-way relay channel. Furthermore, it also presents the BER performance of an algorithm where the two decoders operate independently for the comparison purposes. The simulations use a relatively short $255 \times 175$ binary LDPC code and a long $1057 \times 813$ binary LDPC code. We also assume a quasi-static uncorrelated block fading with unity parameter value. Fig. 2.3 and Fig. 2.4 shows the BER performances of the proposed JCPNC algorithm under the three information exchange schemes. Note that these simulations are carried out for decoding iterations.

The proposed algorithm for a BPSK modulated system shows a considerably better performance, as a result of harnessing the diversity available at the separate transmis-

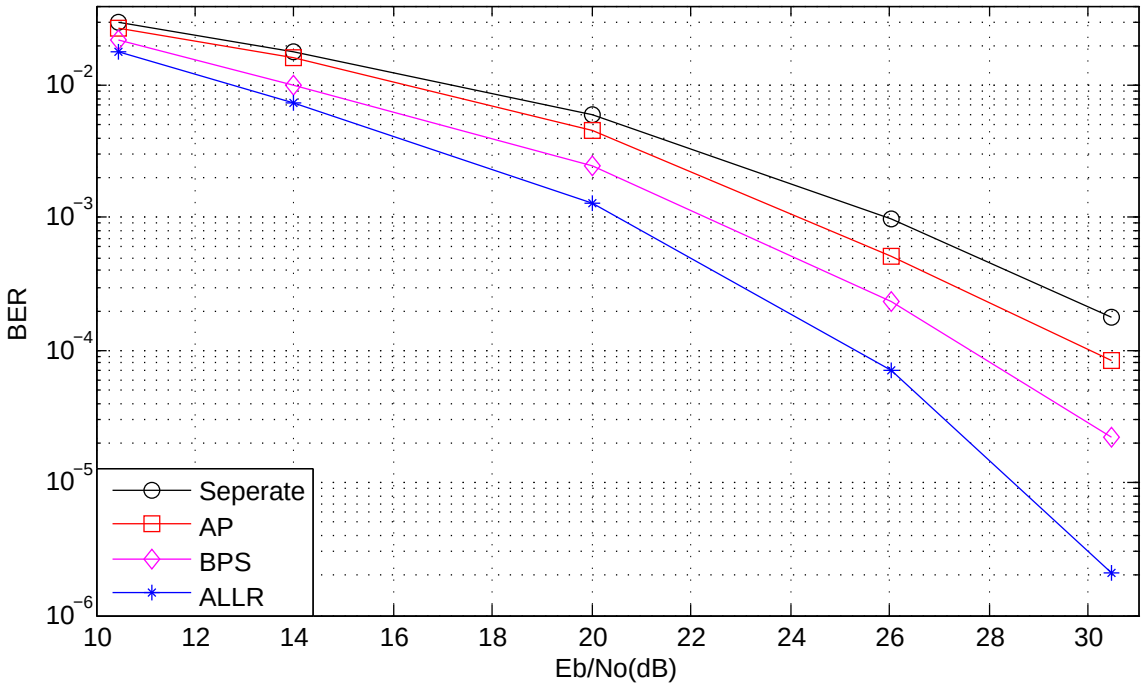


Figure 2.3: Comparison of decoder BER performance for 255 × 175 LDPC code.

sions. Out of the proposed information exchange schemes, the ALLR scheme is providing a better performance compared to other two.

The BER performance of the proposed iterative JCPNC algorithm for a three-way relay channel having MPSK modulation is presented next. We use three different LDPC codes for our experiments, the short 255 × 175 binary LDPC code, a long 1057 × 813 binary LDPC code and a 204 × 102 non-binary LDPC code in GF(4). Uncorrelated quasi-static Rayleigh block fading with unit parameter value is considered. Fig. 2.7, Fig. 2.8 and Fig. 2.9 presents the BER performance after after 10 decoder iterations of the proposed algorithm with QPSK, 8-PSK and 16-PSK modulations. The graphs also present the comparison of BER performance when using three different information

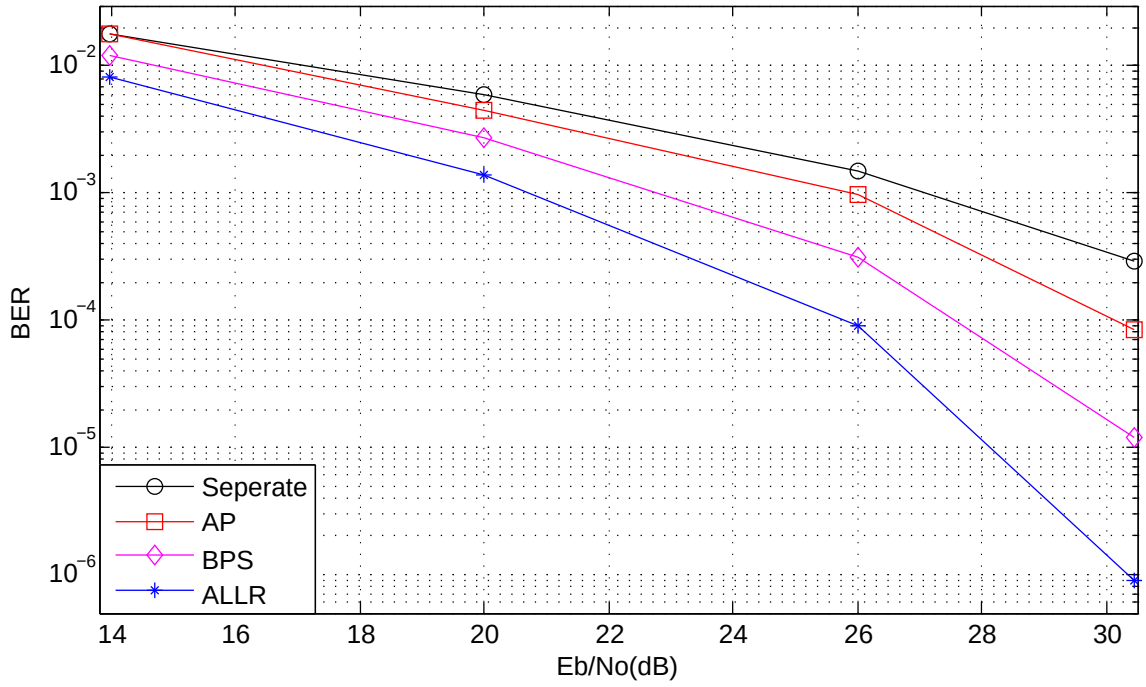


Figure 2.4: Comparison of decoder BER performance for $1057 \times 813$ LDPC code.

exchange schemes proposed. Furthermore, Fig. 2.10 shows the FER performance of the proposed JCPNC algorithm when QPSK modulation is employed. The graphs also show the BER performance when two decoders operate independently, for the comparison purposes.

Proposed JCPNC algorithm for a MPSK modulated system also shows a superior BER performance compared to separate decoding algorithms. Bit or symbol level information exchange between the constituent decoders which enables to harness the diversity of the separate transmissions is the key to this performance improvement. We can also observe that the WSP scheme provides the most superior performance among all proposed information exchange schemes. Moreover, the bit-wise information exchange

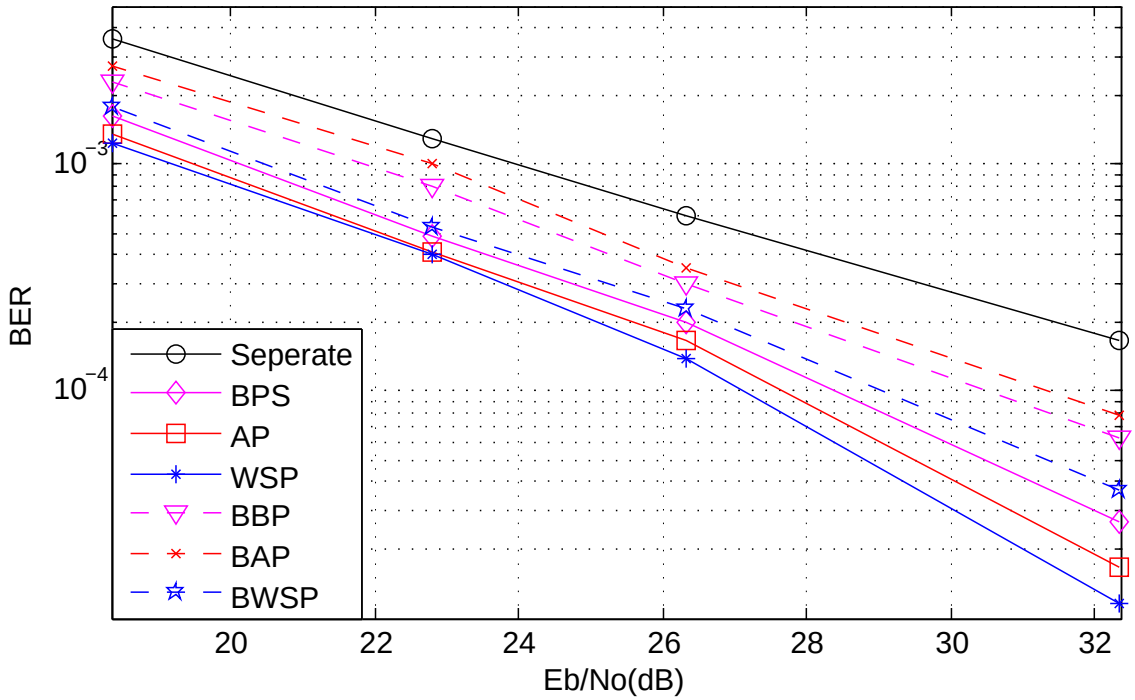


Figure 2.5: BER performance of the proposed algorithm for $255 \times 175$ binary LDPC code with QPSK modulation.

scheme's BER performance is inferior to that of symbol-wise information exchange. Hence, *Lemma 2* presented in Section 2.4.3 is well confirmed by the simulation results. However, it is also worth to note that compared to the other two bit-wise information exchange schemes BWSP scheme's error performance is considerably better.

We also investigate the convergence of the proposed algorithms for a BPSK modulated system using the BER performance for 5, 10 and 20 iterations in the proposed algorithm. For this purpose we use the $255 \times 175$ binary code. Only a negligible BER performance improvement is observed after 10 iterations as shown in Fig. 2.11. These results verify a convergence within a 10 iterations.

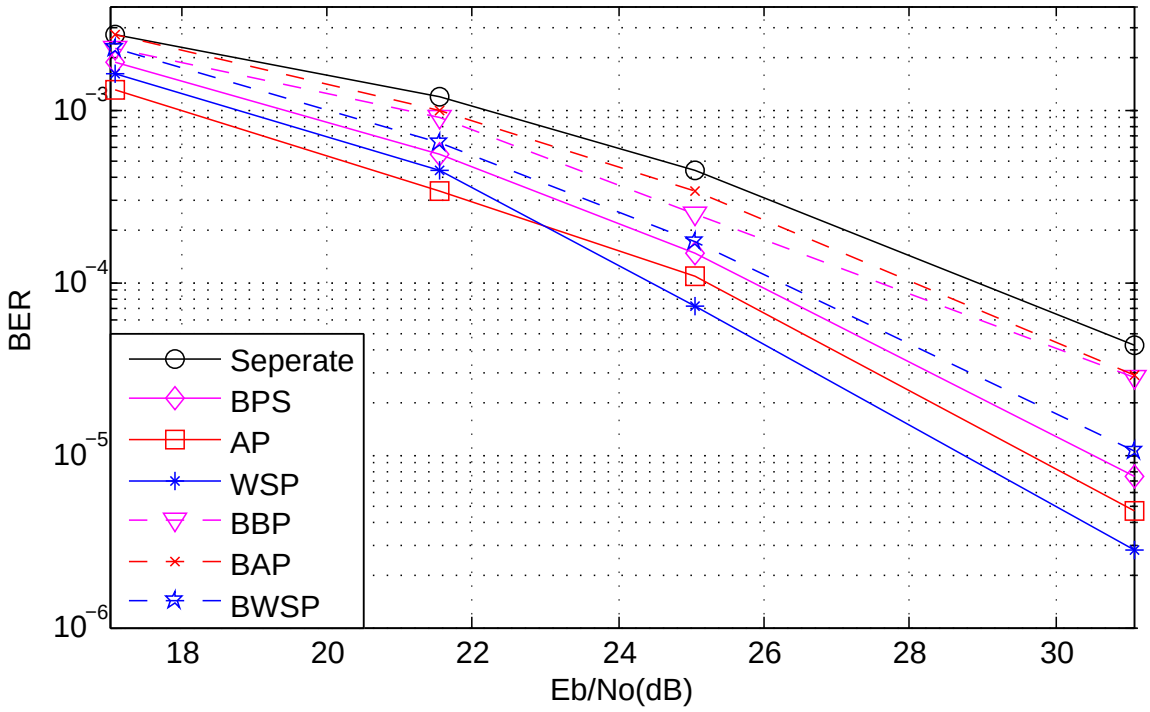


Figure 2.6: BER performance of the proposed algorithm for $1057 \times 813$ binary LDPC code with 8-PSK modulation.

Convergence of the proposed JCPNC algorithm under QPSK modulation is presented in Table 2.3 for 10 decoder iterations and for a $255 \times 175$ LDPC code. From Table 2.3 it can be observed that the proposed JCPNC algorithm attains convergence in more than 93% of the time once one of the symbol level information exchange schemes is used. At the same time, its convergence percentage is more than 87% when bit level information exchange is used. Compared to an algorithm in which the two decoders operate independently where the convergence percentage is 82.8%, the proposed algorithm's convergence is very much superior. Moreover, Fig. 2.12 shows the BER performance of the proposed algorithms for MPSK modulated systems with symbol-wise information exchange after

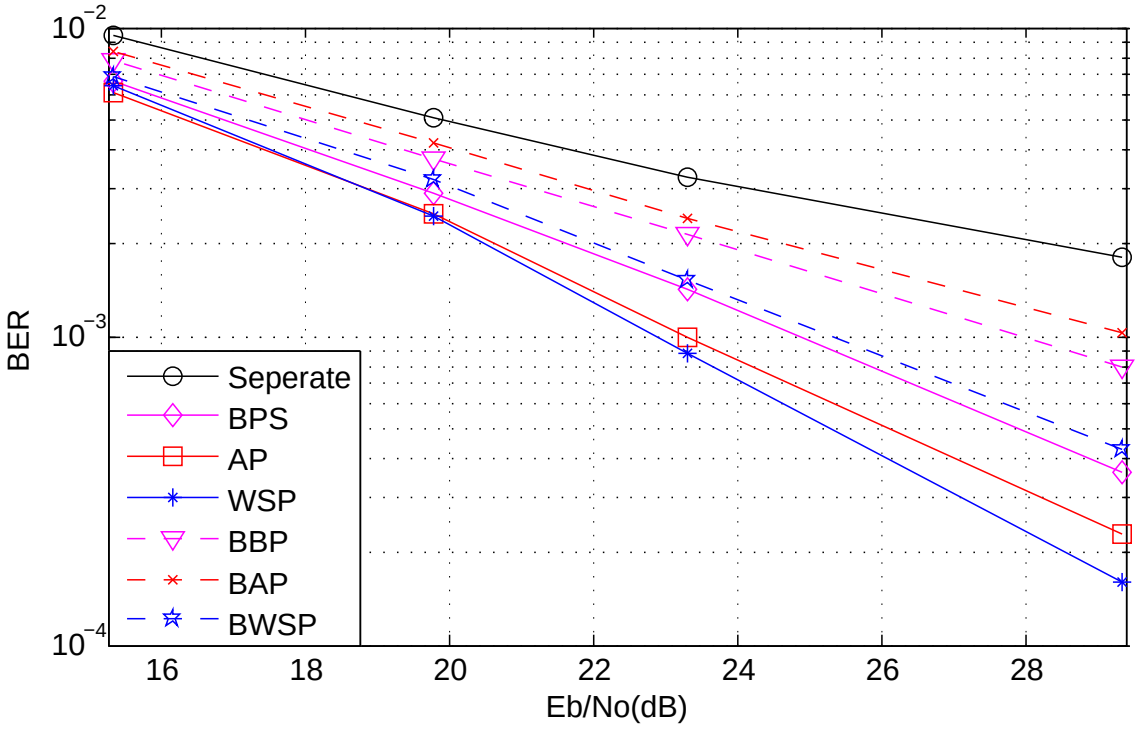


Figure 2.7: BER performance of the proposed algorithm for 255 × 175 binary LDPC code with 16-PSK modulation.

1, 3 and 10 decoder iterations. Here also, a faster convergence compared to the separate decoding is observed when information exchange is carried out.

In Table 2.4, the numerical values for the computational complexity given in Table 2.2 are listed for 255 × 175 LDPC code with $w_r = w_c = 16$ and QPSK modulation.

On the other hand, the BP based decoders consumes 51466240 mathematical operations in average for the probability information update during a single iteration.

It is clear that only a negligible complexity is added by the information exchange step to the overall JCPNC algorithm. For higher orders of modulation, the added complexity by the information exchange step is even less significant. Thus, it is noted that in the

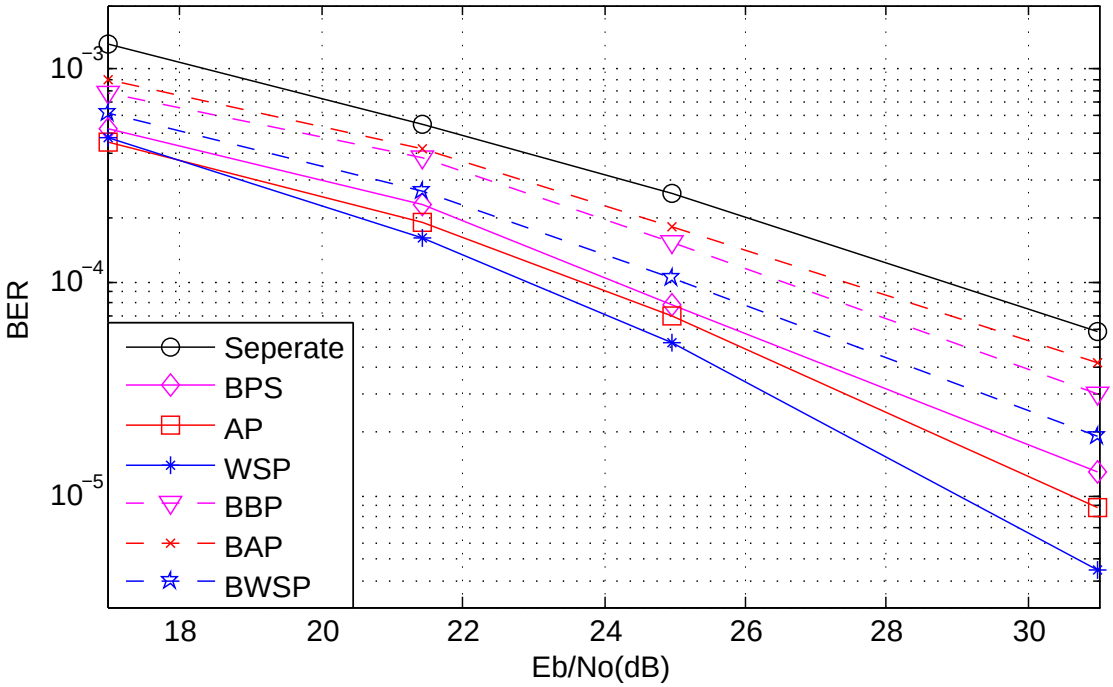


Figure 2.8: BER performance of the proposed algorithm for $204 \times 102$ GF(4) LDPC code with QPSK modulation.

proposed six information exchange schemes a faster convergence and an improved BER performance is achieved without much increment in complexity. Furthermore, WSP obtains a higher BER performance over AP and BPS while BWSP obtains a higher BER performance over BAP and BBP with only a negligible increment in the complexity.

## 2.6 Conclusion

In this chapter a joint decoding algorithm for BPSK-modulated multi-way relay systems employing both physical-layer network coding and LDPC channel coding was presented

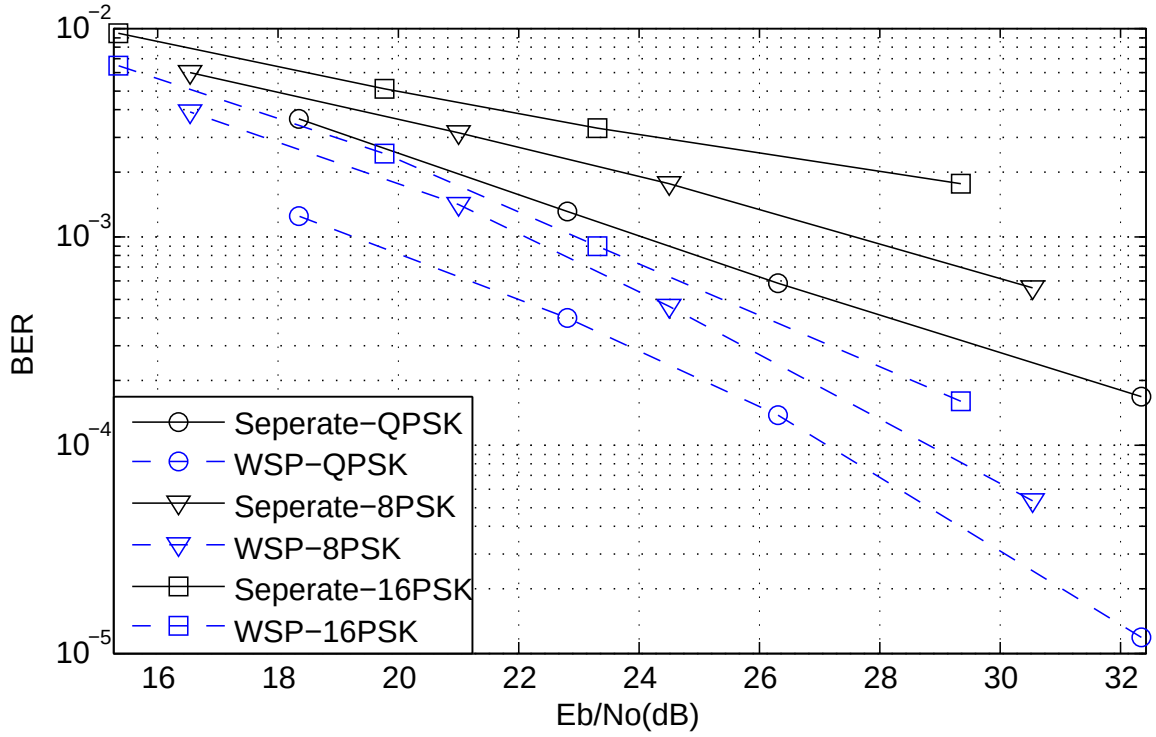


Figure 2.9: BER performance of the proposed algorithm for $255 \times 175$ binary LDPC code under different modulation orders.

and then the above algorithm was extended to MPSK modulated systems. Though we did not specifically present the extension to quadrature amplitude modulation (QAM), the joint decoding algorithm for QAM modulated systems is also the same except for the initialization step. Soft information corresponding to bits or symbols which are transmitted repeatedly during two time-slots of the MAC phase from the chosen communication node is exchanged between the two constitute LDPC channel decoders employed at the relay node. This exchange results in an additional time diversity gain. Moreover, three different information exchange schemes for the BPSK based JCPNC algorithm

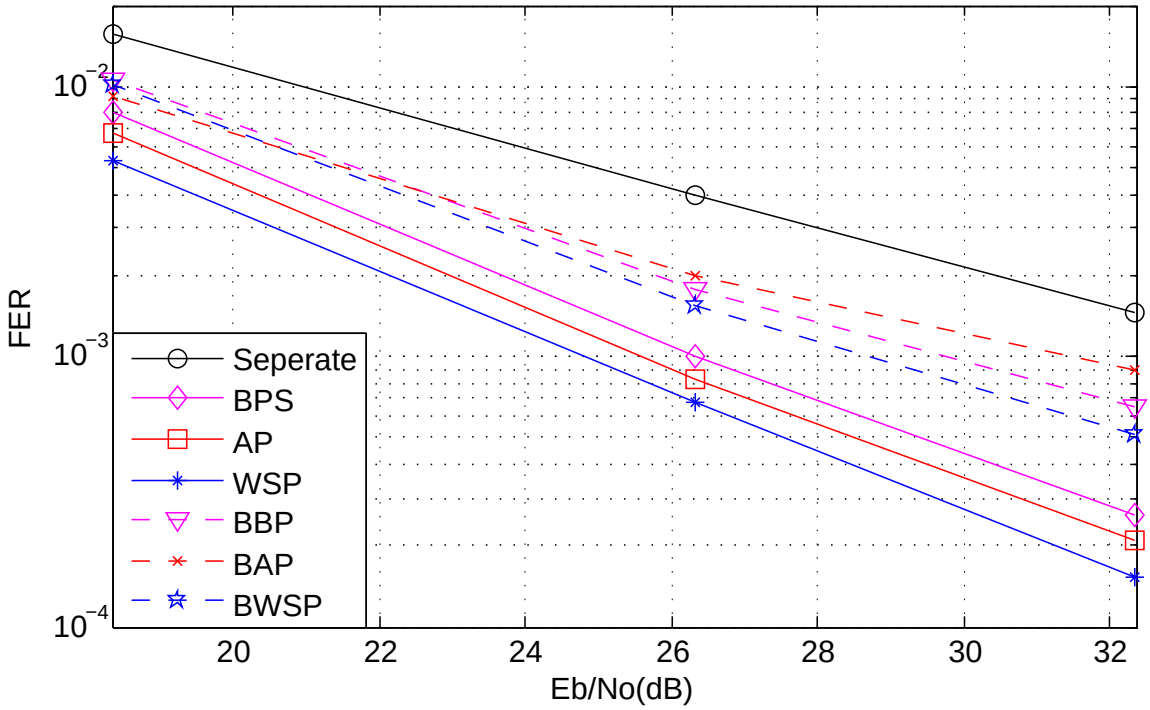


Figure 2.10: FER performance of the proposed algorithm for $255 \times 175$ binary LDPC code with QPSK modulation.

have been proposed while six schemes operating at either the bit-level or symbol-level have been proposed for MPSK based JCPNC algorithm. The simulation results have shown that the proposed joint decoding algorithms offer considerably superior BER performances and superior convergences without much added complexity compared to separate decoding.

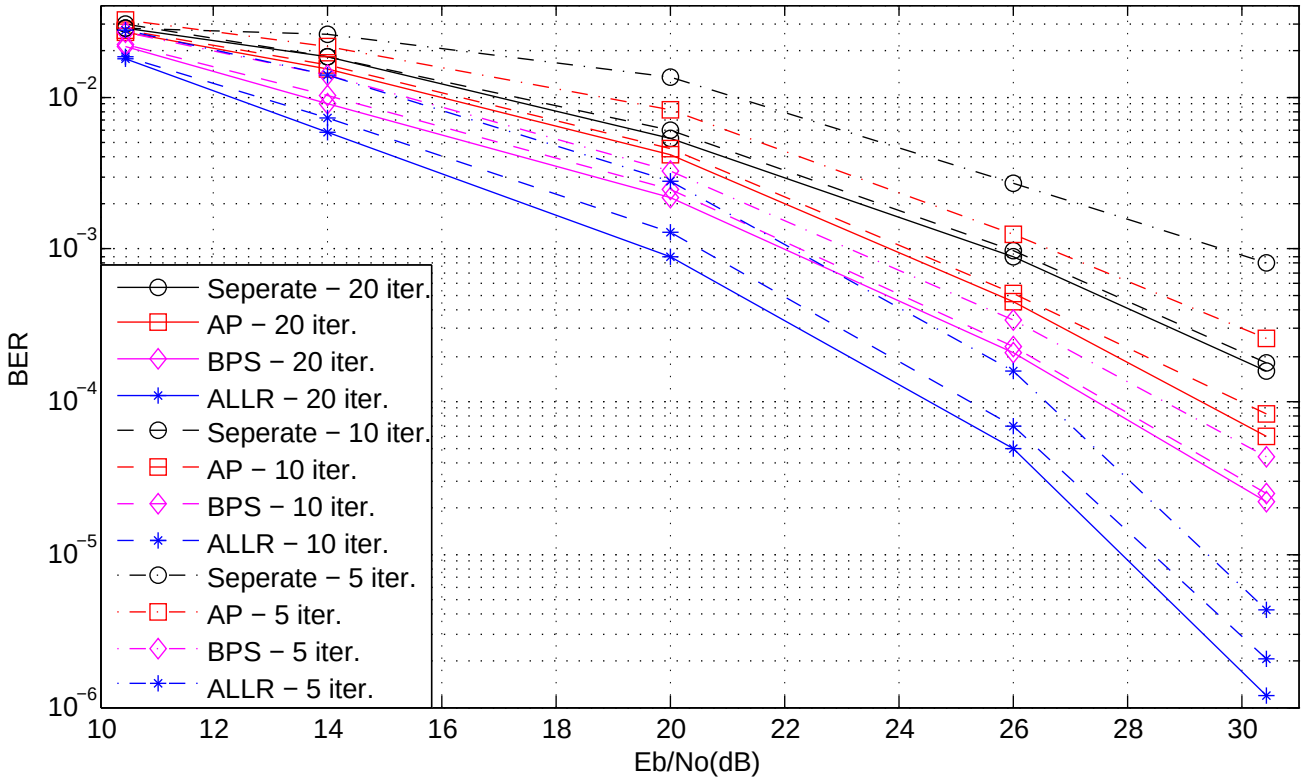


Figure 2.11: Comparison of decoder BER performance for $255 \times 175$ LDPC code for 5, 10 and 20 decoding iterations.

Table 2.3: Percentage number of times the algorithm converges at different number of iterations for $255 \times 175$ LDPC code with QPSK modulation

| Iterations for convergence | 1 | 2 | 3 | 4 | 5 | 6 | 7 | 8 | 9 | 10 |
|---|---|---|---|---|---|---|---|---|---|---|
| Separate | 68.2 | 10.2 | 2.5 | 1.3 | 0 | 0 | 0.6 | 0 | 0 | 0 |
| AP | 91.2 | 1.8 | 0.6 | 0.4 | 0.1 | 0 | 0 | 0.1 | 0 | 0 |
| BPS | 90.4 | 2.1 | 0.9 | 0.1 | 0.1 | 0 | 0 | 0 | 0 | 0 |
| WSP | 90.9 | 2.4 | 0.8 | 0.3 | 0.1 | 0.1 | 0 | 0 | 0 | 0 |
| BAP | 85 | 3.6 | 1.2 | 0 | 0 | 0 | 0 | 0 | 0 | 0 |
| BBP | 84.8 | 1.7 | 0.6 | 0 | 0 | 0 | 0 | 0 | 0 | 0 |
| BWSP | 72.6 | 10.7 | 3.6 | 1.2 | 1.2 | 0 | 0 | 0 | 0 | 0 |

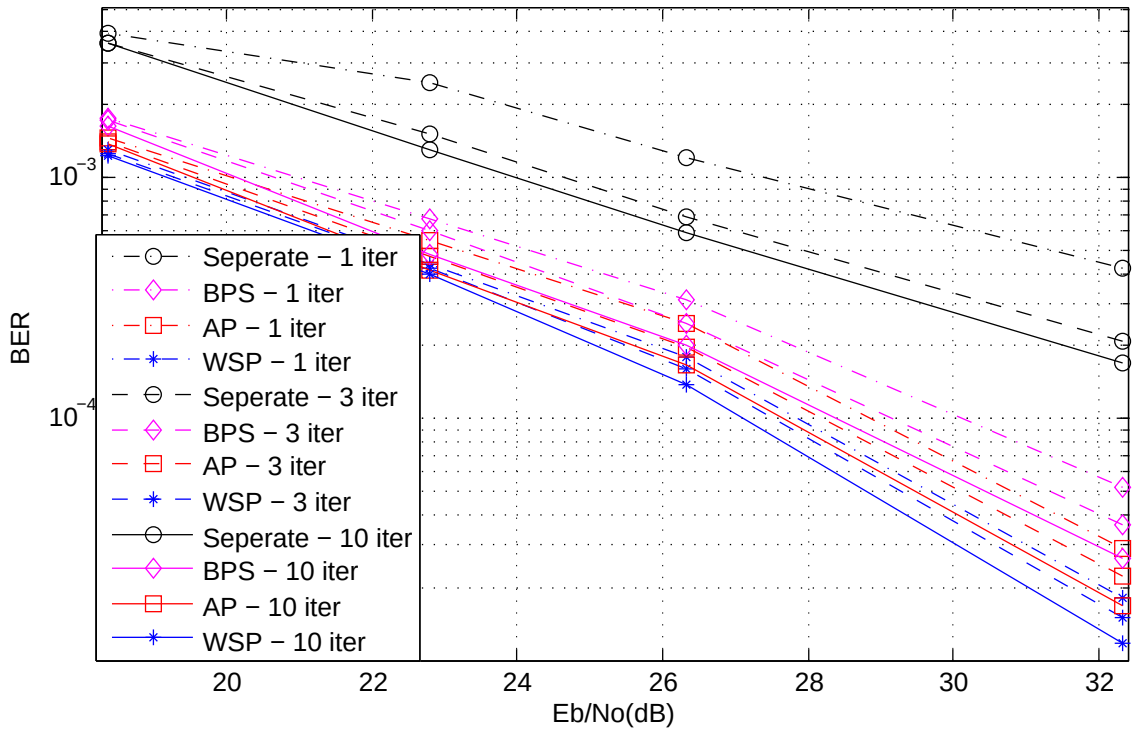


Figure 2.12: BER performance of the proposed algorithm for $255 \times 175$ binary LDPC code with QPSK modulation after 1, 3 and 10 decoder iterations.

Table 2.4: Per iteration, number of mathematical operations involved under different information exchange schemes in $255 \times 175$ binary LDPC code with QPSK modulation

| Scheme | Per iteration, number of mathematical operations |
|---|---|
| Separate | 0 |
| AP | 24480 |
| BPS | 24225 |
| WSP | 28560 |
| BAP | 29580 |
| BBP | 31110 |
| BWSP | 39780 |

# Chapter 3

# Low-Complexity Joint Channel-Network Coding Algorithm for Multi-Way Relay Systems

## 3.1 Introduction

The joint decoding algorithm presented in Chapter 2 and in [61, 62] is based on a BP based channel decoder. However, the complexity added by the BP based channel decoder to the joint decoding process is intolerable in certain conditions. Specially, decoding becomes prohibitively complex for very popular finite geometry LDPC (FG-LDPC) codes.

At the same time, a comparatively low-complexity decoding is provided by the bit-

flipping (BF) algorithm [63, 64]. In each iteration, the decoder calculates the most unreliable bit in the received bit vector and flips the same. The resulting new bit vector is a candidate for a valid codeword. Thus, the decoder heuristically searches for a valid codeword in a multi-dimensional codeword space. In this chapter, it is proposed to employ the BF algorithm in the joint decoder in order to reduce the overall complexity of the joint decoding algorithm. Nevertheless, the application of the existing BF algorithm is not straight-forward as it will not facilitate an information exchange between the two parallel channel decoders. Moreover, in the proposed BF based joint decoder, the flipped symbol-value selection step can be further improved which enables a better BER performance. Therefore, the contribution in this chapter is threefold. First, a modified BF algorithm which can facilitate hard information exchange between the two channel decoders operating parallely is proposed. Second, a technique for information exchange between the parallely operating decoders is presented. Third, an improved flipped symbol-value selection scheme is proposed for the existing non-binary symbol flipping decoder which can be also incorporated to the proposed low-complexity BF based joint decoder.

The rest of the chapter is organized as follows. Section 3.2 presents the system model and Section 3.3 introduces the proposed low-complexity joint decoding algorithm. Then, Section 3.4 presents a complexity analysis. In Section 3.5, a novel flipped symbol-value selection scheme is proposed for the symbol flipping based non-binary LDPC decoder and then this scheme is adopted in the proposed low-complexity joint channel-network

coding algorithm to improve BER performance. Numerical results and a discussion is presented in Section 3.6 followed by a conclusion in Section 3.7.

## 3.2 System Model

In this chapter the same system model presented in Section 2.2 is used, where three nodes A, B and C are to exchange their information via a relay R as shown in Fig.2.2 [61] which can be summarized as follows. Moreover, to present the proposed algorithm, without the loss of generality let us assume that the channel pair selection algorithm in [41, 61] selects nodes A and B to transmit their information first and then B and C to transmit second. Three nodes use the same $(n-\kappa)\times n$ linear block channel code $\Gamma$ to encode their information bit vectors $\mathbf{x}_a, \mathbf{x}_b$ and $\mathbf{x}_c$. This encoding process outputs three code vectors $\mathbf{c}_a = \Gamma(\mathbf{x}_a), \mathbf{c}_b = \Gamma(\mathbf{x}_b)$ and $\mathbf{c}_c = \Gamma(\mathbf{x}_c)$ having $n$ code bits in each. Then the baseband mapping rule $\{0 \to -1, 1 \to +1\}$ maps each element of the codewords to a BPSK symbol. In here we use BPSK modulation in seek of simplicity, though with some modifications to the decoder it can be easily replaced by a higher order modulation scheme. Thereafter, BPSK modulator output symbol-vectors $\mathbf{s}_a, \mathbf{s}_b$ and $\mathbf{s}_c$ are transmitted pair-wise as shown in Fig.2.2.

During the first $n$ time-slots, both nodes A and B transmit their $n$ dimensional symbol vectors $\mathbf{s}_a$ and $\mathbf{s}_b$ simultaneously which are received at the relay as an overlapped signal vector $\mathbf{y}_{ab}$. In [41], after detection, joint network coding and channel decoding is

carried out for this received signal vector to determine the XOR combined bits. After detection the XOR bit vector is again modulated and broadcasted. In comparison, in here, just after the initial detection from $\mathbf{y}_{ab}$, nodes B and C transmit their symbol vectors $\mathbf{s}_b$ and $\mathbf{s}_c$ during the next $n$ bit-intervals. These are received as an overlapped signal at the relay given by $\mathbf{y}_{bc}$. The $j$-th elements of the two such received overlapped signal vectors are given by,

$$y_{ab}(j) = h_{A1}(j)s_a(j) + h_{B1}(j)s_b(j) + n_{ab1}(j) \quad (3.1)$$

$$y_{bc}(j) = h_{B2}(j)s_b(j) + h_{C2}(j)s_c(j) + n_{bc2}(j). \quad (3.2)$$

Here $h_{A1}$ and $h_{B1}$ represent the A-R and B-R channels' channel coefficient during the first $n$ bit-intervals. Also, $h_{B2}$ and $h_{C2}$ represents the B-R and C-R channels' channel coefficients during the second $n$ bit-intervals. $n_{ab1}(j)$ and $n_{bc2}(j)$ are the complex AWGN samples with zero mean and $\sigma^2$ variance per real dimension added at the relay antennas during the two transmissions.

$y_{ab}(j)$ and $y_{bc}(j)$ can be used to detect $x_a \oplus x_b$ and $x_b \oplus x_c$ bits by following a joint decoding process as in [61].

## 3.3 Low-complexity Joint Decoding at the Relay

In this chapter, as stated before we focus on channel decoding and network coding at the relay during the MAC phase where exploiting the time diversity is an important

aspect. Meanwhile, as stated in Section 3.1, a BF based decoding is proposed in order to reduce the overall decoder complexity. However, the BF algorithm deals with the hard information and an information exchange is not possible to be carried out when performing the BF decoding in its original form. Thus, the original version of the BF algorithm is modified and the modified BF algorithm is employed in the joint decoder to explore additional time diversity, while maintaining a low-complexity.

### 3.3.1 Initialization

Let us consider the A and B nodes' communication during $j$-th time-slot ($1 \leq j \leq n$). Further, to simplify, we omit the index $j$. Combined signals map to four equi-probable constellation points $\hat{y}_{ab}$ are given in Table 3.1.

Table 3.1: Combined transmitted signal constellation

| $c_a c_b$ | $\hat{y}_{ab}$ |
|---|---|
| 00 | $-h_A - h_B$ |
| 01 | $-h_A + h_B$ |
| 10 | $h_A - h_B$ |
| 11 | $h_A + h_B$ |

Thus the transmitted combined signal $s_{ab} = \mathcal{S}(i)$'s a priori probability is given by,

$$Pr\left\{s_{ab} = \mathcal{S}(i)\right\} = \frac{1}{4}, \tag{3.3}$$

where $\mathcal{S}(i) \in \{(-1-1), (-1+1), (+1-1), (+1+1)\}$.

Let,

$$Pr\{y_{ab}\,|s_{ab} = \mathcal{S}(i)\} = \frac{1}{2\pi\sigma^2} exp - \left(\frac{\|y_{ab} - \mathcal{S}(i)\|^2}{2\sigma^2}\right) \tag{3.4}$$

denote the probability density of $y_{ab}$ given a certain symbol combination being transmitted. With a received signal $y_{ab}$, is Hence, given the received value $y_{ab}$, the probability that the symbol $\mathcal{S}(i)$ was transmitted is,

$$\begin{aligned} p_i &= Pr\{s_{ab} = \mathcal{S}(i)\,|y_{ab}\} \\ &= Pr\{y_{ab}\,|s_{ab} = \mathcal{S}(i)\} \times \frac{Pr(s_{ab} = \mathcal{S}(i))}{Pr(y_{ab})} \\ &= Pr\{y_{ab}\,|s_{ab} = \mathcal{S}(i)\} \times C \end{aligned} \tag{3.5}$$

where $C = \frac{1}{4Pr(y_{ab})}$ is a constant which can be calculated using the property $\sum P_i = 1$. Hence, the initial hard decision bit combination at the $j$-th position is given by,

$$s_{ab}(j) = \mathcal{S}(\eta), \text{where } \eta = \arg\max_i p_i \tag{3.6}$$

### 3.3.2 Modified Bit-flipping Algorithm

One obvious technique to carry out the low complexity joint channel decoding-network coding is operating the conventional BF algorithm on calculated XORed bit vector using $\mathbf{s}_{ab}$. However, this method does not utilize the complete information available at the joint decoder. Therefore, first an algorithm to harness the complete set of information is

proposed. The novel joint decoding algorithm considers nodes A and B's individual bits to form symbols in a Galois field GF(4) such that $\{00\rightarrow 0,\ 01\rightarrow 1,\ 10\rightarrow 2,\ 11\rightarrow 3\}$. This makes the original binary parity check matrix's parity check equations to be valid for the formed GF(4) symbols under the GF(4) addition operation to replace the binary XOR. However, note that the parity check matrix we use here is binary, so that this scenario is different to that of conventional non-binary channel coding.

We employ a symbol flipping algorithm to perform the joint decoding. At the initial step, hard decision symbol-values are calculated using (3.6) and are assigned to the symbol positions. Then, the rule given below is used to determine the symbol position to be flipped.

Let us denote the reliabilities of the $n$ symbols to be $\mathbf{rel} = [rel_1, rel_2, \ldots, rel_n]$ $= [|llr(s_{ab}(1)|\mathbf{y})|, |llr(s_{ab}(2)|\mathbf{y})|, \ldots, |llr(s_{ab}(n)|\mathbf{y})|]$ where $s_{ab}(j)$ represents the $j$-th position's currently selected symbol. Corresponding to each position $j = 1, \ldots, n$, a reliability metric $\phi_j$ is calculated during each iteration by considering the parity checks in which the given position contributes. Let $\mathcal{N}(i)$, $i = 1, \ldots, \kappa$, denote the set of symbols involved in the parity check equation $i$. Let, $l_i = \min_{j\in\mathcal{N}(i)} rel_j$ and $u_i = \max_{j\in\mathcal{N}(i)} rel_j$. Hence,

$$\phi_{ji} = \begin{cases} rel_j - \frac{l_i}{2} & \text{if } j \in \mathcal{N}(i) \text{ and } \mathrm{z}_i = 0 \\ rel_j - \frac{l_i}{2} - u_i & \text{if } j \in \mathcal{N}(i) \text{ and } \mathrm{z}_i \neq 0, \end{cases} \tag{3.7}$$

where $\mathrm{z}_i$ is the $i$-th parity check GF(4) syndrome symbol calculated using the decoder's

input symbol vector. Thus, the metric can be calculated by,

$$\phi_j = \sum_i \phi_{ji}, \quad j = 1, \ldots, n. \tag{3.8}$$

Note that for low $\phi_j$ values there is a higher probability for the selected symbol to be erroneous. Hence we select the position to be flipped as

$$j' = \arg\min_j \phi_j. \tag{3.9}$$

### 3.3.3 Information Exchange Between Decoders

In the conventionally employed bit-flipping algorithm, the symbol-value at the selected position would be replaced by the symbol-value with the next highest reliability. However, with two information pairs $c_{ab} = \{c_a, c_b\}$ and $c_{bc} = \{c_b, c_c\}$ available at the relay, it is obvious that $c_b$ information is duplicated. This can be viewed as diversity information as in Chapter 2 and [61] and the diversity can be utilized in the new symbol selection process at the two decoders. This can also be explained as an information exchange between the two decoders decoding $c_{ab}$ and $c_{bc}$ information pairs parallelly as shown in Fig. 3.1. Note that the information exchange is occurring at the new symbol selection step.

Let $j$ and $k$ be the two selected positions for flipping from two codewords. Further, let $c_b^{ab}$ and $c_b^{bc}$ represent the $c_b$ hard-decision information corresponding to the $c_{ab}$ and $c_{bc}$

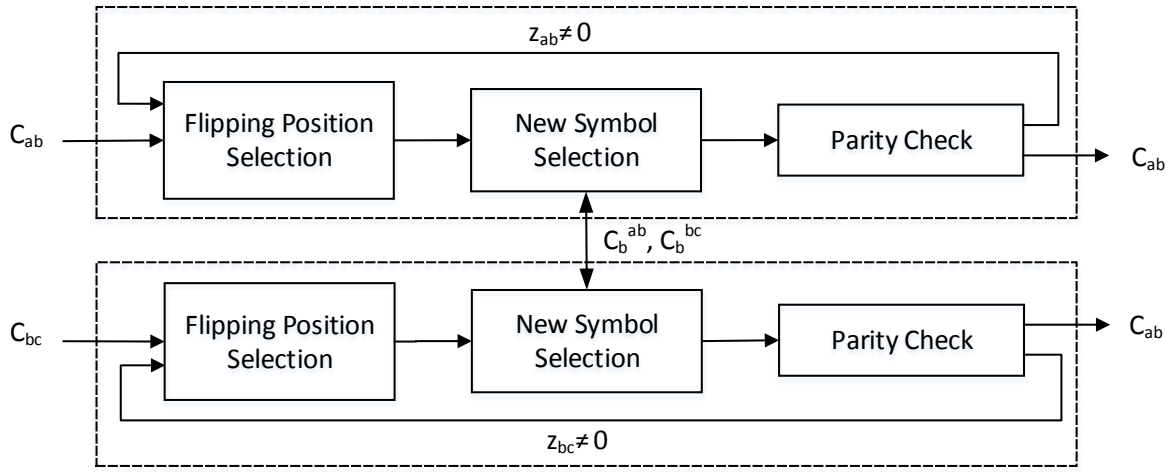


Figure 3.1: Information exchange

Rule 1:

$$(c_{ab}(j), c_{bc}(k)) = \begin{cases} (c_a(j)\overline{c_b(j)}, \overline{c_b(k)}c_c(k)) & \text{if } j = k \text{ and } c_b^{ab}(j) = c_b^{bc}(k) \\ (\overline{c_a(j)}c_b(j), c_b(k)\overline{c_c(k)}) & \text{if } j = k \text{ and } c_b^{ab}(j) \neq c_b^{bc}(k) \\ (\overline{c_a(j)}c_b(j), c_b(k)\overline{c_c(k)}) & \text{if } j \neq k \text{ and } c_b^{ab}(j) = c_b^{bc}(j) \text{ and } c_b^{ab}(k) = c_b^{bc}(k) \\ (\overline{c_a(j)}c_b(j), \overline{c_b(k)}c_c(k)) & \text{if } j \neq k \text{ and } c_b^{ab}(j) = c_b^{bc}(j) \text{ and } c_b^{ab}(k) \neq c_b^{bc}(k) \\ (c_a(j)\overline{c_b(j)}, c_b(k)\overline{c_c(k)}) & \text{if } j \neq k \text{ and } c_b^{ab}(j) \neq c_b^{bc}(j) \text{ and } c_b^{ab}(k) = c_b^{bc}(k) \\ (c_a(j)\overline{c_b(j)}, \overline{c_b(k)}c_c(k)) & \text{if } j \neq k \text{ and } c_b^{ab}(j) \neq c_b^{bc}(j) \text{ and } c_b^{ab}(k) \neq c_b^{bc}(k) \end{cases}$$

MAC phase information transfers respectively. Then the new symbol-value is selected as per the Rule 1. Note that here $\overline{x}$ stands for the bit-wise inversion operation on a binary value $x$.

The decision on the new symbol-value is decided using the fact that if the selected positions are not the same in the two codewords, selected position at one codeword can be updated using the non-selected (hence assumed to be correct) corresponding symbol in the other codeword. On the other hand, if the two selected positions are identical while the two $c_b$ bit values are also identical, we assume the $c_b$ bit values to be erroneous

and flip the same. The reliabilities of the selected new symbols are carried forward to the next iteration as the new reliabilities corresponding to the position.

### 3.3.4 Finalization

At each of the two decoders, at the end of each iteration, a the resultant hard decision symbol vector $\hat{\mathbf{c}}$ is tested for validity. Let the GF(4) syndrome vector be $\mathbf{z} = \hat{\mathbf{c}}\mathcal{H}^T$ where $\mathcal{H}$ is the binary parity check matrix. If the checks result in $\mathbf{z} = \mathbf{0}$, the algorithm is stopped. Otherwise, it proceeds to the next iteration with the resulting symbol vectors as inputs. One other important feature to note in this algorithm is that if only one symbol vector satisfies its parity check, then it is fixed and during the next iteration, only the other decoder is operated. However, during the information exchange, the fixed $c_b$ information is used in correcting the symbol-values of the other decoder.

## 3.4 Computational Complexity Analysis

The computational complexity of the proposed algorithm is analyzed in this section and is compared to that of the joint decoder algorithm using BP proposed in Chapter 2 and also in [61]. Let us consider a joint decoding algorithm's iteration for a relatively short $255 \times 175$ and a long $1023 \times 781$ FG-LDPC codes with row and column weights ($w_r$ and $w_c$ respectively) equal in each and are 16 and 32 respectively. The complexity in terms of real operations (additions and multiplications) can be listed as in Table 3.2.

Table 3.2: Comparison of computational complexity

| | Proposed Algorithm | Algorithm in [61] |
|---|---|---|
| General | $8w_c + (n-1)$ | $4(w_r - 1)(n - m)$ $+28(w_c - 1)n + 20n$ |
| 255x175 LDPC code | 382 | 117000 |
| 1023x781 LDPC code | 1278 | 938432 |

We can observe from Table 3.2 that the computational complexity (per iteration) of the proposed joint decoder is much less than that of the algorithm in [61]. The average number of iterations consumed before converging is also a parameter to be considered along with per iteration complexity, once determining the overall computational complexity. In Figure 3.2, we present the histograms of the average number of iterations required before converging. We also present the histograms corresponding to the algorithm in [61] for comparison. The two histograms show that the proposed algorithm's average number of iterations is only marginally higher than that of the BP based algorithm in [61]. Thus, we can easily conclude the overall complexity of the proposed algorithm to be several orders of magnitude lower than that of the algorithm in [61].

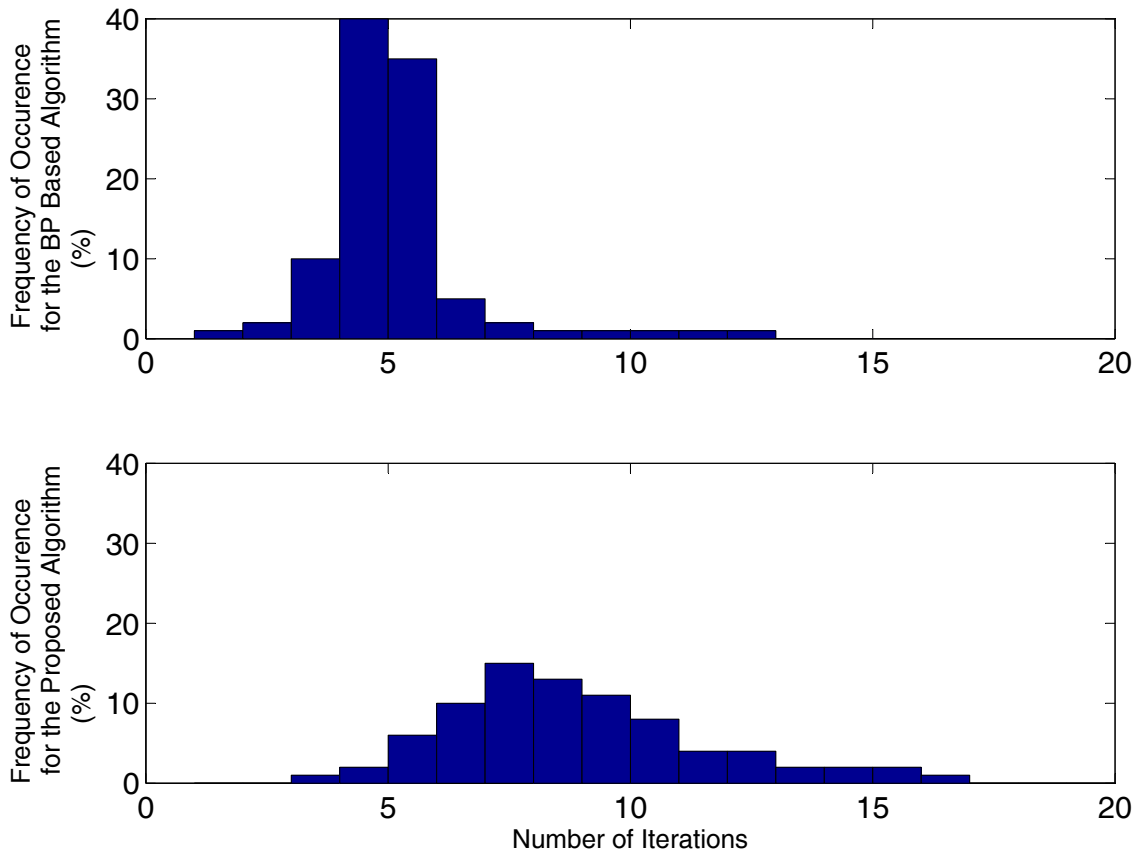


Figure 3.2: Histogram for the average number of iterations per decoded codeword for $255 \times 175$ LDPC code.

## 3.5 Improved Low-complexity Joint Channel Network Coding Algorithms for Multi-Way Relay Systems

One of the major drawbacks of the low-complexity joint decoding algorithm proposed above is the fact that during the new bit combination values selection step using Rule

1, whenever the selected positions are the same in the two decoders' codewords but the corresponding hard decision $c_b$ bits are different we do not find sufficient information to decide on new bit combination values for the selected position. Thus, we take a random new symbol-value selection. However, through simulations it was observed that in a considerable number of instances this random selection leads to an erroneous flip. Thus, a better mechanism is desired for the selection of the new symbol-value. Furthermore, the currently used non-binary LDPC decoding algorithm using symbol flipping too suffers from similar drawbacks. Noting that the new bit combination value selection in the proposed low-complexity joint decoder algorithm is equivalent to a special case of selection of the flipped symbol-value in the non-binary LDPC decoding algorithm using symbol flipping, in this section, an improved symbol-value selection step is proposed for the currently used non-binary LDPC decoding algorithm having symbol flipping. Then the same is incorporated in the low-complexity joint decoding algorithm proposed in Section 3.3.

### 3.5.1 Introduction

A large variety of algorithms have been proposed for non-binary LDPC decoding using a complete hard decision decoding. the key benefit of the hard decision decoding is the l in decoding [65–67]. Two steps constitute one decoder iteration of the aforementioned iterative non-binary LDPC decoding algorithms. At the first step, a symbol position to be flipped is selected considering the now-selected symbol-value reliabilities. Thereafter

a new symbol-value having the next highest reliability is selected to replace the current symbol-value at the selected position. This procedure iteratively performed till a a predefined number of iterations have been performed or a valid codeword is created. Previously done work in this area is only on the improvement of the symbol position to be flipped. To the best of my knowledge, no existing research work has attempted to improve the second step. It is apparent that the second step also has a considerable effect on the error performance of the overall decoding algorithm. At the same time, [68–70] present three researches where flipped symbol-value selection and the flipped symbol position selection are done simultaneously. Nevertheless, a dedicated symbol-value selection step can be expected to have a better overall BER performance. Hence, in this section, a new method is presented for the selection of a new symbol-value to the selected symbol position.

### 3.5.2 System Model

Consider the basic communication model shown in Fig. 3.3, in which a bit-stream is used to form multi-bit symbols. these symbols are then mapped to the symbols of non-binary Galois field of order $q$, $(GF(q = 2^p))$, where $p \in \mathbb{Z}^+$. An $n - \kappa$ dimensional block of symbols is encoded using a $(n, n - \kappa)$ non-binary LDPC code into an $n$ dimensional codeword $\mathbf{s} = [s_1, s_2, \ldots, s_n]$ over $GF(q)$. The codeword is then binary converted to be $\mathbf{c} \in \{0, 1\}^{np}$ and is BPSK modulated to form an $np$ dimensional modulated vector $\mathbf{x} = [x_1, x_2, \ldots, x_{np}]$, where $x_j \in \{-1, 1\}$ for $j \in [1, np]$. It is important to note that

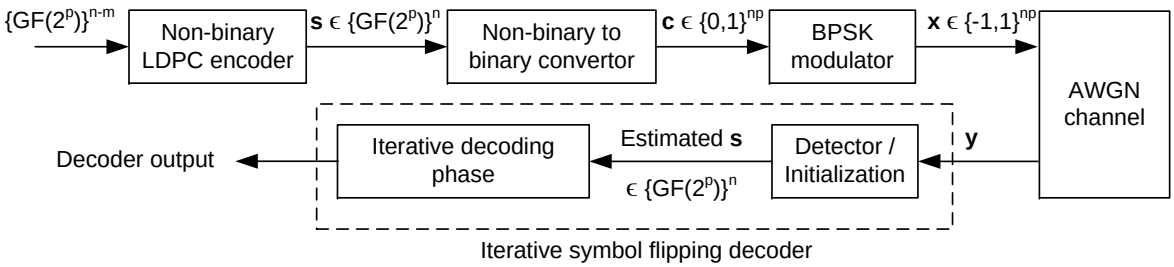


Figure 3.3: System model

any higher-order linear modulation technique can be used here though we considered BPSK modulation in seek of low-complexity. Let us assume an AWGN channel. Thus the received signal vector $\mathbf{y} = [y_1, y_2, \ldots, y_{np}]$ resulting from the transmission of the codeword is,

$$\mathbf{y} = \mathbf{x} + \mathbf{n}. \tag{3.1}$$

Here $\mathbf{n} = [n_1, n_2, \ldots, n_{np}]$. $n_i$, $i \in \{1, \ldots, np\}$ are the iid complex AWGN samples with zero mean and $\sigma^2$ variance per real dimension. Symbol flipping LDPC decoder takes $\mathbf{y}$ as its input.

### 3.5.3 Non-binary LDPC Decoding

Three steps constitute the conventional symbol flipping-based non-binary LDPC decoding algorithm: initialization, flipped symbol position selection and flipped symbol-value selection. In here the last two steps run iteratively till a valid codeword is met [66].

**Initialization**

The a-posteriori probability of the original transmitted $j$-th symbol being $x_j$ provided that the received value is $y_j$,

$$Pr(x_j|y_j) = \frac{f(y_j|x_j)Pr(x_j)}{Pr(y_j)}. \tag{3.2}$$

Furthermore, $f(y_j|x_j) = \frac{1}{2\pi\sigma^2}\exp\left(-\frac{\|y_j-x_j\|^2}{2\sigma^2}\right)$. Let us assume that $Pr(x_j = +1) = Pr(x_j = -1) = \frac{1}{2}$. Hence,

$$Pr(x_j|y_j) = \frac{1}{2C}\exp\left(-\frac{\|y_j - x_j\|^2}{2\sigma^2}\right). \tag{3.3}$$

$C$ is a constant which is to be determined via the property $\sum Pr(x_j|y_j) = 1$.

Let us assume bits constituting a particular symbol $s_k$, $k \in [1, n]$ are independent, thus, $Pr(s_k|\mathbf{y}) = \prod_{j=(k-1)p+1}^{kp} Pr(x_j|y_j)$. The initial hard decision estimate of symbol $s_k$ is obtainable as below:

$$\hat{s}_k = \mathcal{S}(\nu), \tag{3.4}$$

where $\mathcal{S}$ is the $GF(q)$ symbol-space and $\nu = \arg\ \max_\eta Pr(s_k = \mathcal{S}(\eta)|\mathbf{y})$. Furthermore, let

$$llr(s_k = \mathcal{S}(\eta)|\mathbf{y}) = \log\left(\frac{Pr(s_k = \mathcal{S}(\eta)|\mathbf{y})}{1 - Pr(s_k = \mathcal{S}(\eta)|\mathbf{y})}\right) \tag{3.5}$$

define the log-likelihood-ratio (LLR) of symbol $\mathcal{S}(\eta)$ at each symbol position $s_k$.

**Symbol Position Selection**

For the selection of the symbol position to be flipped the single-bit flipping algorithm of [63] and the modified bit-flipping algorithm of Sub-section 3.3.2 is adopted. In here, the symbols' correlation which in turn depends on the structure of the code and the initial symbol reliability values are used to find the symbol position to be flipped.

Let the $n$ symbols' reliability values at the $t$-th iteration be $\mathbf{rel}^{(t)} = [rel_1^{(t)}, \ldots, rel_n^{(t)}] = [|llr(s_1|\mathbf{y})|, |llr(s_2|\mathbf{y})|, \ldots, |llr(s_n|\mathbf{y})|]$ where $s_k$ stands for the now selected symbol at the $k$-th position. During each iteration, a reliability metric $\phi_k$ is calculated, for each symbol $k = 1, \ldots, n$ separately. This calculation is totally based on the set of parity check equations in which the considered symbol is involved in.

Let the symbols those contribute to the $i$-th parity check be given by $\mathcal{N}(i)$, $i = 1, \ldots, \kappa$ and $l_i^{(t)} = \min_{k \in \mathcal{N}(i)} rel_k^{(t)}$ and $u_i^{(t)} = \max_{k \in \mathcal{N}(i)} rel_k^{(t)}$. Then,

$$\phi_{ki}^{(t)} = \begin{cases} rel_k^{(t)} - \frac{l_i^{(t)}}{2} & \text{if } k \in \mathcal{N}(i) \text{ and } \mathrm{z}_i^{(t)} = 0 \\ rel_k^{(t)} - \frac{l_i^{(t)}}{2} - u_i^{(t)} & \text{if } k \in \mathcal{N}(i) \text{ and } \mathrm{z}_i^{(t)} \neq 0, \end{cases} \tag{3.6}$$

where $\mathrm{z}_i^{(t)}$ is the $i$-th parity check syndrome symbol. this syndrome symbol is calculated using the input symbol vector to the decoder during the $t$-th iteration. Then, at the $t$-th iteration and $k$-th symbol position, the metric value can be calculated by

$$\phi_k^{(t)} = \sum \phi_{ki}^{(t)}, \quad k = 1, \ldots, n. \tag{3.7}$$

Note that $\phi_k^{(t)}$ is inversely proportional to the probability of a symbol error.

Therefore, at the end of the $t$-th iteration, we can select a position to be flipped by using

$$k' = \arg\min_k \phi_k^{(t)}. \tag{3.8}$$

**Flipped Symbol-value Selection and Finalization**

In a conventional bit flipping algorithm, at each iteration, the current bit value available is inverted to calculate the new bit value for the selected position. Finally, at the end of each iteration the resultant bit-vector is parity checked. If all the parity checks are satisfied the algorithm is terminated. Otherwise we proceed to the next iteration with the updated hard decision bit vector. Nevertheless, in the case of non-binary LDPC decoding using the symbol flipping algorithm, this is not that simple as the selected position has many candidate symbol values to be placed at that position. In fact we have $q-1$ possible symbol-value candidates out of which we need to select the best. As mentioned in Section 2.1, the currently used symbol flipping algorithms follow two methods to select the new symbol-value for the selected position. In [66,67], the selection of the new flipped symbol-value is considering only the reliabilities of possible candidate symbol-values determined via the initial received signal values. New flipping symbol-value is chosen to be the candidate which has the next best reliability. Alternatively one can convert the selected symbol position over $GF(q)$ into $p$ bit positions where each of these bit positions is associated with a channel output value given by $y_j$, $kp \leq j <$

$(k+1)p$. $|y_j|$ is a measure of the reliability of the bit $j$ [66], thus a set of $f$, $(1 \leq f \leq p)$ bits corresponding to the lowest $|y_j|$ values are selected and inverted. The value $f$ known as *flagbit* is a parameter which starts from 1 at the first decoding iteration and then increments by 1 at each successive iteration. After the flipping, the new symbol value is formed with the use of the newly inverted bit position value and the other $p-1$ bits which constitute the symbol. However, both these methods use only the reliabilities based on initial channel output values. These methods do not use the correlations among bits/symbols introduced due to the channel code in the process of new symbol value selection. In this work we expect the incorporation of this additional correlation information in the flipped symbol-value selection step to produce an improved overall decoding performance. Meanwhile in [68–70] all possible symbols that a position can have are considered in forming the extended symbol combinations set to search for a valid codeword. As already mentioned before we expect a dedicated flipped symbol-value selection to provide an even better performance though the second approach described above considerably improves the decoding performance of the overall non-binary LDPC decoding algorithm.

### 3.5.4 Proposed Symbol-value Selection

In this sub-section a novel symbol-value selection algorithm is proposed for the symbol flipping based non-binary LDPC decoder in seek of an improved performance while retaining the simplicity. The key idea behind the proposed algorithm is the utilization

of the knowledge of both the symbol reliabilities and the correlation available in the channel code.

During every iteration, all other possible candidate symbol-values available at a position selected to be flipped are voted with a positive metric value for every satisfactory parity check the considered symbol-value is involved in. Moreover, for each unsuccessful parity check a symbol is involved in, the symbol value is voted with a negative metric value. Moreover, to incorporate the knowledge available with the initial channel output values, the voting metric values are selected to be related to the initial channel output based reliabilities. This selection eliminates the erroneous decisions made due to erroneous symbol values present at other positions than the position considered.

Let us consider the $t$-th iteration's selected position to be flipped is $k'$ and let $\mathcal{M}(k')$ represent the parity checks in which $s_{k'}$ is involved in. Then one can calculate the candidate symbol-value's metric value as $\mathcal{S}_\nu$ ($\mathcal{S}_\nu \in GF(q)$ and $\mathcal{S}_\nu \neq s_{k'}^{(t)}$) from the $i$-th parity check

$$v_{k',i}^{(t)}(\mathcal{S}_\nu) = \begin{cases} \Gamma_i^{(t)} & \text{if } \mathrm{z}_i^{(t)}(\mathcal{S}_\nu) = 0 \\ -\Gamma_i^{(t)} & \text{if } \mathrm{z}_i^{(t)}(\mathcal{S}_\nu) \neq 0, \end{cases} \tag{3.9}$$

where $\Gamma_i^{(t)} = \left| rel_{k'}^{(t)} - \min_{j \in \mathcal{N}(i)} rel_j^{(t)} \right|$ and $\mathrm{z}_i^{(t)}(\mathcal{S}_\nu)$ represents the $i$-th element of the syndrome vector ($i \in \{1, 2, \ldots, \kappa\}$) with $\mathcal{S}_\nu$ in the $k'$-th symbol position.

An accumulated metric value can be calculate using,

$$v_{k'}^{t}(\mathcal{S}_\nu) = \sum_{i \in \mathcal{M}(k')} v_{k',i}^{t}(\mathcal{S}_\nu). \tag{3.10}$$

Then the new symbol value for the $k'$-th position is given by,

$$s_{k'} = \arg\max_{\mathcal{S}_\nu} v_{k'}^{(t)}(\mathcal{S}_\nu). \tag{3.11}$$

### 3.5.5 Computational Complexity

In this sub-section we evaluate the proposed symbol-value selection algorithm's computational complexity and then compare the same to those of several other existing symbol flipping based non-binary LDPC decoding algorithms. Let us denote the row and the column weight of the parity check matrix and the weight of the syndrome vector by $w_r$, $w_c$ and $w_z$, respectively. Then let us consider an iteration which occurs after the first iteration in order to analyze the computational complexity. As we are considering an iteration after the first iteration we can assume that the LLRs of the symbols and the initial syndrome vector to be available. Thus we do not consider the computations required to calculate these. Furthermore, in seek of simplicity during the search for a valid codeword, the algorithm in [69] considers only a subset of the all possible combinations of symbol vectors having $n$ symbols. This is practically implemented by limiting the number of candidate symbol-values per position and the number of symbol positions considered while calculating the *flipping function* [69]. Let $\epsilon$, ($\epsilon \leq q$) and $\eta$, ($\eta \leq w_r$) denote the symbol-values per position and number of positions respectively. Recall that $\epsilon = 2$ in [69]. Table 3.3 lists the number of real operations needed for the proposed and existing decoding algorithms.

Table 3.3: Number of real operations for the symbol flipping algorithm

| | Symbol Position Selection | symbol-value Selection |
|---|---|---|
| RBA [66] | $(\kappa + w_z)w_r + (w_c - 1)n$ | 0 |
| PSF [68] | | $7\kappa w_r - \kappa$ |
| MVA [69] | | $\kappa\eta\epsilon^{\eta} + (w_c - 1)n\epsilon$ |
| MVPSF [70] | | $7\kappa w_r - n + n\log_2(n)$ |
| Proposed | $(\kappa + w_z)w_r + (w_c - 1)n$ | $2^p w_c + (w_c - 1)(2^p - 1) + 2^p w_c + (2^p - 1)w_c$ |

It is worth to note that the computational complexity of algorithm of [69] has an exponential increment with the $\eta$ value while the complexity of the proposed flipped symbol-value selection step has an exponential complexity increment with the increase order of the Galois field.

Tables 3.4, 3.5 and 3.6 presents the computational complexity of the proposed algorithm together with the other existing algorithms namely, multiple-vote parallel symbol flipping algorithm (MVPSF), multiple-vote symbol flipping algorithm (MVA), parallel symbol flipping algorithm (PSF) and reliability based symbol-value selection algorithm (RBA) in terms of the per iteration required number of real operations. For the simulations we select three non-binary LDPC codes, $1023 \times 781$ LDPC code over GF(16), $63 \times 37$ LDPC code over GF(16) and $204 \times 102$ LDPC code over GF(4). For the $204 \times 102$ LDPC code having $w_c = 3$ and $w_r = 6$, Table 3.4 shows that the on average per iteration real operations required is 1326. Meanwhile in the reliability based algorithms of [66] we require no operations for the symbol selection step while the proposed algorithm requires only 39 real operations for the same. Based on the result we can conclude that the total

number of operations required in the proposed algorithm is very much the same as that the algorithm in [66] for the $204 \times 102$ LDPC code in $GF(4)$. Moreover, compared to the algorithm of [69] the proposed algorithm has significantly less complexity for $\epsilon = 2$ and $\eta = \frac{w_r}{2} = 3$. Though the complexity of the algorithms of [68] and [70] are in the same order as the proposed algorithm, they are approximately 20% and 30% higher in complexity compared to the proposed. Table 3.5 presents the real operations needed per iteration when the $63 \times 37$ LDPC code, with $w_c = w_r = 8$ is used. It is apparent that the symbol position selection step needs 753 operations on average. Meanwhile the symbol selection step of the proposed algorithm consumes 481 operations per iteration in average compared to zero operations in algorithm of [66]. Note that a relatively large number of operations required for the symbol-value selection step due to the higher Galois field order. Anyhow, the increase in the overall complexity as a result of the proposed symbol-value selection step is only marginal for the $63 \times 37$ LDPC code in $GF(16)$ too.

The complexity of the proposed algorithm is still less for $\epsilon = 2$ and $\eta = \frac{w_r}{2} = 4$ when compared to the algorithm of [69]. Table 3.6 shows the computational complexity for the $1023 \times 781$ LDPC code, with $w_c = w_r = 32$. Here the symbol position selection step consumes nearly 43329 operations on average when the proposed algorithm consumes 1969 operations. Once we consider the 559042 operation needed for the algorithm of [69] with $\eta = 8$, proposed algorithm has very much less overall complexity. Moreover, the computational complexities of algorithms of [68] and [70] are approximately 20% and

30% higher than that of the proposed algorithm, respectively.

Table 3.4: Number of real operations for the symbol flipping algorithm for $204 \times 102$, GF(4) LDPC code.

| | Symbol Position Selection | symbol-value Selection |
|---|---|---|
| RBA [66] | 1326 | 0 |
| PSF [68] | | 4182 |
| MVA [69] | | 3264 |
| MVPSF [70] | | 5645 |
| Proposed | 1326 | 39 |

Table 3.5: Number of real operations for the symbol flipping algorithm for $63 \times 37$, GF(16) LDPC code.

| | Symbol Position Selection | symbol-value Selection |
|---|---|---|
| RBA [66] | 753 | 0 |
| PSF [68] | | 1430 |
| MVA [69] | | 2722 |
| MVPSF [70] | | 1769 |
| Proposed | 753 | 481 |

As already mentioned, one of the main drawbacks of the low-complexity joint decoder algorithm presented in Section 3.3 is the lack of sufficient information to decide on a flipped bit combination value whenever the selected positions of the two decoders' codewords are the same but the corresponding hard decision $c_b$ bits are different. To overcome this limitation, the improved symbol-value selection step proposed in Subsection 3.5.4 can be adopted whenever the above mentioned situation occurs.

Table 3.6: Number of real operations for the symbol flipping algorithm for $1023 \times 781$, GF(16) LDPC code.

| | Symbol Position Selection | symbol-value Selection |
|---|---|---|
| RBA [66] | 43329 | 0 |
| PSF [68] | | 53966 |
| MVA [69] | | 559042 |
| MVPSF [70] | | 63173 |
| Proposed | 43329 | 1969 |

## 3.6 Simulation Results and Discussion

The BER performance of the non-binary LDPC decoding algorithm with symbol flipping is investigated here. Note that this algorithm has the proposed symbol-value selection step in extra to the adopted initialization and flipped symbol position selection steps from the algorithm in [63]. This point onwards, we use the term "proposed decoding algorithm" to denote the overall decoding algorithm having the proposed symbol value selection step. We consider a $1023 \times 781$ LDPC code over $GF(16)$, a $63 \times 37$ LDPC code over $GF(16)$ and a $204 \times 102$ LDPC code over $GF(4)$ for the performance investigation. Let's consider an AWGN channel where iid zero-mean Gaussian noise samples are added to the received signal.

In Fig. 3.4, Fig. 3.5 and Fig. 3.6 we present the BER and frame error rate (FER) performances. The BER and FER performances of algorithms of [66], [68], [69] and [70] are also presented for comparison.

Compared to the 2-stage algorithm in [66], the proposed algorithm offers an approximately 0.8 $dB$ BER performance improvement at $10^{-4}$ BER level which is visible in

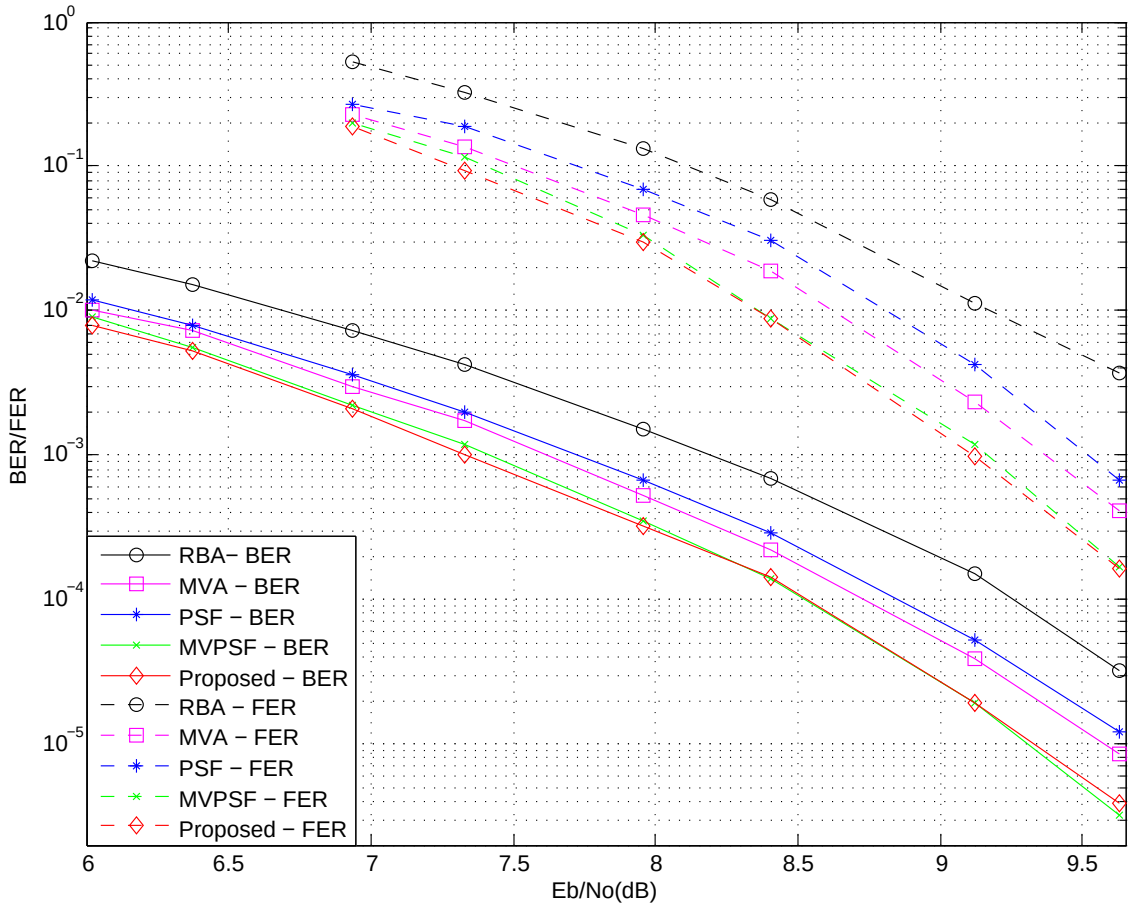


Figure 3.4: Comparison of decoder BER performance for $204 \times 102$, GF(4) LDPC code.

Fig.3.4, Fig.3.5 and Fig.3.6. The reason for this improvement is the use of correlation among the symbols to determine the new flipped-symbol-value. Furthermore, the proposed algorithm is superior than the algorithm of [69] by nearly 0.3 dB and the algorithm of [68] by nearly 0.4 dB in the BER performance at $10^{-4}$ BER level. We can also observe superior FER performances of approximately 1dB, 0.5dB and 0.3dB respectively at $10^{-3}$ when the proposed algorithm is compared to the algorithms of [66], [68] and [69]. The algorithm of [70] has a very much similar BER performance to the proposed. It is

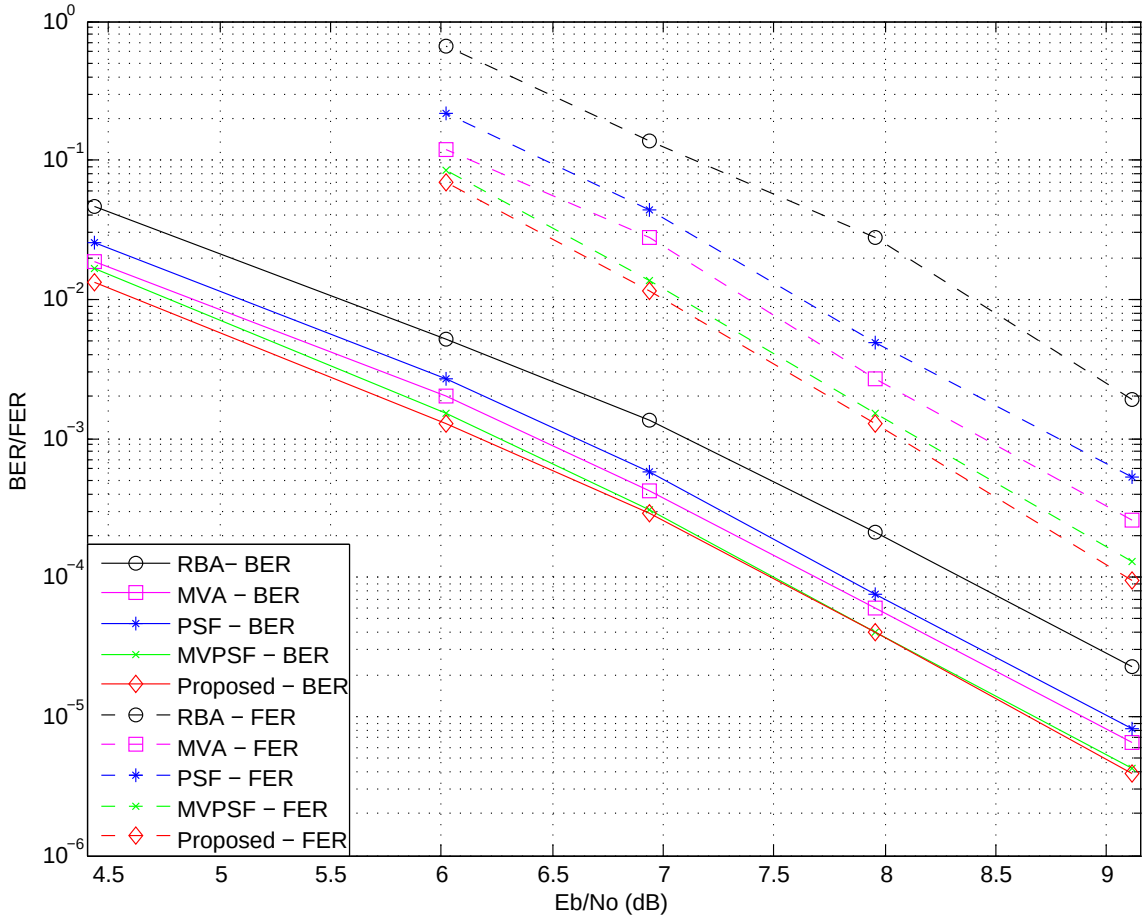


Figure 3.5: Comparison of decoder BER performance for $63 \times 37$, GF(16) LDPC code.

noteworthy that the algorithm of [70] is a combined algorithm of those in [68] and [69], hence it harnesses the coding gains of both the algorithms. We note that the proposed algorithm's novel flipped symbol-value selection step has been able to obtain a coding gain that matches with the high coding gain of the combined algorithm in [70].

Moreover, the simulation results demonstrate that the algorithm of [66] converges after 6.5 iterations on average, while the proposed algorithm converges only in 4.8 iterations on average. Therefore, the overall computational complexity of the proposed algorithm

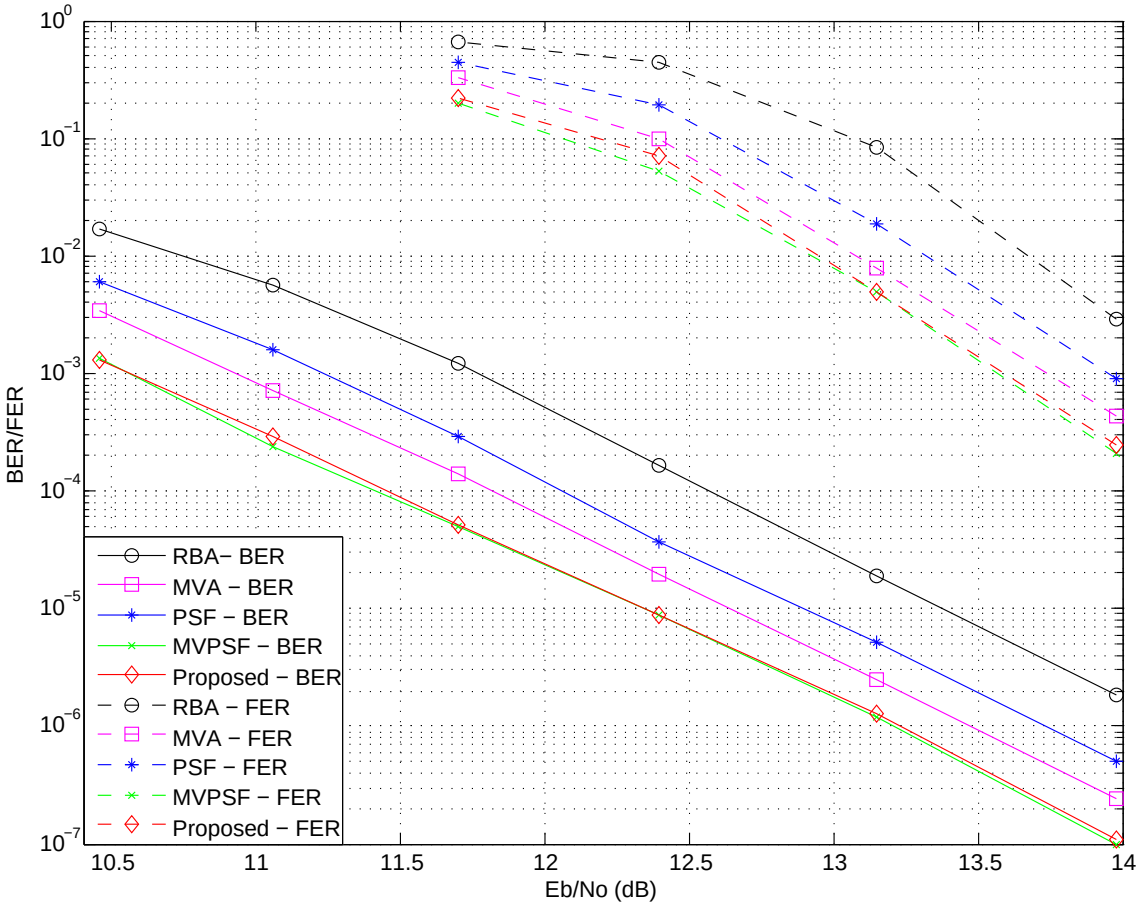


Figure 3.6: Comparison of decoder BER performance for $1023 \times 781$, GF(16) LDPC code.

is only marginally higher than that of the algorithm of [66]. On the other hand, in terms of the real operations required for an iteration, we have a very low-complexity in the proposed algorithm compared to the algorithms of [69] and [70]. In summary, with the proposed flipped symbol-value selection step, it obtains a higher error performance very similar to that of [70], but with much less complexity.

Next, let us investigate the BER performance of the proposed low-complexity joint

channel decoding - physical layer network coding algorithm for the multi-way relay systems. For comparison purposes the BER performance of the separate decoding scheme which doesn't exchange information between decoders is also presented. The BER performance of the joint decoding algorithm proposed in [61] which employs belief propagation for the channel decoder is also produced. Let us consider the same $255 \times 175$ and $1023 \times 781$ FG-LDPC codes used for the computational complexity comparison. Furthermore, let us assume that the channels between the relay and nodes undergo uncorrelated quasi-static Rayleigh block fading with unity parameter value. In Figures 3.7 and 3.8, the BER performances of the proposed improved low-complexity joint channel network coding algorithm is compared with the BP based joint decoding algorithms and BF based algorithm which ignores the additional time diversity. The BER performance of the joint decoder algorithm presented in Section 3.3 is also shown. It can be observed that the BF based low-complexity algorithm presented in Section 3.3 achieves a much superior performance compared to the separately decoding algorithm in which the additional time diversity is not considered. This is further improved in the improved joint decoding algorithm presented in 3.5. Nevertheless, the BP based algorithm in [61]'s BER performance is much superior than the proposed algorithm.

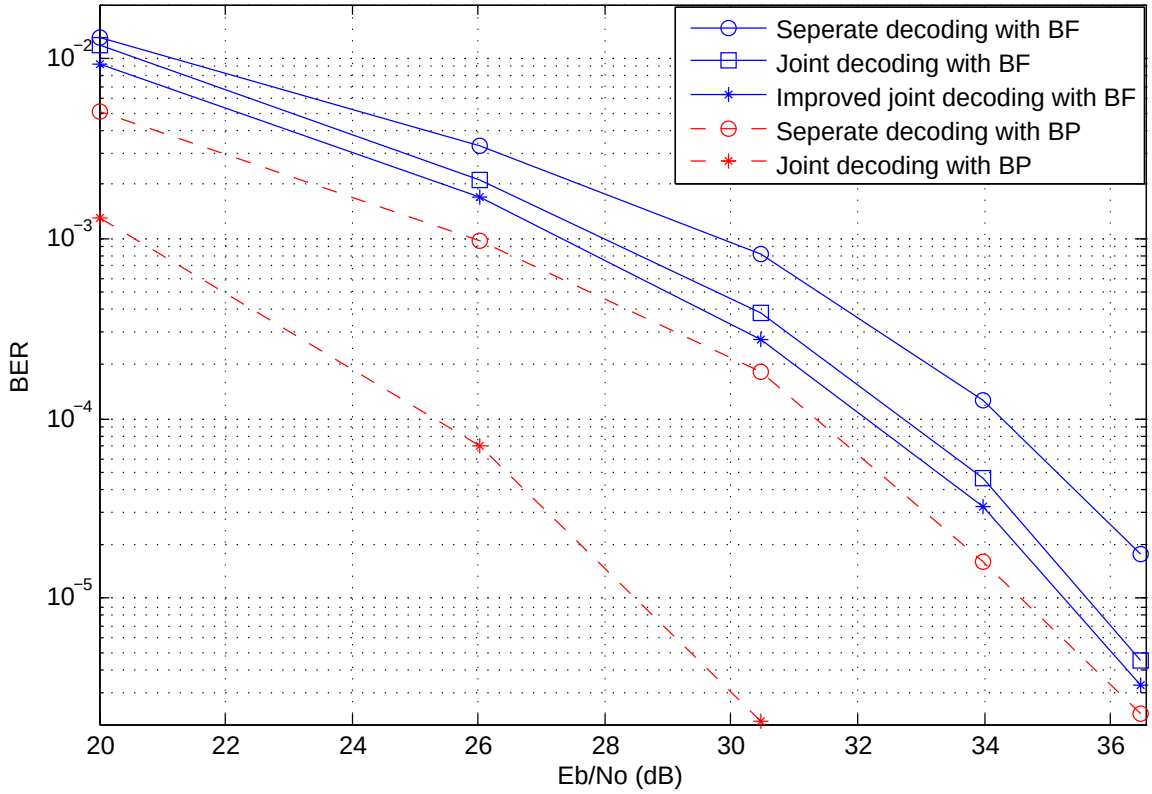


Figure 3.7: Comparison of decoder BER performance for $255 \times 175$ LDPC code.

## 3.7 Conclusion

In this chapter, a low-complexity joint channel-physical layer network coding algorithm had been proposed which is to be deployed in multi-way relay systems [71]. The key element of the proposed decoding algorithm for a 3-way relay system is the exchange of hard information between the two channel decoders operating simultaneously. This information exchange exploits the additional time-diversity gain present due to the duplicated transmission of node B information. Therefore, the proposed algorithm's performance is much superior compared to separately BF based channel decoding and network coding

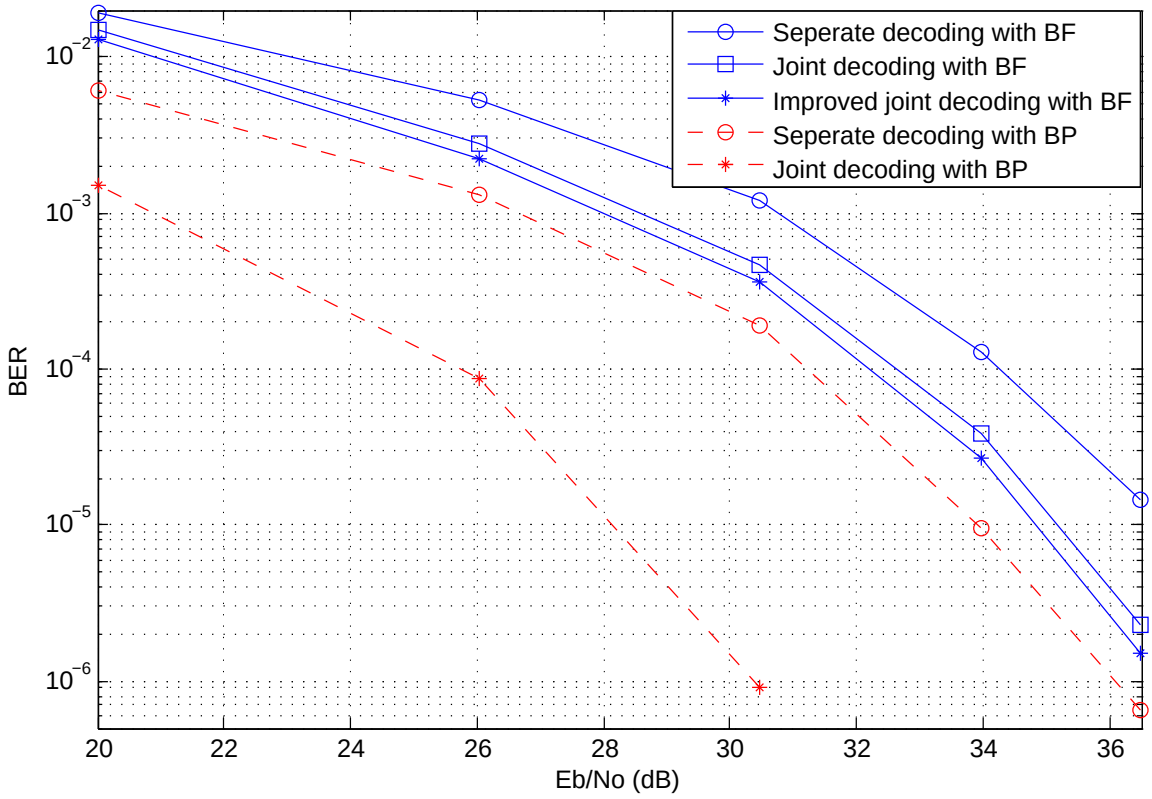


Figure 3.8: Comparison of decoder BER performance for $1023 \times 781$ LDPC code.

algorithm. Also due to the employment of the BF decoder in place of a BP decoder, the joint decoder complexity has greatly reduced.

Furthermore, in seek of an an improved overall BER performance, an improved symbol-value-selection step for the symbol flipping based non-binary LDPC decoder is also proposed [72]. It is apparent from the simulation results that the proposed symbol flipping algorithm obtains a better error performance than all the currently available similar algorithms while maintaining the low-complexity except the algorithm of [70]. Error performance of the proposed algorithm is almost equal to that in [70]. How-

ever, in terms of the decoder complexity, the proposed algorithm is much superior when compared to [70].

However, there is an exponential increment in the computational complexity of the proposed algorithm when the non-binary field's order is increased. This constraint limits the use of higher order non-binary fields which is a major drawback of the proposed algorithm. The proposed flipped symbol-value selection algorithm is then adopted in the low-complexity joint channel-physical layer network coding algorithm for an enhanced BER performance with only a non-significant added complexity.

Further work includes the investigation of the proposed algorithm in continuous time varying channels which will relieve the block fading assumption. Moreover, the the BF algorithm has a tendency to enter in to loops so that the algorithm does not converge in certain cases. Therefore, the investigation of techniques to avoid such loops would also be a future research direction.

# Chapter 4

# Joint Channel-Network Coding in Unequally Error Protected Multi-way Wireless Relay Systems

## 4.1 Introduction

The multi-way wireless relay systems are usually heterogeneous. In other words, the channels from different nodes to the relay may undergo different channel impairment conditions. So far, this research has been focusing on a system model where the multiple nodes transmit to the relay in pairs and the selection of pairs is mainly based on the quality of the channels between the nodes and the relay. However, a scheme of transmission as in [61] and [62] would be ill-treating the nodes associated with poor quality

channels and the throughput of these nodes will be considerably low. Therefore, it may not be very effective to protect all channels with the same channel code. Employing a single channel code with high code rate for all nodes will result in a higher BER as it is incapable of catering poor quality channels. At the same time, a single code with a lower rate employed for all nodes' communication would result in a reduced throughput without producing a significant BER performance improvement. Thus, the need for an asymmetric error protection is obvious to meet a trade-off between error performance and the throughput.

Enlightened by this fact, an asymmetric error protection scheme is proposed for the PNC coded multi-way wireless relay systems. Though asymmetric error protection in multiple channels had been explored in literature [73–76], asymmetric error protection in a JCPNC system is a completely novel contribution. Moreover, a JCPNC algorithm is also proposed to be deployed at the relay of an asymmetrically error protected multi-way relay system. This asymmetric error protection is expected to provide a trade-off between the error performance and the throughput. In this scheme the bit streams communicated poor quality channels are encoded with a larger block length channel code having a low code rate while the communications through good quality channels are encoded with high rate codes with lower block lengths. This ensures that communication from the nodes to relay through poor quality channels are given comparatively higher protection. To facilitate the pairwise joint channel decoding proposed in sub-section 4.4 while providing the aforementioned multi-level protection, each node employs a linear

block channel code whose parity checks are distributed among the multiple nodes. In practice this is achieved by employing a full length channel code with a $k$ number of parity checks for the nodes with poor quality channel while code punctured versions [77, 78] of the original channel code with the number of parity checks $k'(< k)$ are employed at the nodes associated with good quality channels.

The rest of the chapter is organized as follows. Section 4.2 presents the system model followed by the presentation of the throughput enhancement gained by the proposed model over the conventional multi-way relay communication models in Section 4.3. In Section 4.4 we present the proposed JCPNC algorithm for the unequally error protected multi-way relay system. Section 4.5 elaborates on the scaling of the proposed algorithm to higher number of nodes. Section 4.6 and Section 4.7 are dedicated to present simulation results with a discussion and a conclusion respectively.

## 4.2 System Model

Let us consider the same three-way relay system as in Chapter 2 in which nodes A, B and C are exchanging their information via a relay R as shown in Fig.2.1. In order to present the proposed communication system model and the decoder algorithm, let us assume that the channel from node B to relay to have relatively less quality when compared to other two channels. As a result, the node selection for pair-wise transmission selects the nodes A and B for the communication during the first time-slot while nodes B

and C are scheduled to communicate during time-slot 2. It is important to select the nodes associated with the relatively low quality channel to transmit twice when the aforementioned communication scheme is extended to a multi-way relay system.

First, blocks of $n$ bits are formed by grouping the information bit streams of nodes A, B and C. Let $\zeta$ denote a $[n \times (n+k_1+k_2)]$ binary low density parity check (LDPC) code. Let us create two LDPC codes with higher rates after performing code puncturing [77] on $\zeta$. During the code puncturing one should make sure that the parity checks in the two resultant codes are non-overlapping, thus the two punctured codes are uncorrelated. Let us use $\zeta_1 : [n \times (n+k_1)]$ and $\zeta_2 : [n \times (n+k_2)]$ to denote the two codes created. Three bit vectors of lengths $n+k_1+k_2, n+k_1$ and $n+k_2$ are generated by encoding the nodes B, A and C's bit blocks with codes $\zeta, \zeta_1, \zeta_2$, respectively. It is noteworthy that selecting $k_1$ and $k_2$ to be inversely proportional to the quality of the respective associated channel can yield better performances.

Three base-band symbol vectors $\mathbf{s}_a \in \{-1,1\}^{n+k_1}, \mathbf{s}_b \in \{-1,1\}^{n+k_1+k_2}$ and $\mathbf{s}_c \in \{-1,1\}^{n+k_2}$ are generated by BPSK modulating the three coded bit vectors. The output symbol vectors are then transmitted in pairs, first A and B and then B and C as shown in Fig. 4.1. Consider the $j$-th symbol duration ($j = 1, 2, \ldots, n+k_1$) of the first time-slot during which A and B transmission occurs. The received signal at the relay is given by

$$y_{ab}(j) = h_{A1}s_a(j) + h_{B1}s_b(j) + n_{ab1}(j). \tag{4.1}$$

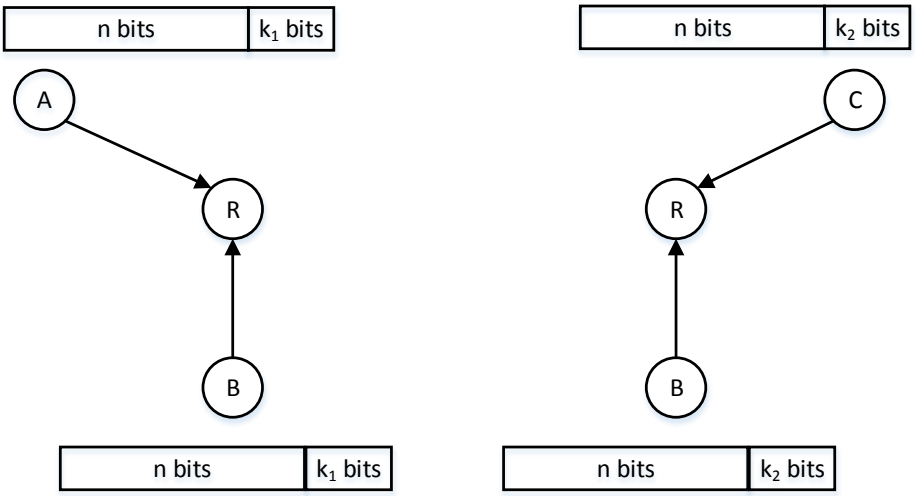


Figure 4.1: Asymmetric information exchange

Similarly, at the $j'$-th symbol duration during the second time-slot ($j' = 1, 2, \ldots, n + k_2$)

$$y_{bc}(j') = h_{B2}s_b(j') + h_{C2}s_c(j') + n_{bc2}(j'), \tag{4.2}$$

is received at the relay. Here $h_{A1}$, $\{h_{B1}, h_{B2}\}$ and $h_{C2}$ are the Rayleigh block fading channel coefficients between the nodes A, B & C and the relay. $n_{ab1}(j)$ and $n_{bc2}(j')$ s are the AWGN samples with zero mean and $\sigma^2$ variance. Relay first decodes $\mathbf{y}_{ab} = \{y_{ab}(1), y_{ab}(2), \ldots, y_{ab}(n + k_1)\}$ and $\mathbf{y}_{bc} = \{y_{bc}(1), y_{bc}(2), \ldots, y_{bc}(n + k_2)\}$ for $\mathbf{c}_a \oplus \mathbf{c}_b$ and $\mathbf{c}_b \oplus \mathbf{c}_c$. Thereafter, relay separately encodes the resulting $n$ dimensional bit vectors using the same $[n \times (n + k_1 + k_2)]$ channel code, BPSK modulates and broadcasts in two time-slots. The individual nodes A, B and C then use the received signals to calculate the information bits coming from other nodes, as shown in [61].

## 4.3 Throughput Enhancement

Recall that the motivation for asymmetric error protection is to have an improved trade-off between the BER performance and the throughput. By employing a a low-rate channel code to encode in the poor quality channel and relatively high-rate channel code to encode in the good quality channels, the corresponding information exchange scheme consumes only $(2n + k_1 + k_2) + 2(n + k_1 + k_2)$ bit-intervals for a full exchange of information. Recall that a conventional three-way relay system using $n + k_1 + k_2$ length channel code for all channels in the system consumes $4(n + k_1 + k_2)$ bit-intervals. Thus, the proposed asymmetric error protection scheme achieves a bit-intervals saving given by

$$\begin{aligned} \varrho &= \frac{k_1 + k_2}{4(n + k_1 + k_2)} \\ &= \frac{1}{4\left(\frac{n}{k_1+k_2} + 1\right)}, \end{aligned} \tag{4.3}$$

which also result in a spectral efficiency of

$$\eta = \frac{1}{1 - \varrho}. \tag{4.4}$$

## 4.4 Iterative Joint Decoding at the Relay

As already mentioned, the main interest in this work is the bit-flipping based hard-decision decoding. This decoding process produces $\mathbf{c}_a \oplus \mathbf{c}_b$ and $\mathbf{c}_b \oplus \mathbf{c}_c$ bit vectors at the relay node. Three key steps constitute the decoding process: initialization, iterative message passing and finalization.

### 4.4.1 Initialization

Considering the simultaneous communication of nodes A and B during the $j$-th bit-interval ($j \in \{1, \ldots, n + k_1\}$), received signal's realization falls on to one of the four equi-probable constellation points given by $\hat{y}_{ab} \in \{-h_{A1} - h_{B1},\ -h_{A1} + h_{B1},\ h_{A1} - h_{B1},\ h_{A1} + h_{B1}\}$. Thus the transmitted combined signal's a-priori probability $s_{ab} = \mathcal{S}(i)$ is given by,

$$Pr\left\{s_{ab} = \mathcal{S}(i)\right\} = \frac{1}{4}, \tag{4.5}$$

where $\mathcal{S}(i) \in \{(-1-1), (-1+1), (+1-1), (+1+1)\}$.

Hence, the conditional probability density function of $y_{ab}$ given a certain symbol combination being transmitted is,

$$Pr\{y_{ab}\,|s_{ab} = \mathcal{S}(i)\} = \frac{1}{2\pi\sigma^2} exp - \left(\frac{\|y_{ab} - \hat{y}_{ab}(i)\|^2}{2\sigma^2}\right). \tag{4.6}$$

Thus, $p_i$, ($i \in \{0, 1, 2, 3\}$) which denotes the probability of symbol $\mathcal{S}(i)$ had been trans-

mitted given the received value $y_{ab}$ is,

$$\begin{aligned} p_i &= Pr\{s_{ab} = \mathcal{S}(i)\,|y_{ab}\} \\ &= Pr\{y_{ab}\,|s_{ab} = \mathcal{S}(i)\} \times \frac{Pr(s_{ab} = \mathcal{S}(i))}{Pr(y_{ab})} \\ &= Pr\{y_{ab}\,|s_{ab} = \mathcal{S}(i)\} \times C. \end{aligned} \tag{4.7}$$

Here, $C = \frac{1}{4Pr(y_{ab})}$ is a constant which can be calculated using the property $\sum p_i = 1$. In the same way, corresponding to each bit position $j' \in \{1, \ldots, n + k_2\}$, $Pr\{s_{bc} = \mathcal{S}(i)\,|y_{bc}\}$ can also be calculated .

### 4.4.2 Iterative Decoding

Let us consider the proposed iterative decoder shown in Fig. 4.2. Let the two four dimensional soft-information vectors at the two decoders decoding $\mathbf{c}_a \oplus \mathbf{c}_b$ and $\mathbf{c}_b \oplus \mathbf{c}_c$ be $[p_0(j), p_1(j), p_2(j), p_3(j)]$ and $[p_0(j'), p_1(j'), p_2(j'), p_3(j')]$. Hence, in a single constituent sub decoder decoding can be carried out as in Chapter 2 and [61].

It is worth to be recalled that a lower rate channel code is employed to encode node B's bit vector seeking a relatively higher error protection. In order A third decoder is employed after the two joint sub-decoders used in Chapter 2 in seek of exploiting this extra coding gain.

During each iteration a decoding operation as in [44] is performed by the two sub-decoders decoding for $\mathbf{c}_a \oplus \mathbf{c}_b$ and $\mathbf{c}_b \oplus \mathbf{c}_c$. Thereafter, the node B's soft-information is

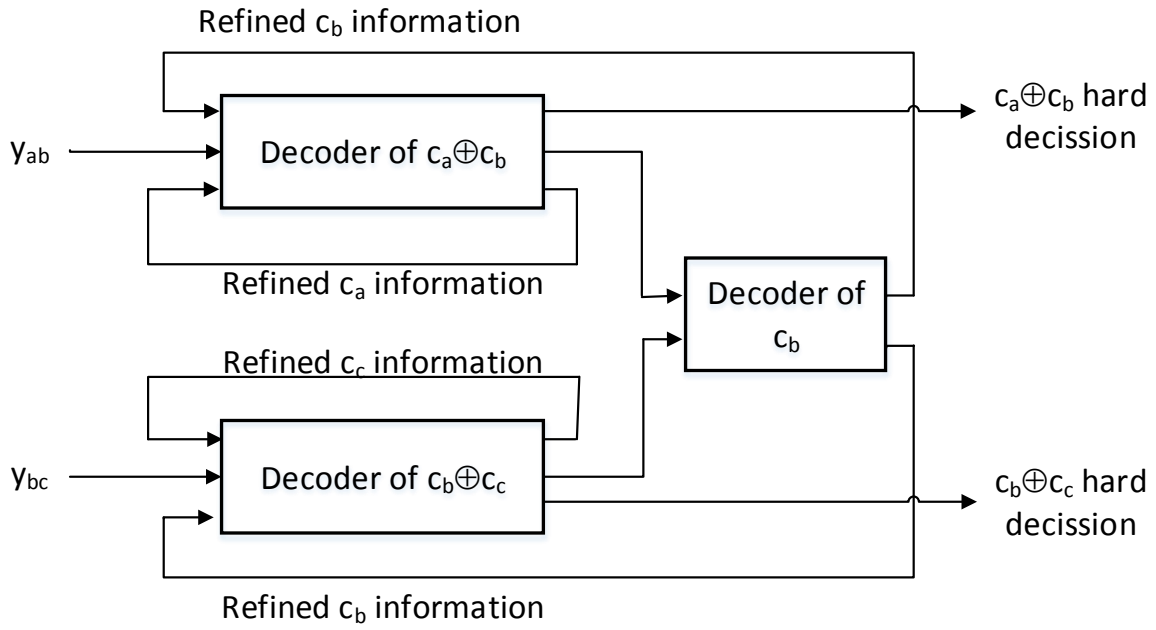


Figure 4.2: Proposed decoder arrangement

extracted at the two sub-decoders as done in the algorithm in Chapter 2. Thereafter the calculation of the combined soft-information corresponding to node B is as follows:

1. Two soft-information sets are present corresponding to the $n$ information bits, which are coming from the output of each of the sub-decoders discussed above. these information can be combined as in Sub-section 2.3.2 and [61],

$$LLR_y(c_b|\Lambda) = \kappa \frac{[LLR_{ab}(c_b|\Lambda) + LLR_{bc}(c_b|\Lambda)]}{2}, \tag{4.8}$$

where $\kappa = \frac{h_{B1}+h_{B2}}{h_{B1}^2+h_{B2}^2}$, $LLR_{ab}(c_b|\Lambda) = \log\left(\frac{P_{ab}(c_b=1|\Lambda)}{P_{ab}(c_b=0|\Lambda)}\right)$ and $LLR_{bc}(c_b|\Lambda) = \log\left(\frac{P_{bc}(c_b=1|\Lambda)}{P_{bc}(c_b=0|\Lambda)}\right)$. This combined soft-information is used to replace node B's soft-information at the two decoders as described in Sub-section 2.3.2 and [61].

2. A soft-information vector corresponding to node B having a dimension of $n+k_1+k_2$ is prepared by using the combined soft-information of the $n$ information bits as given in 1), soft-information corresponding to $k_1$ parity bits coming from the output of the decoder for $\mathbf{c}_a \oplus \mathbf{c}_b$ and soft-information corresponding to $k_2$ parity bits coming from the decoder for $\mathbf{c}_b \oplus \mathbf{c}_c$. The decoder of $\mathbf{c}_b$ codeword is using this $n+k_1+k_2$ dimensional complete soft-information vector as its input.

3. At the output of the decoder for $\mathbf{c}_b$ codeword we have further refined node B's soft-information. During the next iteration, this refined information is again combined with the soft-information of node A and then is fed as apriori information to the $\mathbf{c}_a \oplus \mathbf{c}_b$ decoder.

$$\begin{aligned} p_0 &= Pr(c_a = 0|\Lambda)Pr(c_b = 0|\Lambda) \\ p_1 &= Pr(c_a = 0|\Lambda)Pr(c_b = 1|\Lambda) \\ p_2 &= Pr(c_a = 1|\Lambda)Pr(c_b = 0|\Lambda) \\ p_3 &= Pr(c_a = 1|\Lambda)Pr(c_b = 1|\Lambda). \end{aligned} \tag{4.9}$$

In the same manner, the probabilities $\{p_0, p_1, p_2, p_3\}$ at the input of the decoder of $\mathbf{c}_b \oplus \mathbf{c}_c$ can also be determined and this soft-information is used in the $\mathbf{c}_b \oplus \mathbf{c}_c$ decoder at the next iteration.

### 4.4.3 Finalization

A PNC mapping is performed at the end of each full iteration as per the rule,

$$c_{ab}(j) \;=\; \mathcal{C}_{\eta}. \tag{4.10}$$

Here, $\eta = \arg\max_i \;\; p_i(j)$. $p_i(j)$ where $i \in \{0, 1, 2, 3\}$ are the elements of the output soft-information vector at the $j$-th symbol position at the decoder of $\mathbf{c}_a \oplus \mathbf{c}_b$.

$$c_{bc}(j') \;=\; \mathcal{C}_{\eta'}, \tag{4.11}$$

where $\eta' = \arg\max_i \;\; p_i(j')$. $p_i(j')$ where $i \in \{0, 1, 2, 3\}$ are the elements of the output soft-information vector at the $j'$-th symbol position at the decoder of $\mathbf{c}_b \oplus \mathbf{c}_c$.

Finally a parity checking is carried out for the resultant XORed codewords. The proposed algorithm is terminated upon the satisfaction of all parity checks or reaching a pre-defined number of iterations.

## 4.5 Extending the Unequal Error Protection Scheme to $\mathcal{M} > 3$

We so far considered a three-way relay system in seek of simplicity. Nevertheless, the number of participating nodes in a real world multi-way relay system can be more such

that $\mathcal{M}$ ($\mathcal{M} > 3$). However the same unequally error protection scheme can be extended to such a relay system. Let $\mathcal{M}$ number of nodes are denoted as $A_1, A_2, \ldots, A_{\mathcal{M}}$ so that the nodes $A_1$ and $A_{\mathcal{M}}$ are associated with the two best quality channels. $A_1$ and $A_2$ transmit symbol vectors having a dimension $n + k_1$ in each,to the relay, during the first time-slot. $A_2$ and $A_3$ transmit symbol vectors having a dimension $n + k_2$ during the second time-slot. Next, $A_3$ and $A_4$ transmit $n+k_1$ dimensional symbol vectors during the third time-slot. In this manner all node pairs transmit using either $k_1$ or $k_2$ parity bits at a time. It is worth to note here that the information bits from nodes $\{A_2, \ldots, A_{\mathcal{M}-1}\}$ are transmitted twice. Thus, this duplicated transmission can be exploited to obtain an additional diversity gain. All $\mathcal{M} - 1$ decoded XOR bit vectors are broadcasted during the broadcast phase,taking $\mathcal{M} - 1$ time-slots, each having $n + k_1 + k_2$ coded bits.

### 4.5.1 Throughput

A $[(n + k_1) + (n + k_2) + \ldots] + (\mathcal{M} - 1)(n + k_1 + k_2)$ total number of bit-intervals are needed when completing a full information exchange using the proposed algorithm. On the other hand, $2(\mathcal{M} - 1)(n + k_1 + k_2)$ number of bit-intervals are required when using a full length code for all nodes. Thus, the proposed scheme obtains a bit-interval saving,

$$\varrho = \begin{cases} \frac{1}{4\left(\frac{n}{k_1+k_2}+1\right)} & \text{if } \mathcal{M} \text{ is odd} \\ \frac{\frac{\mathcal{M}}{\mathcal{M}-1} - \frac{2}{\mathcal{M}-1}\left(\frac{k_1}{k_1+k_2}\right)}{4\left(\frac{n}{k_1+k_2}+1\right)} & \text{if } \mathcal{M} \text{ is even.} \end{cases} \tag{4.12}$$

When $k_1 = k_2$, we get an identical bit-interval saving for both odd and even number of nodes which only depends on the code rate. Therefore, the throughput enhancement in turn depends only on the code rate.

### 4.5.2 Scaled Joint Decoder Algorithm

The JCPNC algorithm proposed in Section 4.4 for an asymmetric three-way relay system can easily be extended to a multi-way relay system where $\mathcal{M} > 3$. In this extended decoder algorithm, the soft-information corresponding to nodes $\{A_2, \ldots, A_{\mathcal{M}-1}\}$ are individually decoded and fedback to the joint sub-decoders during each iteration which are again used by the joint sub-decoders during the next iteration. In comparison to a decoding scheme employed in a symmetrically error protected system, the proposed algorithm is expected to yield an improved BER performance.

## 4.6 Numerical Results and Discussion

This section first presents the throughput enhancement gained by the proposed asymmetrically error protected scheme. Bit-intervals saving factor and the corresponding spectral efficiency for the two extreme possible code rates and for a code rate value of 0.5 are listed in Table 4.1. Moreover, the variation of spectral efficiency ($\eta$) with the code rate is shown in Fig. 4.3. Note that the throughput enhancement is equal to $1 - \eta$. Hence, the upper bound for the throughput improvement achieved via the

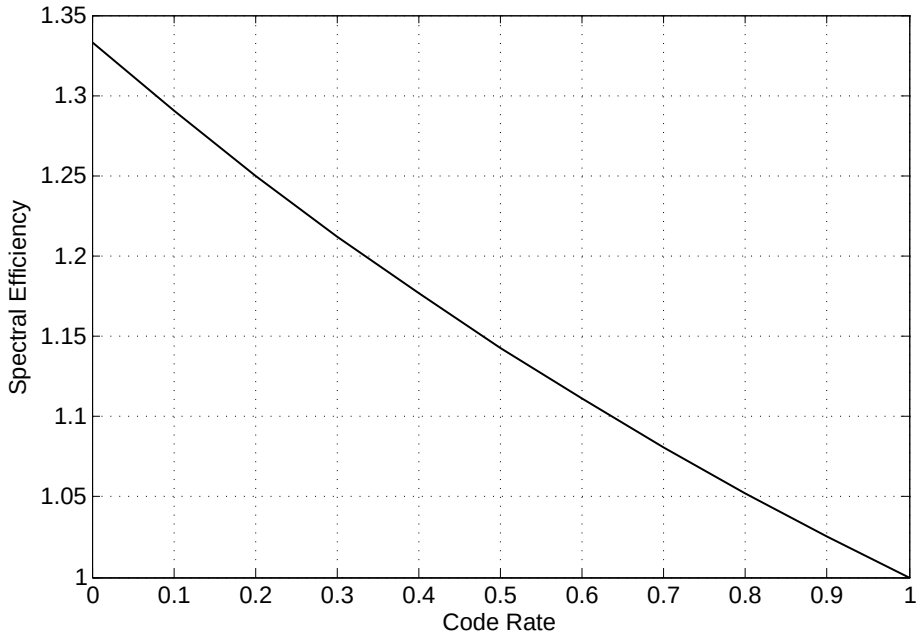


Figure 4.3: Spectral efficiency for different code rates

proposed scheme is 33.33%, while this throughput improvement is above 20% for code rates below 0.33. Note that this is an additional throughput improvement over that is gained by the deployment of PNC.

Table 4.1: Spectral efficiency for different code rates

| Code Rate | $\frac{n}{k_1+k_2}$ | $\varrho$ | $\eta$ |
|---|---|---|---|
| 0 | 0 | 0.25 | 1.33 |
| 0.5 | 1 | 0.125 | 1.14 |
| 1 | $\infty$ | 0 | 1 |

Next the BER performance of the proposed JCPNC algorithm for asymmetrically error protected three-way relay systems is investigated. In seek of simplicity it is assumed that $k_1 = k_2$. However, selecting the $k_1$ and $k_2$ values inversely proportional to the

channel coefficient, is expected to yield better results. A $63 \times 37$ very short LDPC code and also a $255 \times 175$ medium length LDPC code are used for the simulations. By applying code puncturing [77], $50 \times 37$ and $215 \times 175$ two higher rate punctured LDPC codes are obtained each. In order to compare, the BER performance of the algorithm presented in [61] is also considered under symmetric error protection with $50 \times 37$ high rate LDPC code and $63 \times 37$ full length original LDPC code. We also assume the Raleigh fading to be static over a block period having unity parameter value. Fig. 4.4 and Fig. 4.5 presents the BER performance obtained via the proposed decoder algorithm. It can be easily observed that our proposed scheme outperforms a scheme in which the high rate channel code is used in all nodes, by nearly a 3dB additional coding gain. On the other hand its BER performance is less than about 3dB once compared with a system fully error protected with the low rate code in all nodes. Convergence is obtained in the proposed decoder algorithm within 5 decoder iterations as shown in Fig. 4.6. We also present the BER performance for a four-way relay system in Fig. 4.7 which verifies the superior BER performance than the symmetrically error protected systems.

## 4.7 Conclusion

This chapter presents a new asymmetrically error protected communication system model which is to be employed in the multi-way wireless relay systems which is expected to provide a better trade off between the BER performance and the spectral

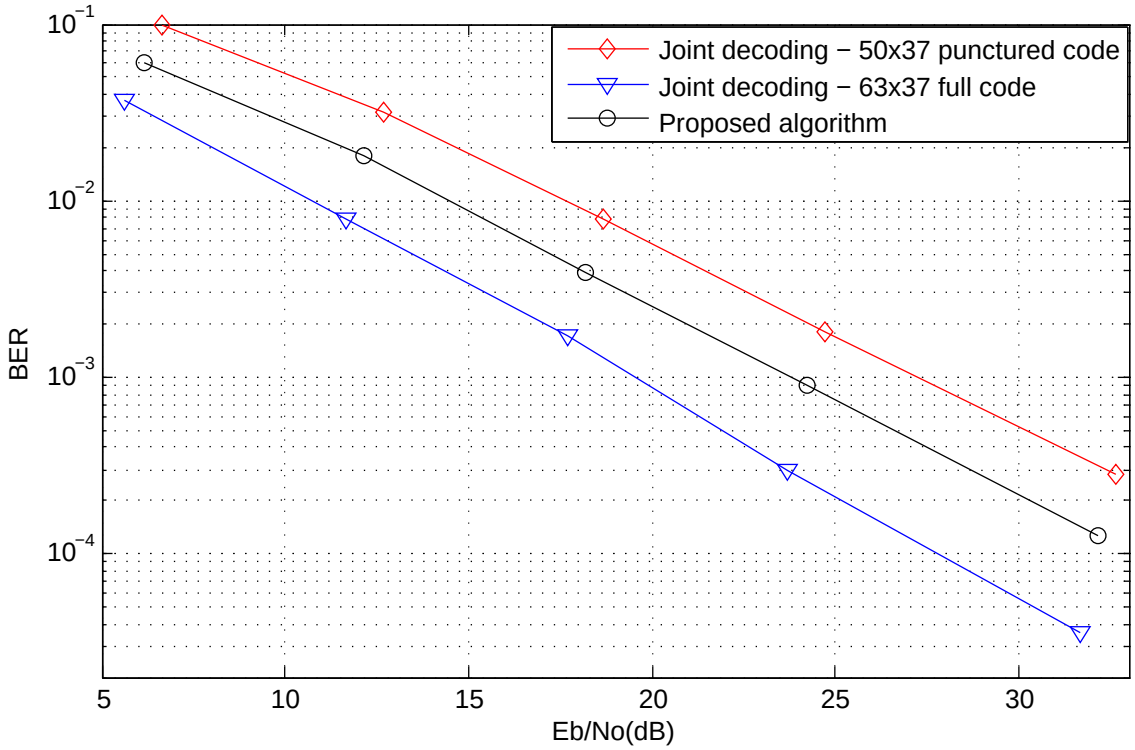


Figure 4.4: BER performance for $63 \times 37$ LDPC code

efficiency. Moreover, a novel JCPNC algorithm for the asymmetrically error protected system is also presented which has three constituent low density parity check decoders. By using the joint information present at the two decoders decoding for $\mathbf{c}_a \oplus \mathbf{c}_b$ and $\mathbf{c}_b \oplus \mathbf{c}_c$, the presented algorithm extracts soft-information corresponds to $\mathbf{c}_b$. After combining different versions of soft-information corresponding to node B, it then carries out an extra decoding iteration for which involves an extended LDPC code. The full length LDPC code's decoding yields a additional coding gain for $\mathbf{c}_b$. Furthermore, with this additional coding gain, an improved BER performance is obtained in the decoders of $\mathbf{c}_a \oplus \mathbf{c}_b$ and $\mathbf{c}_b \oplus \mathbf{c}_c$.

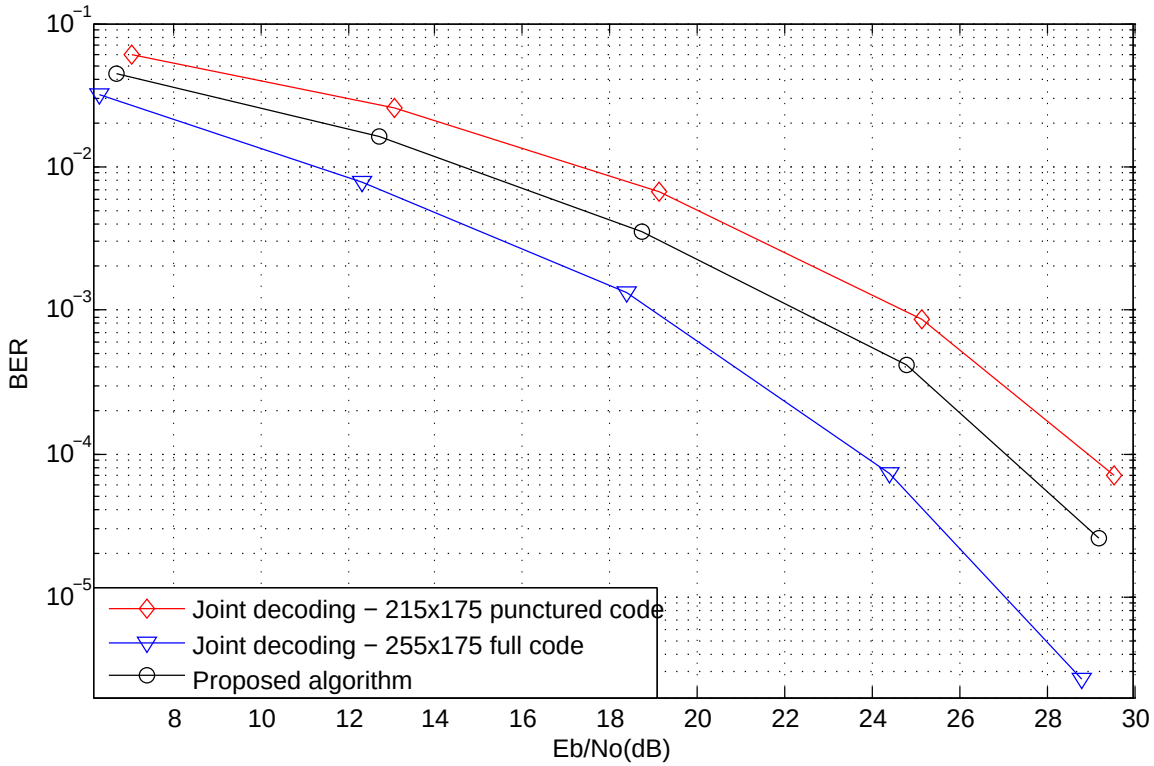


Figure 4.5: BER performance for $255 \times 175$ LDPC code

A superior BER performance of the proposed algorithm is observed from the simulation results when unequal error protection is employed in multi-way relay systems. Meanwhile by performing the unequal error protection, the additional spectral efficiency gained is above 20% when code rates fall below 0.33. This is a practically viable solution to improve the error resiliency and the spectral efficiency together. One of the key issues in the proposed scheme is that when the proposed communication scheme is applied in a practical relay system, we are unable to match the optimum coding rate required for each and every channel as we are compelled to use either $k_1$ or $k_2$ parity bits for error protection. In this work quasi-static block fading channels were considered, thus future

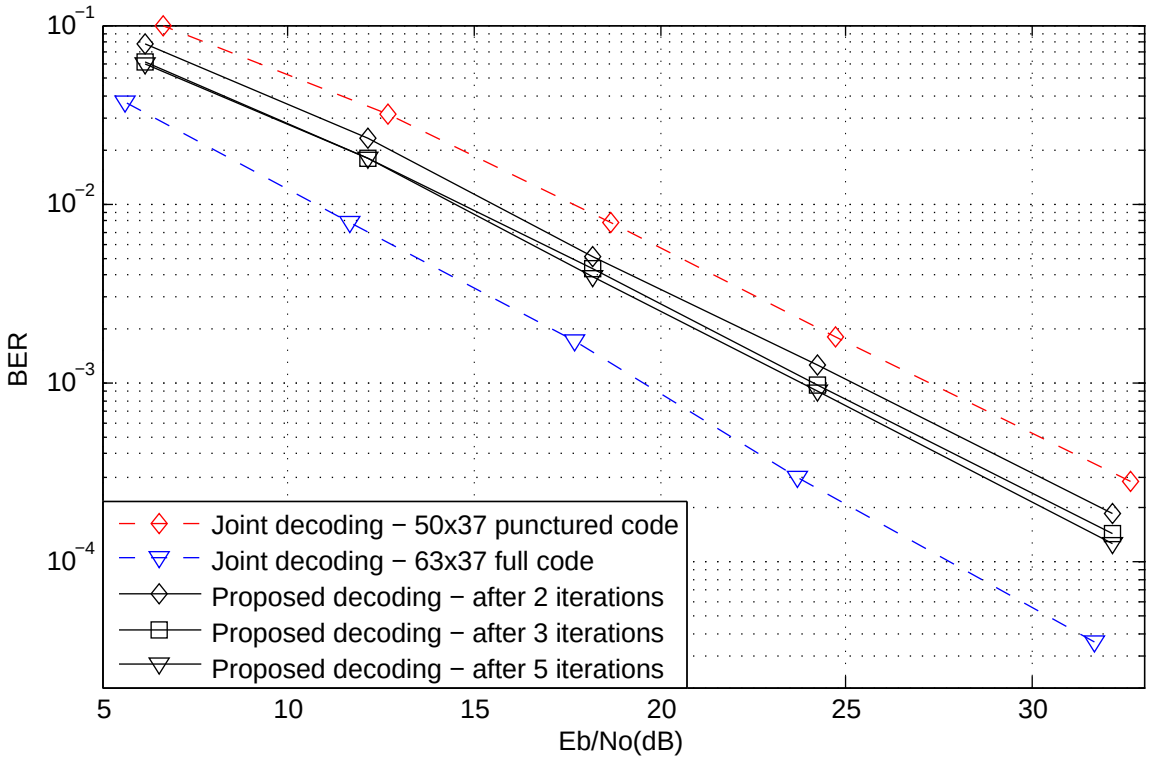


Figure 4.6: Convergence of the proposed decoder algorithm

work includes extending the proposed algorithm to continuous time-varying channels which would be a more realistic channel behavior in practical applications.

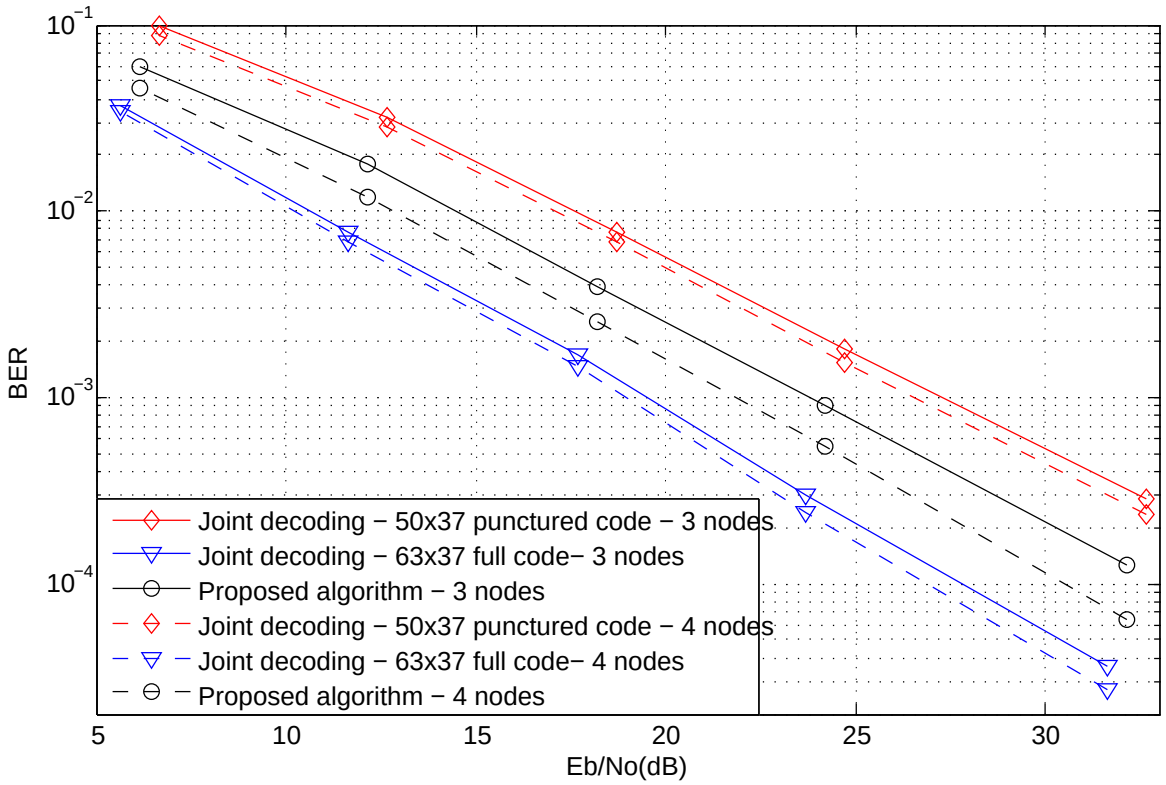


Figure 4.7: BER performance for a four-way relay system

# Chapter 5

# EXIT Analysis of the JCPNC Algorithm

## 5.1 Introduction

Extrinsic information transfer (EXIT) chart analysis had been a very powerful tool both in analyzing the convergence of iterative decoding algorithms and also in designing codes to gain the best performance [79–83]. EXIT chart analysis has been employed in Turbo code design, Repeat Accumulate code design and also in LDPC code design [84–87]. Furthermore, EXIT chart analysis has been extended to the non-binary LDPC codes design [88, 89]. However, an EXIT chart analysis has not been carried out to analyze the performance of the JCPNC algorithms. In this chapter, EXIT chart technique is first used to analyze the performance of the JCPNC algorithm in [42]. Moreover in

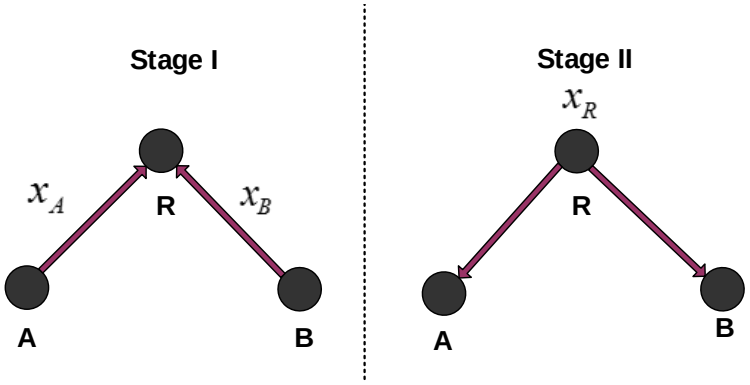


Figure 5.1: Two-way relay system (I) MAC phase of A & B transfer (II) Broadcast phase of A & B transfer

Chapter 2 and in [61, 62], an improved algorithm has been proposed for the JCPNC in multi-way wireless relay systems employing opportunistic pair-wise information exchange. Secondly the performance of this improved algorithm in [61] is analysed using EXIT analysis.

## 5.2 System Model

Let us consider a two-way relay system where nodes A and B exchange their information via a relay R as shown in Fig. 5.1. Let us focus only on transfer of information from each node to relay R and the joint decoding at the relay. Both nodes encode their $(n-\kappa)$ dimensional information bit vectors using the same $(n-\kappa)\times n$ binary LDPC channel code producing two vectors of code bits $\mathbf{c}_a$ and $\mathbf{c}_b$. These vectors are then BPSK modulated using the bits to BPSK symbol mapping rule $\{0,1\}\rightarrow\{-1,1\}$ to form two $n$ dimensional symbol vectors $\mathbf{x}_a$ and $\mathbf{x}_b$ at nodes A and B, respectively. Though we

have already considered MPSK modulated systems in Chapter 2, considering higher order modulations for EXIT analysis of the JCPNC algorithm is prohibitively complex. Hence, let us restrict the EXIT analysis to BPSK modulation only.

During the first time-slot, both A and B transmit their $n$-long symbol vectors $\mathbf{x}_A$ and $\mathbf{x}_B$ simultaneously. The overlapped signal received at the relay can be given as

$$\mathbf{y}_r = h_A \mathbf{x}_a + h_B \mathbf{x}_b + \mathbf{n}_r \tag{5.1}$$

where $h_A$ and $h_B$ are the static channel coefficients from A-R and B-R channels respectively. Here too, considering a Gaussian channel with a path loss is considered over a fading channel in seek of avoiding the prohibitively high complexity in the EXIT analysis of the JCPNC algorithm. $\mathbf{n}_r$ represents the $n$ dimensional AWGN vector added at the relay antenna with zero mean and $\sigma^2$ variance per dimension. Using $\mathbf{y}_r$, the relay receiver estimates the bit combination $\mathbf{c}_{ab} = \{\mathbf{c}_a, \mathbf{c}_b\}$ through a joint decoding process as illustrated in [42]. The joint decoder in [42] carries out an iterative decoding process where probability soft information is iteratively exchanged between check nodes and variable nodes in a Tanner graph [16] corresponding to the channel code.

## 5.3 Log Domain Joint Decoder

Note that the decoder in [42] passes four probability values $p_0 = Pr\left(c_{ab} = \{0,0\}|\Lambda\right)$, $p_1 = Pr\left(c_{ab} = \{0,1\}|\Lambda\right)$, $p_2 = Pr\left(c_{ab} = \{1,0\}|\Lambda\right)$ and $p_3 = Pr\left(c_{ab} = \{1,1\}|\Lambda\right)$ in every

message exchanged between the variable nodes and check nodes during the iterative decoding process with $\Lambda$ representing the prior information resulted from previous iterations. However, in order to perform an EXIT analysis we require to calculate the mutual information between the channel inputs and the LLR soft information values at different stages in the decoder. This in turn requires the LLR information available at different stages of the decoder. Hence, in this section a log domain decoder is derived, corresponding to the probability domain decoder proposed in [42,49]. In the log domain let us define three LLR values based on these probabilities.

$$\begin{aligned} L^{01} &\triangleq \log\left(\frac{p_1}{p_0}\right) \\ L^{10} &\triangleq \log\left(\frac{p_2}{p_0}\right) \\ L^{11} &\triangleq \log\left(\frac{p_3}{p_0}\right). \end{aligned} \tag{5.2}$$

The decoding algorithm is run as shown in Fig. 5.2 where the variable node decoder (VND) and the check node decoder (CND) operate iteratively. Furthermore, $L_{ch}, L_{VND}$ and $L_{CND}$ refers to the LLR soft information corresponding to the output of the channel, output of the VND and the output of the CND, respectively.

### 5.3.1 Initialization

Based on the received signal and the maximum likelihood detection rule, three LLR values can be calculated to represent the initial received value based information at the

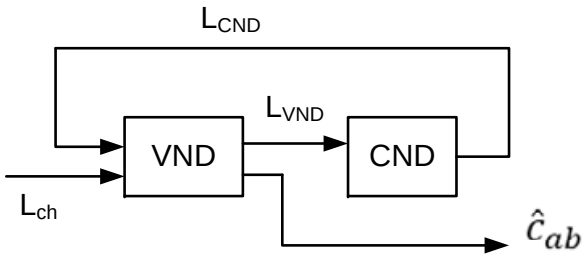


Figure 5.2: Iterative decoder

channel output as follows. Consider the received value at the $j$-th bit index $y_r(j) = h_A x_a(j) + h_B x_b(j) + n_r(j)$. Let us omit the bit index $j$ for simplicity. Assuming that the complete channel state information is available at R, the received value LLRs $\mathbf{L}_{ch} = \{L^{01}, L^{10}, L^{11}\}$ are given by,

$$\begin{aligned} L^{01} &= \log\left(\frac{Pr\left(c_{ab}=\{0,1\}|y_r\right)}{Pr\left(c_{ab}=\{0,0\}|y_r\right)}\right) \\ &= \log\left(\frac{\frac{1}{\sqrt{2\pi\sigma^2}}e^{-\left(\frac{(y_r+h_A-h_B)^2}{2\sigma^2}\right)}}{\frac{1}{\sqrt{2\pi\sigma^2}}e^{-\left(\frac{(y_r+h_A+h_B)^2}{2\sigma^2}\right)}}\right) \\ &= \frac{2h_Ah_B}{\sigma^2} + \frac{2h_Ah_B}{\sigma^2}x_a + \frac{2h_B^2}{\sigma^2}x_b + \frac{2h_B}{\sigma^2}n_r. \end{aligned} \tag{5.3}$$

Similarly,

$$L^{10} = \frac{2h_Ah_B}{\sigma^2} + \frac{2h_Ah_B}{\sigma^2}x_b + \frac{2h_A^2}{\sigma^2}x_a + \frac{2h_A}{\sigma^2}n_r. \tag{5.4}$$

$$L^{11} = \frac{2(h_A+h_B)h_A}{\sigma^2}x_a + \frac{2(h_A+h_B)h_B}{\sigma^2}x_b + \frac{2(h_A+h_B)}{\sigma^2}n_r. \tag{5.5}$$

It is clear from (5.3), (5.4) and (5.5) that $L^{01}, L^{10}$ and $L^{11}$ are Gaussian distributed conditioned on $\{x_a, x_b\}$ with the mean and variance values given in Table 5.1.

Table 5.1: Mean and variance values for LLR

| | Mean ($\mu$) | Variance ($V$) | $\frac{V}{\mu}$ |
|---|---|---|---|
| $L^{01}$ | $\frac{2h_B}{\sigma^2}\left[h_A \pm h_A \pm h_B\right]$ | $\frac{4h_B^2}{\sigma^2}$ | $\frac{2h_B}{h_A \pm h_A \pm h_B}$ |
| $L^{10}$ | $\frac{2h_A}{\sigma^2}\left[h_B \pm h_B \pm h_A\right]$ | $\frac{4h_A^2}{\sigma^2}$ | $\frac{2h_A}{h_B \pm h_B \pm h_A}$ |
| $L^{11}$ | $\frac{2(h_A+h_B)}{\sigma^2}\left[\pm h_A \pm h_B\right]$ | $\frac{4(h_A+h_B)^2}{\sigma^2}$ | $\frac{2(h_A+h_B)}{\pm h_A \pm h_B}$ |

### 5.3.2 Variable Node Decoder

VND output message of the joint decoder algorithm of [42] is given by $\beta\left[\prod_{i\in\mathcal{M}_j} p_0(i), \prod_{i\in\mathcal{M}_j} p_1(i), \prod_{i\in\mathcal{M}_j} p_2(i), \prod_{i\in\mathcal{M}_j} p_3(i)\right]$ when $\mathcal{M}_j$ represents the set of parity checks which are contributed by bit $j$ and $\beta$ is a constant which can be calculated using the property $\sum_{\forall k} p_k = 1$. In the log domain this message becomes $L_{VND} = \left[\sum_{i\in\mathcal{M}_j} L^{01}(i), \sum_{i\in\mathcal{M}_j} L^{10}(i), \sum_{i\in\mathcal{M}_j} L^{11}(i)\right]$. Note that if the output of the CND is Gaussian distributed with mean to variance ratios are as given in Table 5.1, all three elements of $L_{VND}$ are Gaussian distributed conditioned on $x_a$ and $x_b$ with ratio between mean and variance being same as in Table 5.1.

### 5.3.3 Check Node Decoder

Let $\mathcal{N}_i$ represents the set of bits (variables) which contribute to the parity check $i$. The output probability message passed to a variable node $j$ from a check node $i$ connected with two other contributing variable nodes $j'$ and $j''$ having the input probability messages $\mathbf{p}(j') = [p_0(j'), p_1(j'), p_2(j'), p_3(j')]$ and $\mathbf{p}(j'') = [p_0(j''), p_1(j''), p_2(j''), p_3(j'')]$ is

given by [42],

$$CND(\mathbf{p}(j'),\mathbf{p}(j'')) = \begin{pmatrix} p_0(j')p_0(j'') + p_1(j')p_1(j'') + p_2(j')p_2(j'') + p_3(j')p_3(i'') \\ p_0(j')p_1(j'') + p_1(j')p_0(j'') + p_2(j')p_3(j'') + p_3(j')p_2(i'') \\ p_0(j')p_2(j'') + p_1(j')p_3(j'') + p_2(j')p_0(j'') + p_3(j')p_1(i'') \\ p_0(j')p_3(j'') + p_1(j')p_2(j'') + p_2(j')p_1(j'') + p_3(j')p_0(i'') \end{pmatrix}^T . \tag{5.6}$$

The output CND message of a check node with multiple contributing variable nodes can be calculated as $CND(\mathbf{p}(j'),\mathbf{p}(j''),\ldots) = CND(\mathbf{p}(j'),CND(\mathbf{p}(j''),CND(\ldots)))$.

Thus, log domain CND output message passed from a check node $i$ to a contributing variable node $j$ can be derived as follows.

$$\begin{aligned} L^{01}(j) &= \log\left(\frac{p_0(j')p_1(j'') + p_1(j')p_0(j'') + p_2(j')p_3(i'') + p_3(j')p_2(j'')}{p_0(j')p_0(j'') + p_1(j')p_1(j'') + p_2(j')p_2(j'') + p_3(j')p_3(i'')}\right) \\ &= \log\left(\frac{\frac{p_1(j'')}{p_0(j'')} + \frac{p_1(j')}{p_0(j')} + \frac{p_2(j')}{p_0(j')}\frac{p_3(i'')}{p_0(j'')} + \frac{p_3(j')}{p_0(j')}\frac{p_2(j'')}{p_0(j'')}}{1 + \frac{p_1(j')}{p_0(j')}\frac{p_1(j'')}{p_0(j'')} + \frac{p_2(j')}{p_0(j')}\frac{p_2(j'')}{p_0(j'')} + \frac{p_3(j')}{p_0(j')}\frac{p_3(i'')}{p_0(j'')}}\right) \\ &= \log\left(\frac{e^{L^{01}_{j''}} + e^{L^{01}_{j'}} + e^{L^{10}_{j'}+L^{11}_{j''}} + e^{L^{11}_{j'}+L^{10}_{j''}}}{1 + e^{L^{01}_{j'}+L^{01}_{j''}} + e^{L^{10}_{j'}+L^{10}_{j''}} + e^{L^{11}_{j'}+L^{11}_{j''}}}\right). \end{aligned} \tag{5.7}$$

Thus,

$$\mathbf{L}_{CND}(\mathbf{L}_{j'},\mathbf{L}_{j''})(j) = [L^{01}(j), L^{10}(j), L^{11}(j)] = \begin{pmatrix} \log\left(\frac{e^{L^{01}_{j''}}+e^{L^{01}_{j'}}+e^{L^{10}_{j'}+L^{11}_{j''}}+e^{L^{11}_{j'}+L^{10}_{j''}}}{1+e^{L^{01}_{j'}+L^{01}_{j''}}+e^{L^{10}_{j'}+L^{10}_{j''}}+e^{L^{11}_{j'}+L^{11}_{j''}}}\right) \\ \log\left(\frac{e^{L^{10}_{j''}}+e^{L^{10}_{j'}}+e^{L^{01}_{j'}+L^{11}_{j''}}+e^{L^{11}_{j'}+L^{01}_{j''}}}{1+e^{L^{01}_{j'}+L^{01}_{j''}}+e^{L^{10}_{j'}+L^{10}_{j''}}+e^{L^{11}_{j'}+L^{11}_{j''}}}\right) \\ \log\left(\frac{e^{L^{11}_{j''}}+e^{L^{11}_{j'}}+e^{L^{01}_{j'}+L^{10}_{j''}}+e^{L^{10}_{j'}+L^{01}_{j''}}}{1+e^{L^{01}_{j'}+L^{01}_{j''}}+e^{L^{10}_{j'}+L^{10}_{j''}}+e^{L^{11}_{j'}+L^{11}_{j''}}}\right) \end{pmatrix}^T .$$

Let us define an operator $\oslash$ such that $\oslash(t_1,t_2,\ldots) = \log(e^{t_1}+e^{t_2}+\ldots)$. Then,

$$\mathbf{L}_{CND}(\mathbf{L}_{j'},\mathbf{L}_{j''})(j) = \begin{pmatrix} \oslash\left(L_{j''}^{01}, L_{j'}^{01}, L_{j'}^{10}+L_{j''}^{11}, L_{j'}^{11}+L_{j''}^{10}\right) \\ \oslash\left(L_{j''}^{10}, L_{j'}^{10}, L_{j'}^{01}+L_{j''}^{11}, L_{j'}^{11}+L_{j''}^{01}\right) \\ \oslash\left(L_{j''}^{11}, L_{j'}^{11}, L_{j'}^{01}+L_{j''}^{10}, L_{j'}^{10}+L_{j''}^{01}\right) \end{pmatrix}^T - \oslash\left(0, L_{j'}^{01}+L_{j''}^{01}, L_{j'}^{10}+L_{j''}^{10}, L_{j'}^{11}+L_{j''}^{11}\right)\mathbf{e}$$

where $\mathbf{e}$ is a $1 \times 3$ row vector with all unit elements.

Through extensive simulation it was observed that the elements of $\mathbf{L}_{CND}(j)$ are approximately Gaussian distributed conditioned on $x_a$ and $x_b$. Moreover, mean to variance ratios of the elements of $\mathbf{L}_{CND}(j)$ are approximately following the ratio values given in Table 5.1.

### 5.3.4 Finalization

At the end of each iteration, the value $L^{\eta}(j) = max\left[L^{01}(j), L^{10}(j), L^{11}(j)\right]$ is calculated. Then the hard decision bit pair estimate is based on the rule:

$$\hat{c}_{ab}(j) = \begin{cases} 00 & \text{if } L^{\eta}(j) < 0 \\ \eta & \text{if } L^{\eta}(j) \geq 0 \end{cases} \tag{5.8}$$

## 5.4 EXIT Analyzis for the JCPNC

In this section the EXIT analysis for the joint decoder is developed.

### 5.4.1 $J_V$ Function

To derive the EXIT characteristics of the VND block we need to model the input to the VND. Note that there are two inputs to the VND block, one from the channel output and the other from the CND output. Recall that the channel output values are Gaussian distributed with mean and variance values as given in Table 5.1. Furthermore, careful simulations demonstrated that for the regular binary LDPC codes the output three LLR elements of the CND block too are approximately Gaussian distributed. Therefore, the mutual information between the channel input and the output LLR of the VND or CND block can be calculated as follows.

$$\begin{aligned} I\left(x_A, x_B; L^{01}\right) &= \sum_{x_A=\pm 1}\sum_{x_B=\pm 1}\int_{-\infty}^{\infty} f\left(x_A, x_B, L^{01}\right)\log_2\frac{f\left(x_A, x_B, L^{01}\right)}{Pr(x_A, x_B)f(L^{01})}dL^{01} \\ &= \frac{1}{4}\sum_{x_A=\pm 1}\sum_{x_B=\pm 1}\int_{-\infty}^{\infty} f\left(L^{01}|x_A, x_B\right)\log_2\frac{4f\left(L^{01}|x_A, x_B\right)}{\sum_{x_A=\pm 1}\sum_{x_B=\pm 1} f\left(L^{01}|x_A, x_B\right)}dL^{01} \\ &= 2-\frac{1}{4}\sum_{x_A=\pm 1}\sum_{x_B=\pm 1}\int_{-\infty}^{\infty} f\left(L^{01}|x_A, x_B\right)\log_2\frac{\sum_{x_A=\pm 1}\sum_{x_B=\pm 1} f\left(L^{01}|x_A, x_B\right)}{f\left(L^{01}|x_A, x_B\right)}dL^{01} \\ &= 2-\frac{1}{4}\sum_{x_A=\pm 1}\sum_{x_B=\pm 1}\int_{-\infty}^{\infty} f\left(L^{01}|x_A, x_B\right)\log_2\left(\Psi\right)dL^{01} \end{aligned} \tag{5.9}$$

where $\Psi = 1 + e^{\lambda_1(x_A,x_B)}e^{L^{01}\nu_1(x_A,x_B)} + e^{\lambda_2(x_A,x_B)}e^{L^{01}\nu_2(x_A,x_B)} + e^{\lambda_3(x_A,x_B)}e^{L^{01}\nu_3(x_A,x_B)}$ and the values of the $\lambda(.)$ and $\nu(.)$ functions are listed in Table 5.2. Here $\mu_0, \mu_1, \mu_2, \mu_3$ refers to mean value of the LLR distributions when $x_A x_B = \{-1-1, -1+1, +1-1, +1+1\}$ respectively while $\sigma_L^2$ is the common variance of the LLR distributions.

It is apparent that $I\left(x_A, x_B; L^{01}\right)$ is a function of $\sigma_{L^{01}}$ only. Thus, it can be defined

Table 5.2: $\lambda(.)$ and $\nu(.)$ functions

| $x_A x_B$ | $\lambda_1(x_A, x_B)$ | $\lambda_2(x_A, x_B)$ | $\lambda_3(x_A, x_B)$ | $\nu_1(x_A, x_B)$ | $\nu_2(x_A, x_B)$ | $\nu_3(x_A, x_B)$ |
|---|---|---|---|---|---|---|
| -1-1 | $-\frac{\left(\mu_1^2-\mu_0^2\right)}{2\sigma_L^2}$ | $-\frac{\left(\mu_2^2-\mu_0^2\right)}{2\sigma_L^2}$ | $-\frac{\left(\mu_3^2-\mu_0^2\right)}{2\sigma_L^2}$ | $\frac{\mu_1-\mu_0}{\sigma_L^2}$ | $\frac{\mu_2-\mu_0}{\sigma_L^2}$ | $\frac{\mu_3-\mu_0}{\sigma_L^2}$ |
| -1+1 | $-\frac{\left(\mu_0^2-\mu_1^2\right)}{2\sigma_L^2}$ | $-\frac{\left(\mu_2^2-\mu_1^2\right)}{2\sigma_L^2}$ | $-\frac{\left(\mu_3^2-\mu_1^2\right)}{2\sigma_L^2}$ | $\frac{\mu_0-\mu_1}{\sigma_L^2}$ | $\frac{\mu_2-\mu_1}{\sigma_L^2}$ | $\frac{\mu_3-\mu_1}{\sigma_L^2}$ |
| +1-1 | $-\frac{\left(\mu_0^2-\mu_2^2\right)}{2\sigma_L^2}$ | $-\frac{\left(\mu_1^2-\mu_2^2\right)}{2\sigma_L^2}$ | $-\frac{\left(\mu_3^2-\mu_2^2\right)}{2\sigma_L^2}$ | $\frac{\mu_0-\mu_2}{\sigma_L^2}$ | $\frac{\mu_1-\mu_2}{\sigma_L^2}$ | $\frac{\mu_3-\mu_2}{\sigma_L^2}$ |
| +1+1 | $-\frac{\left(\mu_0^2-\mu_3^2\right)}{2\sigma_L^2}$ | $-\frac{\left(\mu_1^2-\mu_3^2\right)}{2\sigma_L^2}$ | $-\frac{\left(\mu_2^2-\mu_3^2\right)}{2\sigma_L^2}$ | $\frac{\mu_0-\mu_3}{\sigma_L^2}$ | $\frac{\mu_1-\mu_3}{\sigma_L^2}$ | $\frac{\mu_2-\mu_3}{\sigma_L^2}$ |

as,

$$J_V^{01}(\sigma_{L^{01}}) = I\left(x_A, x_B; L^{01}\right). \tag{5.10}$$

Similarly, $J_V^{10}(\sigma_{L^{10}}) = I\left(x_A, x_B; L^{10}\right)$ and $J_V^{11}(\sigma_{L^{11}}) = I\left(x_A, x_B; L^{11}\right)$ can too be calculated in a similar manner as in (5.9) where, $\sigma_{L^{10}}$ and $\sigma_{L^{11}}$ are the standard deviations of $L^{10}$ and $L^{11}$ respectively.

### 5.4.2 VND EXIT Curve

Let the mutual information between output of the CND block and $\{x_A, x_B\}$ be denoted by $\{I_{CND}^{01}, I_{CND}^{10}, I_{CND}^{11}\}$. Similarly, let the mutual information between output of the VND block and $\{x_A, x_B\}$ be denoted by $\{I_{VND}^{01}, I_{VND}^{10}, I_{VND}^{11}\}$. Now we can define the output of the VND block as a function of its inputs given by,

$$\begin{aligned} I_{VND}^{01} &= J_V^{01}\left(\sqrt{(w_c-1)[J_V^{01^{-1}}(I_{CND}^{01})]^2 + V^{01}}\right) \\ I_{VND}^{10} &= J_V^{10}\left(\sqrt{(w_c-1)[J_V^{10^{-1}}(I_{CND}^{10})]^2 + V^{10}}\right) \end{aligned} \tag{5.11}$$

$$I_{VND}^{11} = J_V^{11}\left(\sqrt{(w_c-1)[J_V^{11^{-1}}(I_{CND}^{11})]^2 + V^{11}}\right)$$

where $w_c$ is the column weight of the regular LDPC parity check matrix.

### 5.4.3 CND EXIT Curve

The relationship between the inputs and the outputs of the CND block can be expressed as,

$$\begin{aligned} I_{CND}^{01} &= J^{01}\left[f_{01}\left(J^{01^{-1}}\left(I_{VND}^{01}\right), J^{10^{-1}}\left(I_{VND}^{10}\right), J^{11^{-1}}\left(I_{VND}^{11}\right)\right)\right] \\ I_{CND}^{10} &= J^{10}\left[f_{10}\left(J^{01^{-1}}\left(I_{VND}^{01}\right), J^{10^{-1}}\left(I_{VND}^{10}\right), J^{11^{-1}}\left(I_{VND}^{11}\right)\right)\right] \\ I_{CND}^{11} &= J^{11}\left[f_{11}\left(J^{01^{-1}}\left(I_{VND}^{01}\right), J^{10^{-1}}\left(I_{VND}^{10}\right), J^{11^{-1}}\left(I_{VND}^{11}\right)\right)\right]. \end{aligned} \tag{5.12}$$

with $f$ standing for a certain one to one function. However, it is not possible to derive a closed form expression to define the output of the CND block as a function of its inputs. Therefore the CND EXIT characteristics are estimated through simulations.

Using 5.4.2 and 5.4.3, a theoretical average convergence trajectory can be derived for a given code, under given channel coefficients and at a certain $E_b/N_0$ value.

## 5.5 Example EXIT Analysis for the JCPNC Algorithm

In this section, let us investigate the average convergence characteristics of the JCPNC algorithm using proposed EXIT analysis technique. To present the novel EXIT analysis, consider a $255 \times 175$ LDPC code with row and column weight of 16. Let us consider a two-way relay communication channel with A and B nodes communicating via a relay R under four scenarios.

1. The channel coefficients are fixed such that $h_A = 0.3$ and $h_B = 0.5$. $E_b/N_0 = 2\ dB$.
2. The channel coefficients are fixed such that $h_A = 0.3$ and $h_B = 0.5$. $E_b/N_0 = 7\ dB$.
3. The channel coefficients are fixed such that $h_A = 0.9$ and $h_B = 1.1$. $E_b/N_0 = 3\ dB$.
4. The channel coefficients are fixed such that $h_A = 0.9$ and $h_B = 1.1$. $E_b/N_0 = 5\ dB$.

The selection of the arbitrary real valued channel coefficients is due to the fact that we use BPSK modulation, hence the signals are real.

Tables 5.3, 5.4, 5.5 and 5.6 present the EXIT trajectories for the four cases considered, where the labels T and S refer to theoretical and simulated mutual information values. Note that we deal with 2 bits at a symbol so that the attainable maximum information is 2 bits. Attaining 2 bits of mutual information represents the convergence. The BER performances of two decoders are also presented in Fig. 5.5. From Fig. 5.5 it is clear that the decoder does not converge at $Eb/No = 2dB$ and it converges at

$Eb/No = 7dB$ when $h_A = 0.3$ and $h_B = 0.5$, which is also visible in the EXIT analysis in Tables 5.3 and 5.4. Moreover, when $h_A = 0.9$ and $h_B = 1.1$, the decoder converges at $Eb/No = 5dB$, but not at $Eb/No = 3dB$ which is depicted in Tables 5.5 and 5.6 and Fig. 5.5.

Table 5.3: EXIT trajectory for $E_b/N_0 = 2dB$ when $h_A = 0.3$ and $h_B = 0.5$

| Iteration | | | 1 | 2 | 3 | 4 | 5 | 6 | 7 | 8 | 9 | 10 |
|---|---|---|---|---|---|---|---|---|---|---|---|---|
| $I_a$ | $L^{01}$ | T | 0.0024 | 0.0024 | 0.0024 | 0.0024 | 0.0024 | 0.0024 | 0.0024 | 0.0024 | 0.0024 | 0.0024 |
| | | S | 0.0028 | 0.0033 | 0.0028 | 0.0029 | 0.0054 | 0.0068 | 0.0008 | 0.0004 | 0.0069 | 0.0060 |
| | $L^{10}$ | T | 0.0267 | 0.0267 | 0.0267 | 0.0267 | 0.0267 | 0.0267 | 0.0267 | 0.0267 | 0.0267 | 0.0267 |
| | | S | 0.0266 | 0.0310 | 0.0269 | 0.0269 | 0.0309 | 0.0280 | 0.0260 | 0.0284 | 0.0261 | 0.0283 |
| | $L^{11}$ | T | 0.0038 | 0.0038 | 0.0038 | 0.0010 | 0.0038 | 0.0010 | 0.0038 | 0.0038 | 0.0038 | 0.0038 |
| | | S | 0.0049 | 0.0017 | 0.0009 | 0.0074 | 0.0033 | 0.0003 | 0.0015 | 0.0061 | 0.0014 | 0.0019 |
| $I_e$ | $L^{01}$ | T | 0.7295 | 0.7674 | 0.7674 | 0.7674 | 0.7674 | 0.7674 | 0.7674 | 0.7674 | 0.7674 | 0.7674 |
| | | S | 0.7335 | 0.7650 | 0.7647 | 0.7683 | 0.7697 | 0.7715 | 0.7663 | 0.7677 | 0.7662 | 0.7691 |
| | $L^{10}$ | T | 0.7422 | 0.8653 | 0.8048 | 0.8048 | 0.8048 | 0.8653 | 0.8048 | 0.8048 | 0.8048 | 0.8653 |
| | | S | 0.7452 | 0.8684 | 0.8058 | 0.8052 | 0.8079 | 0.8700 | 0.8045 | 0.8031 | 0.8033 | 0.8646 |
| | $L^{11}$ | T | 0.7342 | 0.7580 | 0.7580 | 0.7580 | 0.7580 | 0.7580 | 0.7580 | 0.7580 | 0.7580 | 0.7580 |
| | | S | 0.7366 | 0.7553 | 0.7601 | 0.7585 | 0.7581 | 0.7606 | 0.7557 | 0.7615 | 0.7556 | 0.7580 |

Table 5.4: EXIT trajectory for $E_b/N_0 = 7dB$ when $h_A = 0.3$ and $h_B = 0.5$

| Iteration | | | 1 | 2 | 3 | 4 | 5 | 6 | 7 | 8 | 9 | 10 |
|---|---|---|---|---|---|---|---|---|---|---|---|---|
| $I_a$ | $L^{01}$ | T | 0.3669 | 1.6971 | 1.9924 | 2.0000 | 2.0000 | 2.0000 | 2.0000 | 2.0000 | 2.0000 | 2.0000 |
| | | S | 0.3667 | 1.6374 | 1.9369 | 2.0000 | 2.0000 | 2.0000 | 2.0000 | 2.0000 | 2.0000 | 2.0000 |
| | $L^{10}$ | T | 0.5445 | 1.5637 | 1.9777 | 2.0000 | 2.0000 | 2.0000 | 2.0000 | 2.0000 | 2.0000 | 2.0000 |
| | | S | 0.5426 | 1.5515 | 1.9266 | 2.0000 | 2.0000 | 2.0000 | 2.0000 | 2.0000 | 2.0000 | 2.0000 |
| | $L^{11}$ | T | 0.2109 | 1.4767 | 1.9346 | 2.0000 | 2.0000 | 2.0000 | 2.0000 | 2.0000 | 2.0000 | 2.0000 |
| | | S | 0.2035 | 1.4145 | 1.9337 | 2.0000 | 2.0000 | 2.0000 | 2.0000 | 2.0000 | 2.0000 | 2.0000 |
| $I_e$ | $L^{01}$ | T | 1.2751 | 1.7573 | 2.0000 | 2.0000 | 2.0000 | 2.0000 | 2.0000 | 2.0000 | 2.0000 | 2.0000 |
| | | S | 1.2790 | 1.7619 | 1.9967 | 2.0000 | 2.0000 | 2.0000 | 2.0000 | 2.0000 | 2.0000 | 2.0000 |
| | $L^{10}$ | T | 1.2751 | 1.8872 | 2.0000 | 2.0000 | 2.0000 | 2.0000 | 2.0000 | 2.0000 | 2.0000 | 2.0000 |
| | | S | 1.2755 | 1.8889 | 1.9982 | 2.0000 | 2.0000 | 2.0000 | 2.0000 | 2.0000 | 2.0000 | 2.0000 |
| | $L^{11}$ | T | 1.2751 | 1.5925 | 2.0000 | 2.0000 | 2.0000 | 2.0000 | 2.0000 | 2.0000 | 2.0000 | 2.0000 |
| | | S | 1.2781 | 1.5956 | 1.9979 | 2.0000 | 2.0000 | 2.0000 | 2.0000 | 2.0000 | 2.0000 | 2.0000 |

Table 5.5: EXIT trajectory for $E_b/N_0 = 3dB$ when $h_A = 0.9$ and $h_B = 1.1$

| Iteration | | | 1 | 2 | 3 | 4 | 5 | 6 | 7 | 8 | 9 | 10 |
|---|---|---|---|---|---|---|---|---|---|---|---|---|
| $I_a$ | $L^{01}$ | T | 0.0119 | 0.0119 | 0.0119 | 0.0265 | 0.0265 | 0.0119 | 0.0119 | 0.0265 | 0.0265 | 0.0265 |
| | | S | 0.0113 | 0.0104 | 0.0094 | 0.0280 | 0.0262 | 0.0101 | 0.0156 | 0.0299 | 0.0251 | 0.0308 |
| | $L^{10}$ | T | 0.0393 | 0.0393 | 0.0393 | 0.0393 | 0.0393 | 0.0393 | 0.0393 | 0.0393 | 0.0393 | 0.0393 |
| | | S | 0.0365 | 0.0378 | 0.0381 | 0.0418 | 0.0370 | 0.0366 | 0.0379 | 0.0372 | 0.0411 | 0.0370 |
| | $L^{11}$ | T | 0.0081 | 0.0036 | 0.0081 | 0.0081 | 0.0081 | 0.0081 | 0.0081 | 0.0081 | 0.0081 | 0.0081 |
| | | S | 0.0087 | 0.0026 | 0.0058 | 0.0100 | 0.0127 | 0.0060 | 0.0109 | 0.0072 | 0.0066 | 0.0116 |
| $I_e$ | $L^{01}$ | T | 0.8673 | 0.9064 | 0.9444 | 0.9444 | 0.9444 | 0.9444 | 0.9444 | 0.9444 | 0.9444 | 0.9444 |
| | | S | 0.8633 | 0.9071 | 0.9394 | 0.9428 | 0.9445 | 0.9407 | 0.9442 | 0.9490 | 0.9410 | 0.9394 |
| | $L^{10}$ | T | 0.8848 | 1.0204 | 1.0204 | 1.0204 | 1.0204 | 1.0204 | 1.0204 | 1.0204 | 1.0204 | 1.0204 |
| | | S | 0.8849 | 1.0240 | 1.0175 | 1.0212 | 1.0220 | 1.0211 | 1.0206 | 1.0193 | 1.0206 | 1.0159 |
| | $L^{11}$ | T | 0.8752 | 0.8967 | 0.8967 | 0.8967 | 0.8967 | 0.8967 | 0.8967 | 0.8967 | 0.8967 | 0.8967 |
| | | S | 0.8736 | 0.8920 | 0.9003 | 0.8933 | 0.8941 | 0.8928 | 0.9016 | 0.8950 | 0.8994 | 0.8980 |

Table 5.6: EXIT trajectory for $E_b/N_0 = 5dB$ when $h_A = 0.9$ and $h_B = 1.1$

| Iteration | | | 1 | 2 | 3 | 4 | 5 | 6 | 7 | 8 | 9 | 10 |
|---|---|---|---|---|---|---|---|---|---|---|---|---|
| $I_a$ | $L^{01}$ | T | 0.7858 | 1.8332 | 2.0000 | 2.0000 | 2.0000 | 2.0000 | 2.0000 | 2.0000 | 2.0000 | 2.0000 |
| | | S | 0.7794 | 1.7473 | 2.0000 | 2.0000 | 2.0000 | 2.0000 | 2.0000 | 2.0000 | 2.0000 | 2.0000 |
| | $L^{10}$ | T | 0.7857 | 1.7881 | 2.0000 | 2.0000 | 2.0000 | 2.0000 | 2.0000 | 2.0000 | 2.0000 | 2.0000 |
| | | S | 0.7781 | 1.7276 | 2.0000 | 2.0000 | 2.0000 | 2.0000 | 2.0000 | 2.0000 | 2.0000 | 2.0000 |
| | $L^{11}$ | T | 0.4433 | 1.8172 | 2.0000 | 2.0000 | 2.0000 | 2.0000 | 2.0000 | 2.0000 | 2.0000 | 2.0000 |
| | | S | 0.4348 | 1.7291 | 2.0000 | 2.0000 | 2.0000 | 2.0000 | 2.0000 | 2.0000 | 2.0000 | 2.0000 |
| $I_e$ | $L^{01}$ | T | 1.4377 | 1.7037 | 2.0000 | 2.0000 | 2.0000 | 2.0000 | 2.0000 | 2.0000 | 2.0000 | 2.0000 |
| | | S | 1.4403 | 1.7054 | 2.0000 | 2.0000 | 2.0000 | 2.0000 | 2.0000 | 2.0000 | 2.0000 | 2.0000 |
| | $L^{10}$ | T | 1.4437 | 1.7061 | 2.0000 | 2.0000 | 2.0000 | 2.0000 | 2.0000 | 2.0000 | 2.0000 | 2.0000 |
| | | S | 1.4482 | 1.7077 | 2.0000 | 2.0000 | 2.0000 | 2.0000 | 2.0000 | 2.0000 | 2.0000 | 2.0000 |
| | $L^{11}$ | T | 1.4330 | 1.6215 | 2.0000 | 2.0000 | 2.0000 | 2.0000 | 2.0000 | 2.0000 | 2.0000 | 2.0000 |
| | | S | 1.4369 | 1.6252 | 2.0000 | 2.0000 | 2.0000 | 2.0000 | 2.0000 | 2.0000 | 2.0000 | 2.0000 |

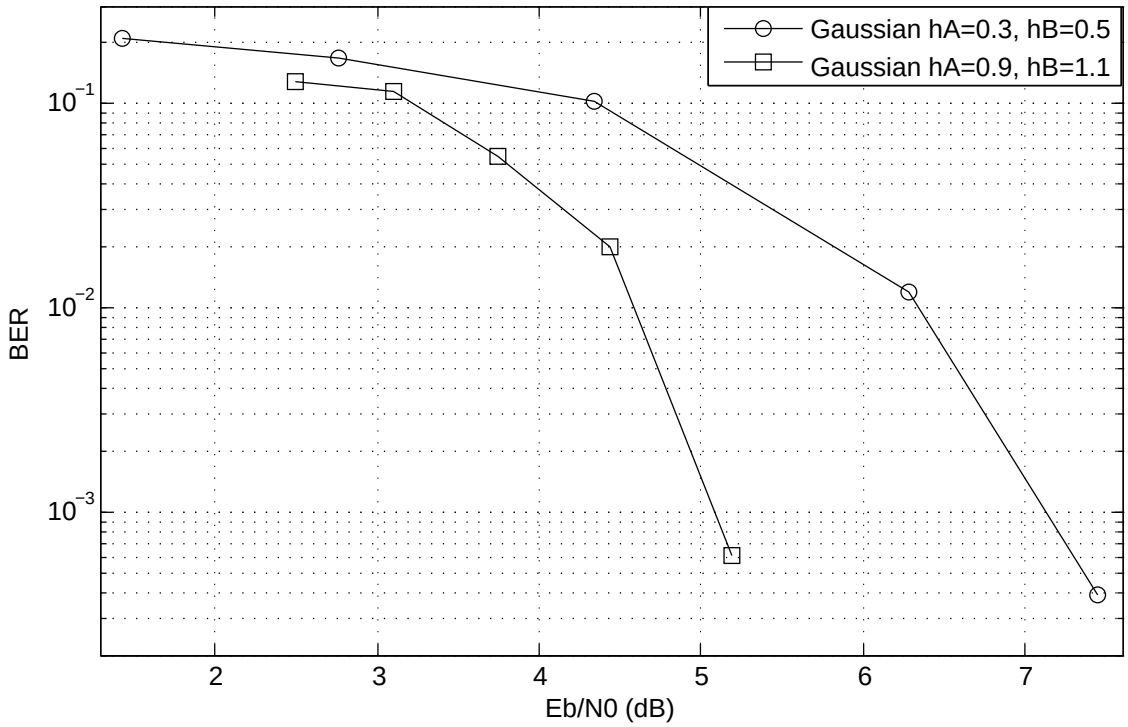


Figure 5.3: BER performance of the individual AB and BC decoders for $255 \times 175$ binary LDPC code

## 5.6 EXIT Analyzis for the JCPNC in Multi-way Relay Systems

Recall that the algorithm proposed in [61] presents an improved joint decoder for multi-way wireless relay system, to be employed at the common relay. Let us investigate the effect of information exchange between the parallely operating decoders in [61] using EXIT analysis. For simplicity let us consider a 3-way relay system where A and B nodes communicate first to the relay under $h_A = 0.3$ and $h_B = 0.5$ and B and C nodes communicate to the relay next with $h_B = 0.9$ and $h_C = 1.1$. Let us analyze the EXIT

characteristics at $E_b/N_0 = 4\ dB$, $E_b/N_0 = 5\ dB$ and $E_b/N_0 = 7\ dB$. Tables 5.7 and 5.8 show the convergence of BC decoder at $E_b/N_0 = 5\ dB$ and the convergence of the AB decoder at $E_b/N_0 = 7\ dB$ at a much lesser number of iterations compared to non-information exchanging decoder pair, which is a result of the information exchange. Tables 5.9 and 5.10 shows that the BC decoder converges at $E_b/N_0 = 4\ dB$ which was not converging without information exchange while AB decoder still does not converge. Same behavior is reconfirmed from the BER plots in Figure 5.6. With these results it is clear that the information exchange has improved the convergence of the two decoders.

Table 5.7: EXIT trajectory of the BC decoder for $E_b/N_0 = 5dB$ with information exchange

| Iteration | | 1 | 2 | 3 | 4 | 5 | 6 | 7 | 8 | 9 | 10 |
|---|---|---|---|---|---|---|---|---|---|---|---|
| $I_a$ | $L^{01}$ | 2.0000 | 2.0000 | 2.0000 | 2.0000 | 2.0000 | 2.0000 | 2.0000 | 2.0000 | 2.0000 | 2.0000 |
| | $L^{10}$ | 2.0000 | 2.0000 | 2.0000 | 2.0000 | 2.0000 | 2.0000 | 2.0000 | 2.0000 | 2.0000 | 2.0000 |
| | $L^{11}$ | 2.0000 | 2.0000 | 2.0000 | 2.0000 | 2.0000 | 2.0000 | 2.0000 | 2.0000 | 2.0000 | 2.0000 |
| $I_e$ | $L^{01}$ | 1.1152 | 2.0000 | 2.0000 | 2.0000 | 2.0000 | 2.0000 | 2.0000 | 2.0000 | 2.0000 | 2.0000 |
| | $L^{10}$ | 1.8322 | 2.0000 | 2.0000 | 2.0000 | 2.0000 | 2.0000 | 2.0000 | 2.0000 | 2.0000 | 2.0000 |
| | $L^{11}$ | 1.6669 | 2.0000 | 2.0000 | 2.0000 | 2.0000 | 2.0000 | 2.0000 | 2.0000 | 2.0000 | 2.0000 |

Table 5.8: EXIT trajectory of the AB decoder for $E_b/N_0 = 7dB$ with information exchange

| Iteration | | 1 | 2 | 3 | 4 | 5 | 6 | 7 | 8 | 9 | 10 |
|---|---|---|---|---|---|---|---|---|---|---|---|
| $I_a$ | $L^{01}$ | 0.6908 | 1.7169 | 1.9933 | 2.0000 | 2.0000 | 2.0000 | 2.0000 | 2.0000 | 2.0000 | 2.0000 |
| | $L^{10}$ | 0.4078 | 1.5785 | 1.9709 | 2.0000 | 2.0000 | 2.0000 | 2.0000 | 2.0000 | 2.0000 | 2.0000 |
| | $L^{11}$ | 0.3822 | 1.4723 | 1.9160 | 2.0000 | 2.0000 | 2.0000 | 2.0000 | 2.0000 | 2.0000 | 2.0000 |
| $I_e$ | $L^{01}$ | 1.4613 | 1.9145 | 2.0000 | 2.0000 | 2.0000 | 2.0000 | 2.0000 | 2.0000 | 2.0000 | 2.0000 |
| | $L^{10}$ | 1.5335 | 1.7536 | 2.0000 | 2.0000 | 2.0000 | 2.0000 | 2.0000 | 2.0000 | 2.0000 | 2.0000 |
| | $L^{11}$ | 1.2588 | 1.6871 | 2.0000 | 2.0000 | 2.0000 | 2.0000 | 2.0000 | 2.0000 | 2.0000 | 2.0000 |

Table 5.9: EXIT trajectory of the BC decoder for $E_b/N_0 = 4dB$ with information exchange

| Iteration | | 1 | 2 | 3 | 4 | 5 | 6 | 7 | 8 | 9 | 10 |
|---|---|---|---|---|---|---|---|---|---|---|---|
| $I_a$ | $L^{01}$ | 1.4377 | 1.7129 | 1.8991 | 2.0000 | 2.0000 | 2.0000 | 2.0000 | 2.0000 | 2.0000 | 2.0000 |
| | $L^{10}$ | 1.5403 | 1.7712 | 1.9296 | 2.0000 | 2.0000 | 2.0000 | 2.0000 | 2.0000 | 2.0000 | 2.0000 |
| | $L^{11}$ | 0.4685 | 1.1895 | 1.6236 | 2.0000 | 2.0000 | 2.0000 | 2.0000 | 2.0000 | 2.0000 | 2.0000 |
| $I_e$ | $L^{01}$ | 0.5212 | 1.8591 | 2.0000 | 2.0000 | 2.0000 | 2.0000 | 2.0000 | 2.0000 | 2.0000 | 2.0000 |
| | $L^{10}$ | 1.4991 | 1.8866 | 2.0000 | 2.0000 | 2.0000 | 2.0000 | 2.0000 | 2.0000 | 2.0000 | 2.0000 |
| | $L^{11}$ | 1.0373 | 1.5743 | 1.8059 | 2.0000 | 2.0000 | 2.0000 | 2.0000 | 2.0000 | 2.0000 | 2.0000 |

Table 5.10: EXIT trajectory of the AB decoder for $E_b/N_0 = 4dB$ with information exchange

| Iteration | | 1 | 2 | 3 | 4 | 5 | 6 | 7 | 8 | 9 | 10 |
|---|---|---|---|---|---|---|---|---|---|---|---|
| $I_a$ | $L^{01}$ | 0.0025 | 0 | 0 | 0 | 0 | 0 | 0 | 0 | 0 | 0 |
| | $L^{10}$ | 0.0068 | 0 | 0 | 0 | 0 | 0 | 0 | 0 | 0 | 0 |
| | $L^{11}$ | 0 | 0 | 0 | 0 | 0 | 0 | 0 | 0 | 0 | 0 |
| $I_e$ | $L^{01}$ | 0.4078 | 0.2868 | 0.2482 | 0.2482 | 0.2482 | 0.2482 | 0.2482 | 0.2482 | 0.2482 | 0.2482 |
| | $L^{10}$ | 0.8653 | 0.3399 | 0.2738 | 0.2738 | 0.2738 | 0.2738 | 0.2738 | 0.2738 | 0.2738 | 0.2738 |
| | $L^{11}$ | 0.4078 | 0.2577 | 0.2577 | 0.2577 | 0.2577 | 0.2577 | 0.2577 | 0.2577 | 0.2577 | 0.2577 |

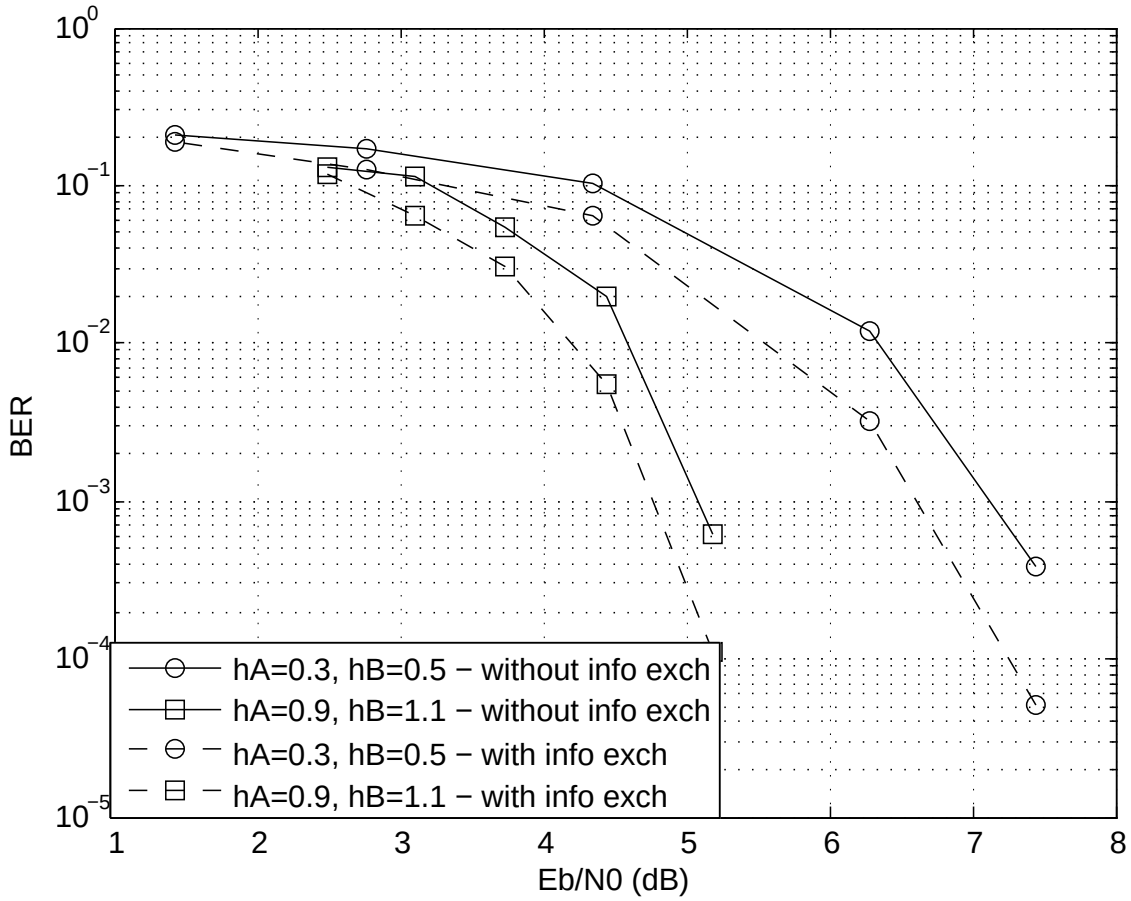


Figure 5.4: BER performance of the joint decoder for $255 \times 175$ binary LDPC code

## 5.7 Conclusion

In this chapter the log domain decoder has been derived for the LDPC decoder presented in [42]. Furthermore, an EXIT analysis was carried out for this decoder which verified the non-convergence behavior of the decoder at certain channel conditions. Moreover, it is shown that the joint decoder in [61] can improve the performance of the decoding process by information exchange, using EXIT analysis. Furthermore, the proposed EXIT analysis technique for the joint decoder can be utilized to predict the convergence

behavior and also to predict the average number of iterations for convergence.

# Chapter 6

# Conclusion and Suggestions for Further Work

## 6.1 Conclusion

Joint channel-physical layer network coding has attracted an attention as a promising technique to have a good trade-off between BER performance and spectral efficiency in data communication over wireless relay channels. However, use of joint channel-physical layer network coding in multi-way wireless relay systems had not been well studied. Thus, this thesis first presented an improved JCPNC algorithm for multi-way wireless relay systems which yields the additional time-diversity gain available due to the pair-wise multi-way information exchange between the nodes. Though the joint decoder algorithm was first defined for BPSK modulated systems, later the same was extended

for a general MPSK modulated system. The key element in harnessing this additional diversity gain is the exchange of soft information between the constitute sub-decoders employed at the relay. For this information exchange, nine different schemes were also proposed. Proposed joint channel physical layer network coding algorithm provides an appealing BER performance-spectral efficiency trade-off as presented in Chapter 2.

In Chapter 3, a novel joint channel-physical layer network coding algorithm was proposed which again harnessed the available time diversity gain due to the transmission of same information twice in two time-slots, during the pair-wise multi-way relay communication. One specialty of this algorithm is the low complexity compared to the algorithm presented in Chapter 2, which is a result of the use of the BF decoder in place of the BP decoder. However, with the use of the BF decoder, the information flowing in the system is hard information, hence a novel information exchange scheme was also proposed to exchange information between the constituent decoders operating parallely. Chapter 3 also presented an improved symbol value-selection algorithm for symbol flipping based non-binary LDPC decoding which is then employed in the low complexity JCPNC algorithm to improve the performance of hard information exchange. Simulation results have confirmed that the proposed low complexity JCPNC algorithm outperforms the BF based separately channel decoding and network coding algorithm while providing far less complexity compared to the algorithm proposed in Chapter 2.

Considering the fact that most of the practical deployments consist of heterogeneous channels in the multi-way wireless relay system, a scheme with unequal error protection

for different channels in the multi-way relay system and an associated distributed channel coding scheme has been proposed in Chapter 4. A joint decoding algorithm for the unequally error protected system has also been developed. In this novel LDPC channel decoder, an additional LDPC decoder takes the decoded soft information corresponding to the bit information transmitted twice, from the decoders decoding for the pair-wise joint information, and performs an additional decoding using an extended LDPC code. Extended decoding produces an additional gain compared to the decoder algorithm in Chapter 2. Through simulation results it had been demonstrated that this is a practically viable solution to improve the error resiliency and the spectral efficiency together, in heterogeneous wireless relay systems.

In Chapter 5, the performance of the developed improved multi-way JCPNC algorithm has been analyzed using EXIT analysis technique. In Chapter 5, first a log domain decoder was derived for joint channel-physical layer network coding for which the EXIT analysis had been performed. Second, the EXIT analysis had been extended to the improved JCPNC algorithm presented in Chapter 2 of this thesis. EXIT analysis has verified the convergence behavior and the additional diversity gain obtained by the information exchange between the constituent decoders.

The communication requirements of today's world is growing at a rapid rate than never before. A wide array of bandwidth hungry applications have been introduced and the number of communication subscribers have also grown exponentially. Meeting all these new requirements is a challenge for the communication engineer. Amid all this,

IoT has been a very popular novel communication trend in which multi-way relaying is very common. Thus, the novel set of algorithms presented in this thesis would be of immense value to achieve an efficient communication in such multi-way wireless relay systems.

The proposed set of algorithms will be able to add high reliability in multi-way relay systems. Consequently, the high error resiliency gained through the proposed algorithms would enable the nodes to reduce their transmit power, in view of a greener communication. On the other hand, high error resiliency can lead to a low latency in networks. Moreover, the reduced hardware complexity with the use of the proposed low-complexity algorithm will lead us to faster performance and cost effective hardware at nodes. The proposed communication scheme and the decoding algorithm for the practical asymmetric multi-way relay systems will benefit the communication with added spectral efficiency.

## 6.2 Further Work

Though the proposed set of algorithms have shown to provide a very good trade-off between the BER performance and the spectral efficiency when communicating over multi-way wireless relay systems, these were evaluated under the block fading channel conditions. An investigation of their performance under realistic practical channel conditions will be a good topic for future research. At the same time, this research work

assumed that all channel state information is available freely to all nodes. In reality, a separate mechanism has to be implemented to estimate the channel conditions which may vary time to time. Channel estimation technique has a significant effect on the overall performance of the joint decoder, thus analysis of such effects is also important. Moreover, the error performances of the proposed joint decoding algorithms were investigated only using simulations. Therefore, in order to confirm the potential benefits of the proposed algorithms, it is worthwhile to further investigate the performances in practical experimental setups which would guide us to the viability of the proposed algorithms and the modifications required to adopt them in real life communication systems.

Non-orthogonal multiple access (NOMA) is a highly embraced multiple access technique in fifth generation mobile communication systems. The extension of the proposed joint decoding algorithms to JCPNC with NOMA would also be an interesting research topic.

# Bibliography

[1] J.G. Proakis and M. Salehi, *Digital Communications,* McGraw-Hill, 5th ed., 2008.

[2] A. Goldsmith, *Wireless Communications,* Cambridge University Press, 2nd ed., 2005.

[3] R. Ahlswede, N. Cai, S. Y. R. Li and R.W. Yeung, "Network Information Flow," *IEEE Transactions on Information Theory,* , Vol. 46, 2000, pp. 1204-1216.

[4] S. Y. R. Li, R. W. Yeung and N. Cai, "Linear Network Coding," *IEEE Transactions on Information Theory,* , Vol. 49, No. 2, Feb 2003, pp. 371 - 381.

[5] M. Medard and A. Sprintson, *Network Coding: Fundamentals and Applications,* Elsevier, 2012.

[6] R. W. Yeung, *Information Theory and Network Coding,* Springer, 2008.

[7] C. Fragauli and E. Soljanin, *Network Coding Fundamentals,* Now Publishers Inc, 2007.

[8] S. Zhang, S. C. Liew, and P. Lam, "Hot Topic: Physical Layer Network Coding," *in Proc. International Conference on Mobile Computing and Networking (MobiCom),* Los Angeles, CA, USA, 2006, pp. 358-365.

[9] S. C. Liew, S. Zhang and L. Lu, "Physical-layer Network Coding: Tutorial, Survey, and Beyond," *Physical Communication,* , Vol. 6, Mar 2013, pp. 4-42.

[10] P. Popovski and H. Yomo, "The Anti-packets Can Increase the Achievable Throughput of a Wireless Multi-hop Network," *in Proc. IEEE ICC 2006,* June 2006, pp. 3885-3890.

[11] S. Zhang and S. C. Liew, "Applying Physical-Layer Network Coding in Wireless Networks," *EURASIP Journal on Wireless Communications and Networking,* , Vol. 2010, Mar 2010.

[12] Y. Wu, P. A. Chou, S. Y. Kung, "Information Exchange in Wireless Networks with Network Coding and Physical-layer Broadcast," *in Proc. 39th Annual Conf. Inform. Sci. and Systems (CISS),* 2005.

[13] C. Schnurr, T. J. Oechtering, and S. Stanczak, "On Coding for the Broadcast Phase in the Two-Way Relay Channel," *in Proc. Conference on Information Sciences and Systems (CISS07),* March 2007.

[14] P. Popovski, and H. Yomo, "Physical Network Coding in Two-Way Wireless Relay Channels," *in Proc. ICC 2007,* 2007.

[15] K. Lu, S. Fu, Y. Qian, H. Chen, "SER Performance Analysis of Physical Layer Network Coding over AWGN Channels," *in Proc. IEEE GLOBECOM'09,* 2009, pp. 1-6.

[16] S. Lin and D. J. Costello, *Error Control Coding,* Prentice-Hall, 2003.

[17] C. Berrou, A. Glavieux, and P. Thitimajshima, "Near Shannon limit error correcting coding and decoding: Turbo codes," *in Proc. of the IEEE International Conference on Communications,* Geneva, Switzerland, May 1993.

[18] R. Gallager "Low-density Parity-Check Codes," *IRE Trans. Information Theory,* Vol. 8, 1962, pp. 21-28.

[19] D.J. Mackay and R.M. Neal, "Near Shannon limit performance of low-density parity-check codes," *IEE Electronics Letters*, Vol. 32, Aug. 1996, pp. 1645 – 1646.

[20] T. M. Cover, and J. A. Thomas, *Elements of Information Theory,* New York: Wiley, 1991.

[21] D. Divsalar, H. Jin, and R. J. McEliece, "Coding theorems for 'turbo-like' codes," *in Proc. of the 36th Allerton Conf. on Communications, Control, and Computing,* Sept. 1998, pp. 201-210.

[22] A. Chakrabarthi, A. Baynast, A. Sabharwal and B. Aazhang, "Low Density Parity Check Codes for the Relay Channel," *IEEE Journal on Selected Areas in Communications,* Vol.25, No. 2, Feb. 2007, pp. 280-291.

[23] C. Hausl and J. Hagenauer, "Iterative network and Channel Coding for the Two-Way Relay Channels," *in Proc. IEEE ICC06,* June 2006.

[24] X. Xu, M. F. Flanagan, N. Goertz and J. Thompson, "Joint Channel and Network Coding for Cooperative Diversity in a Shared-Relay Environment," *IEEE Transactions on Wireless Communications,* , Vol. 9, No. 8, Aug 2010, pp. 2420-2423.

[25] X. Wu, C. Zhao, and X. You, "Joint LDPC and Physical-layer Network Coding for Asynchronous Bi-directional Relaying," *IEEE Journal on Selected Areas in Communications,* , Vol. 31, Issue 8, Aug 2013, pp. 1446-1454.

[26] E. Benamira, F. Merazka and G. K. Kurt, "Joint Channel Coding and Cooperative Network Coding on PSK Constellations in Wireless Networks," *in Proc. International Conference on Smart Communications in Network Technologies (SaCoNeT)*, 2018, pp. 132-137.

[27] Y. Zid, R. Bouallgue and S. Z. Ammar, "Joint channel network coding for multiple access relay channel with correlated sources," *25th International Conference on Software, Telecommunications and Computer Networks (SoftCOM)*, 2017, pp. 1-4.

[28] W. Liu, "Joint channel coding network coding for multi-way relay systems," *in Proc. SAI Computing Conference (SAI)*, 2016, pp. 615-621.

[29] S. Zhang, S. C. Liew, and P. Lam, "Physical Layer Network Coding Schemes over Finite and Infinite Feilds," *in Proc. IEEE GLOBECOM '08,* 2008, pp. 3784-3789.

[30] S. Zhang, S. C. Liew, and K. B. Letaief, "Joint Design of Network Coding and Channel Decoding for Wireless Networks," *in Proc. International Conference on Neural Networks and Signal processing,* Nanjing, 2008, pp. 512-516.

[31] S. Zhang and S. C. Liew, "Channel Coding and Decoding in a Relay System Operated with Physical Layer Network Coding," *IEEE Journal on Selected Areas in Communications,* Vol.27, No. 5, June. 2009, pp. 788-796.

[32] Z. He and S. Roy, "LDPC Coded Two-way MIMO Relay Networks with Physical Layer Network Coding," *in Proc. 25th IEEE Binomial Symposium on Communications,* 2010, pp. 301-304.

[33] S. Yan and R. Koetter , "Network Coding over a Noisy Channel: A Belief Propagation Approach ," *in Proc. IEEE International Symposium on Information theory,* France, 2007.

[34] T. Tran, T. Nguyen and B. Bose, "A Joint Network-Channel Coding Technique for Single-hop Wireless Networks ," *in Proc. IEEE NETCOD,* China, 2008.

[35] M. P. Wilson, K. Narayana, H. Pfister and A. Sprintson, "Joint Physical Layer Coding and Network Coding for Bidirectional Relaying," *IEEE Transactions on Information theory,* Vol.56, No. 11, Sept. 2010, pp. 5641-5654.

[36] B. Nazer and M. Gapster, "Reliable Physical Layer Network Coding," *in Proc. the IEEE,* Vol.99, Issue 3, March 2011, pp. 438-460.

[37] F. Gao, Y. Wang and Y. Zhang, "Joint channel-vertical physical-layer network coded modulation based on PAM for two-way relay channel," in Proc. IEEE International Conference on Signal Processing, Communications and Computing (ICSPCC), 2017, pp. 1-4.

[38] S. Chaudhary, R. Johari, R. Bhatia, K. Gupta and A. Bhatnagar, "CRAIoT: Concept, Review and Application(s) of IoT, "*4th International Conference on Internet of Things: Smart Innovation and Usages (IoT-SIU)*, 2019, pp. 1-4.

[39] K. Routh and T. Pal, "A survey on technological, business and societal aspects of Internet of Things by Q3, 2017, "*3rd International Conference on Internet of Things: Smart Innovation and Usages (IoT-SIU)*, 2018, pp. 1-4.

[40] M. K. Shukla, H. H. Nguyen and O. J. Pandey, "Multiuser Full-Duplex IoT Networks With Wireless-Powered Relaying: Performance Analysis and Energy Efficiency Optimization," *IEEE Transactions on Green Communications and Networking*, Vol. 4, No. 4, Dec. 2020, pp. 982-997.

[41] Y. Jeon, Y. Kim, M. Park and I. Lee, "Oppertunistic Scheduling for Three-way Relay Syetems with Physical Layer Network Coding ," *in Proc. IEEE 73rd Vehicular Technology Conference,* 2011, pp. 1-5.

[42] D. Wubben and Y. Lang, "Generalized Sum-Product Algorithm for Joint Channel Decoding and Physical Layer Network Coding in Two-Way Relay Systems," *in Proc. IEEE GLOBECOM,* 2010, pp. 1-5.

[43] Y. Lang, D. Wubben and K. D. Kammeyer, "An Improved Physical Layer Network Coding Scheme for Two-Way relay Systems," *in Proc. International ITG Workshop on Smart Antennas (WSA),* Bremen, Germany, Feb. 2010.

[44] Y. Lang and D. Wubben, "Generalized Joint Channel Coding and Physical Network Coding for Two-Way Relay Systems," *in Proc. IEEE 71st Vehicular Technology Conference,* 2010, pp. 1-5.

[45] D. To and J. Choi, "Convolutional Codes in Two-Way Relay Networks with Physical-Layer Network Coding," *IEEE Transactions in Wireless Communication,* Vol.9, No. 9, Sept. 2010, pp. 2724-2729.

[46] Jie Hou, C. Hausl, and R. Kotter, "Distributed Turbo Coding Schemes for Asymmetric Two-Way Relay Communication ," *in Proc. 5th International Symposium on Turbo Codes and Related Topics,* 2008, pp. 237 - 242.

[47] J. Kang, B. Zhou, Z. Ding and S. Lin, "LDPC Coding Schemes for Error Control in a Multicast Network ," *in Proc. IEEE International Symposium on Information Theory,* Toronto, Canada, Jul 2008.

[48] Z. Guo, J. Huang, J.H. Cui, S, Zhou and P. Willet, "A Practical Joint Network-Channel Coding Scheme for Reliable Communication in Wireless Networks," *in Proc. 10th International Symposium on Mobile Ad-hoc Networking and Computing (MobiHoc),* 2009, pp. 1-10.

[49] D. Wubben, "Joint Channel Decoding and Physical-layer Network Coding in Two-way QPSK Relay Systems by a Generalized Sum-product Algorithm ," *in Proc. International Symposium on Wireless Communication Systems (ISWCS),* 2010, pp. 576-580.

[50] C. Hausl and P. Dupraz, "Joint Network-Channel Coding for Multiple Access Relay Channel," *in Proc. International Conference on Sensors, Ad-hoc Communication and Networks(SECON),* 2006, pp. 817-822.

[51] Z. Lin, Y. Li and B. Vucetic, "Distributed Network-Channel Coding for Multiple-Access Relay Interference Channels ," *in Proc. IEEE 71st Vehicular Technology Conference,* 2010, pp. 1-5.

[52] C. H. Liu and A. Arapostathis, "Joint Network Coding and Superposition Coding for Multi-user Information Exchange Wireless Relaying Networks," *Proc. of the IEEE GLOBECOM*, Dec 2008, pp. 1 – 6.

[53] D. Xu, Z. Bai, A. Waadt, G. H. Bruck, P. Jung, "Combining MIMO with Network Coding: A Viable Means to Provide Multiplexing and Diversity in Wireless Relay Networks ," *in Proc. International Conference on Communications '10,* 2010, pp. 1-5.

[54] H. A. Suraweera, H. Q. Ngo, T. Q. Duong, C. Yuen and E. G. Larsson, "Multi-pair Amplify-and-forward Relaying with Large Antenna Arrays," *in Proc. International Conference on Communications '13*, 2013, pp. 3228-3233.

[55] M. Park and S. K. Oh, "An Iterative Network Code Optimization for Three-way Relay Channels," *Proc. of the IEEE Conf. Vehicular Technology*, Sep 2009, pp. 1 – 5.

[56] H. Yomo and P. Popovski, "Opportunistic Scheduling for Wireless Network Coding," *Proc. of the IEEE Intern. Conf. on Communications*, June 2007, pp. 5610 – 5615.

[57] D.G. Brennan, "Linear Diversity Combining Techniques," *Proc. of the IRE*, Vol.47, No. 1, June 1959, pp.1075-1102.

[58] R. Comroe and D. Costello, "ARQ Schemes for Data Transmission in Mobile Radio Systems," *IEEE Journal on Selec. Areas in Comm.,* 1984, pp. 472-481.

[59] I. Hughes and T. Hase, *Measurements and Their Uncertainties: A Practical Guide to Modern Error Analysis,* 1st Ed., Oxford University Press, 2010.

[60] J.R. Taylor, *An Introduction to Error Analysis: The Study of Uncertainties in Physical Measurements,* 2nd Ed., University Science Books, 1997.

[61] N. Balasuriya and C. Wavegedara, "Joint Channel-Physical Layer Network Coding in Multi-Way Wireless Relay Systems," *in Proc. IEEE ICIIS,* 2013, pp. 213-218.

[62] N. Balasuriya and C. Wavegedara, "A Joint Decoder for Network and Channel Coded Multi-way Relay Systems with MPSK Modulation, *IET Communications,* Vol.13, Issue. 15, Sep 2019, pp. 2273-2279.

[63] Z. Liu and D.A. Pados, "A Decoding Algorithm for Finite-geometry LDPC Codes," *IEEE Trans. on Comm.*, Vol. 53, No. 3, Mar. 2005, pp. 415 – 421.

[64] T. Ngatched, F. Takawira & M. Bossert, "An Improved Decoding Algorithm for Finite-geometry LDPC Codes," *IEEE Trans. on Comm.*, Vol. 57, no 2, Feb. 2009, pp. 302-306.

[65] M.C. Davey, D. MacKay, "Low Density Parity Check Codes Over GF(q)," *IEEE Comm. Letters*, Vol. 2, Issue 6, June. 1998, pp. 165-167.

[66] B. Liu, J. Gao, G. Dou & W. Tao, "Weighted Symbol-flipping Decoding for Non-binary LDPC Codes ," *Proc. of the IEEE Intern. Conf. on Network Security, Wireless Communications and Trusted Computing* , Apr. 2010, pp. 223-226.

[67] B. Liu, J. Gao, G. Dou & W. Tao, "Majority Decision Based Weighted Symbol-flipping Decoding for Non-binary LDPC Codes ," *Proc. of the 2nd Intern. Conf. on Future Computer and Communication*, May. 2010, pp. V3.6-V3.10.

[68] C. Huang, C. Wu, C. Chen & C. Chao, "Parallel Symbol-flipping Decoding for Non-binary LDPC Codes ," *IEEE Comm. Letters*, Jun. 2013, Vol. 17, Issue 6, pp. 1228-1231.

[69] F. Garcia Herrero, E. Li, D. Declercq & J. Valls, "Multiple-vote Symbol-flipping Decoder for Non-binary LDPC Codes," *IEEE Trans. on VLSI Sys.*, Vol. 22, Issue 11, Feb. 2014.

[70] N. Nhan, T.M.N. Ngatched, O.A. Dobre, P. Rostaing, K. Amis,E. Radoi, Multiples-Votes Parallel Symbol-Flipping Decoding Algorithm for Non-Binary LDPC Codes, *IEEE Comm. Letters*, 19(6), pp. 905 - 908, (2015).

[71] N. Balasuriya and C. Wavegedara, "Low Complexity LDPC Decoder for Physical Layer Network Coded Multi-way Wireless Relay Systems," *in Proc. IEEE ICIIS,* 2015, pp. 226-231.

[72] N. Balasuriya and C. B. Wavegedara, "Improved Symbol Value Selection for Symbol Flipping Based Non-binary LDPC Decoding," *EURASIP Journal on Wireless Communications and Networking,* , Vol. 2017:105, June 2017.

[73] Y. H. Tahir, C.Kyun Ng, N. K. Noordin, B. A. Ali and S. Khatun, "Unequally Error Protected Wireless Data Transmission Using Channel State Information and Adaptive Encoders," *Journal of Computer Science,* Vol.5, Issue 12, 2009, pp. 1095-1100.

[74] S. Borade, B. Nakiboglu and L. Zheng, "Unequal Error Protection: An Information-Theoretic Perspective," *IEEE Transactions on Information Theory,* Vol.55, Issue 12, 2009, pp. 5511-5539.

[75] H. X. Nguyen, H. H. Nguyen and T. Le-Ngoc, "Signal Transmission With Unequal Error Protection in Wireless Relay Networks," *IEEE Transactions on Vehicular Technology,* Vol.59, Issue 5, June 2010, pp. 2166-2178.

[76] I. Shahid and P. Yahampath, "Distributed Joint Source-Channel Coding Using Unequal Error Protection LDPC Codes," *IEEE Transactions on Communications,* Vol.61, No. 8, Aug 2013, pp. 3472-3482.

[77] J. Ha, J. Kim, D. Klinc and S. W. McLaughlin, "Rate-compatible Punctured Low-density Parity-check Codes with Short block lengths," *IEEE Tans. on Info. Theory,* Vol. 52, Issue 2, Feb. 2006, pp. 728-738.

[78] S. Zhou, D.G.M. Mitchell, N. Goertz and D. J. Costello, "A Puncturing Algorithm for Rate-compatible LDPC Convolutional Codes," *in Proc. 7th International Symposium on Turbo Codes and Iterative Information Processing,* 2012, pp. 255-259.

[79] A. Grant, "Convergence of Non-binary Iterative Decoding," *in Proc. IEEE GLOBECOM,* 2001, pp. 1058-1062.

[80] J. Hagenauer, "The Exit Chart - Introduction to Extrinsic Information Transfer in Iterative Processing," *In proc. 12th European Signal Processing Conference,* 2004, pp. 1541-1548.

[81] M. El-Hajjar and L. Hanzo, "EXIT Charts for System Design and Analysis," *IEEE Commun. Surveys Tutorials,* Vol.16, No. 1,2014, pp. 127-153.

[82] A. Bennatan and D. Burshtein, "Design and Analysis of Nonbinary LDPC Codes for Arbitrary Discrete-memoryless Channels," *IEEE Trans. on Info. Theory*, Vol. 52, Issue 2, Feb. 2006, pp. 549 – 583.

[83] C. Wavegedara and V. Bhargava, "Convergence Analysis of Turbo Equalizers in ST Block-coded MIMO Systems," *in Proc. IEEE ICIIS,* 2009, pp. 104-111.

[84] A. Ashikhmin, G. Kramer, and S. T. Brink, "Extrinsic Information Transfer Functions: Model and Erasure Channel Properties," *IEEE Transactions on Information Theory,* Vol.50, No. 11, Nov. 2004, pp. 2657-2673.

[85] S. T. Brink and G. Kramer, "Design of RepeatAccumulate Codes for Iterative Detection and Decoding," *IEEE Transactions on Signal Processing,* Vol.51, No. 11, Nov. 2003, pp. 2764-2772.

[86] S. T. Brink, G. Kramer and A. Ashikmin, "Design of Low-Density Parity-Check Codes for Modulation and Detection," *IEEE Transactions on Communications,* Vol.52, No. 4, Apr. 2004, pp. 670-678.

[87] Y. Yang, H. Changqing and Z. Haibin, "Design of Low-density Parity-check Codes Using Linear Programming for Modulation and Detection," *in Proc. 62nd IEEE Vehicular Technology Conference*, 2005, pp. 532-535.

[88] J. Kliewer, S. X. Ng, and L. Hanzo, "Efficient Computation of EXIT Functions for Non-binary Iterative Decoding," *IEEE Transactions on Communications,* Vol.54, No. 12, Dec. 2006, pp. 2133-2136.

[89] G. J. Byers and F. Takawira, "EXIT Charts for Non-Binary LDPC Codes," *in Proc. IEEE ICC,* 2005, pp. 652-657.